STUDY OF HOMOGENEOUS AND HETEROGENIZED RUTHENIUM / TIN HETEROBIMETALLIC COMPLEXES: SYNTHESIS, ELECTROCHEMISTRY AND CATALYTIC PROPERTIES

By

COREY R. ANTHONY

A DISSERTATION PRESENTED TO THE GRADUATE SCHOOL
OF THE UNIVERSITY OF FLORIDA IN PARTIAL FULFILLMENT
OF THE REQUIREMENTS FOR THE DEGREE OF
DOCTOR OF PHILOSOPHY

UNIVERSITY OF FLORIDA

2006

This dissertation is dedicated to my grandfather, Leonard Legister,
September 30th, 1900 – March 4th, 2004.
You may be gone POPPA but you will never be forgotten.

ACKNOWLEDGMENTS

I would like to first thank God because with him all things are possible.

I would now like to acknowledge the strong women who have had a positive impact in my life. First and foremost I thank my mother, a remarkable single parent who made countless sacrifices in raising three children. To her I owe my strong work ethic, drive for education and will always love unconditionally. I want to also acknowledge my lovely wife for all her love, support and patience which kept me focused during many endless nights of research. To her I owe a tremendous debt of gratitude for being my rock these last two years. I also wish to thank my sisters Charmaine and Cheryl and my cousin Heather for always being there and making this PhD dream of mine a reality.

I would now like to thank my advisor, another strong woman Dr. Lisa McElwee-White. To her I express gratitude for all the discussions and advice during the six years I have apprenticed with her. Under her tutelage I was able to grow both as a chemist and as a person. I'd like to also thank the McElwee-White group members past and present. Special thanks from me go out to Dr. Keisha-Gay Hylton, Dr. Corey Wilder, Dr. Ying Yang and Daniel Serra. I would also like to thank Dr. Khalil Abboud for solving the X-ray crystal structures presented in this dissertation.

TABLE OF CONTENTS

LIST OF TABLES

LIST OF FIGURES

Abstract of Dissertation Presented to the Graduate School
of the University of Florida in Partial Fulfillment of the
Requirements for the Degree of Doctor of Philosophy

STUDY OF HOMOGENEOUS AND HETEROGENIZED
RUTHENIUM / TIN HETEROBIMETALLIC COMPLEXES:
SYNTHESIS, ELECTROCHEMISTRY AND CATALYTIC PROPERTIES

By

Corey R. Anthony

May 2006

Chair: Dr. Lisa McElwee-White
Major Department: Chemistry

This dissertation describes the synthesis, electrochemistry and catalytic properties of a series of Ru/Sn complexes. A single oxidation wave, attributed to the Ru(II/III) couple was observed in the cyclic voltammograms of the Ru/Sn complexes. The electrocatalytic properties of these complexes were investigated during the electrooxidation of methanol. The oxidation products observed are dimethoxymethane (DMM) and methyl formate (MF). The formation of DMM is favored when the catalysis is performed with the Ru/Sn complexes. The selectivity of the catalysts can be tuned by varying the anodic potential. The highest current efficiency (92.4 %) and selectivity (100 %) were obtained from the electrooxidation of methanol with $CpRu(TPPMS)_2(SnCl_3)$ (**23**). Chemically modified electrodes were also prepared by attaching Ru/Sn complexes to the electrode surface. The electrochemical properties and stability of these heterogenized complexes were studied using cyclic voltammetry.

A novel Ru/Hg complex $CpRu(PPh_3)(\mu\text{-}Cl)(\mu\text{-}dppm)HgCl_2$ (**16**) was synthesized and characterized. X-ray crystallography revealed a unique chloride and dppm linker in **16**, the first time a Ru/Hg complex was isolated with these bridging moieties.

CHAPTER 1
LITERATURE REVIEW

Oxidation of Organic Molecules

In inorganic chemistry, oxidation is clearly defined as the loss of an electron by an atom, molecule or ion accompanied with an increase in the formal oxidation state. For organic chemists the concepts of oxidation states and electron transfer are less easily applied, hence the definition of oxidation differs slightly from inorganic to organic chemistry. Organic chemists have defined the oxidation of an organic molecule as either 1) the loss of hydrogen or 2) the replacement of hydrogen with a more electronegative atom such as oxygen or a halogen.

The oxidation of organic molecules has a long history[1] stemming to the 1780's and Lavoisier's explanation of combustion. Observations in the 19th century linked the deterioration of many organic materials such as rubber and natural oils to the adsorption of dioxygen. The control of oxidation is desirable not only for inhibiting the degradation of commercially important materials such as plastics, gasoline, and rubbers but also for promoting the selective oxidation of hydrocarbon feedstocks such as olefins, alkanes and aromatic hydrocarbons.

The first observation of a catalyzed oxidation reaction is attributed to Davy who showed in 1820 that ethanol is oxidized to acetic acid (Eq. 1.1) in the presence of

$$CH_3CH_2OH + O_2 \xrightarrow{[\ Pt\ ]} CH_3COOH + H_2O \qquad (1.1)$$

platinum. Since then the scope of the catalyzed oxidation reaction of organic molecules has grown tremendously, becoming basic to organic chemistry and the petrochemical

industry. Catalytic oxidation of ethylene to acetaldehyde (Eq. 1.2, Wacker process) was the first industrial scale reaction that used an organopalladium catalyst. The catalytic

$$CH_2{=}CH_2 + H_2O \xrightarrow[CuCl_2]{[PdCl_4]^{2-}} CH_3CHO \qquad (1.2)$$

oxidation of organic molecules is now widely used in the synthesis of fine chemicals. These reactions are now well understood and can be utilized in synthesizing a wide array of functional groups (Scheme 1-1).[2]

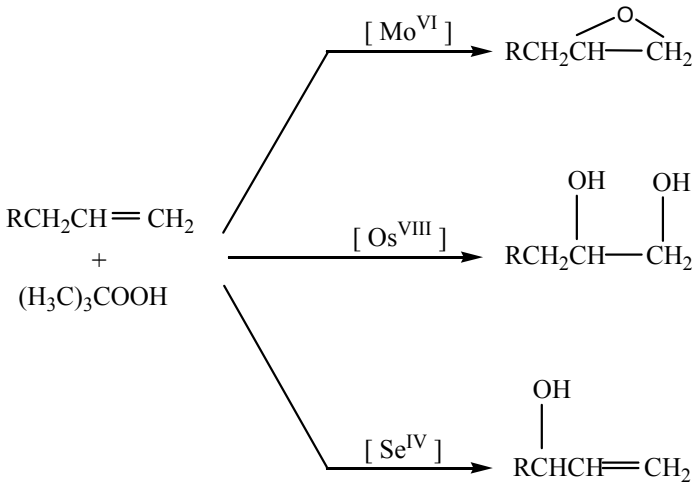

Scheme 1-1. Adapted from reference 2.

Oxidation of Alcohols

The selective oxidation of alcohols to the corresponding aldehyde, ketone or carboxylic acid is of significance not only to fundamental research but also for commercial manufacturing processes. Traditionally the oxidation of alcohols is performed with high oxidation state metal reagents such as chromium (VI), Mn (VI) and ruthenium (VIII). These methods have been reviewed extensively[2,3] and will not be covered within this dissertation. Another area of emphasis is the use of transition metal catalysts along with a chemical co-oxidant such as oxygen,[4-9] peroxide[7,8,10] or an amine

N-oxide.[11,12] The above transformations have also been extensively studied and are beyond the scope of this review. One area which has recently received significant interest from the scientific community is the electrochemical oxidation of alcohols. The literature on electrochemical oxidation of alcohols can be roughly grouped into two sets: heterogeneous[13,14] (fuel cell) and homogeneous studies.

Electrochemical Oxidation of Methanol in Fuel Cells

Fuel cells have been postulated as the power generation system of the immediate future, poised to replace not only internal combustion engines[15,16] but also advanced alkali[16,17] batteries. Due to their simplicity, high energy efficiency and low pollution, direct methanol fuel cells (DMFCs) are especially suited for use in portable electronic devices.[16,17] In DMFCs aqueous methanol is electrochemically oxidized at the anode (Eq. 1.3) to CO_2

Anodic Reaction: $CH_3OH + H_2O \longrightarrow CO_2 + 6\ H^+ + 6\ e^-$ (1.3)

while oxygen is reduced at the cathode (Eq. 1.4) to form water.

Cathodic Reaction: $3/2\ O_2 + 6\ H^+ + 6e^- \longrightarrow 3\ H_2O$ (1.4)

When combined, the two half reactions result in an electromotive force of 1.18 V for the overall reaction (Eq. 1.5).

Overall Reaction: $3/2\ O_2 + CH_3OH \longrightarrow CO_2 + 2\ H_2O \quad \Delta E = 1.18\ V$ (1.5)

The mechanism for this oxidation has been reviewed[18,19] extensively and can be summarized in two key steps:

- Physisorption and dehydrogenation of methanol on the electrode surface
- Formation of CO_2 from adsorbed carbonaceous intermediates

Very few electrode materials are capable of performing both reactions, and of these only platinum and platinum based electrodes have displayed any encouraging activity and stability in an acidic medium.

Mechanism

The surface catalyzed electrooxidation of methanol has been studied exhaustively,[18,20-22] and because of this the reaction mechanism is now well understood. The mechanism was elucidated using a variety of electrochemical and spectroscopic methods. These methods include cyclic voltammetry, steady-state galvanostatic polarizations, chronoamperometry, mass spectrometry, FTIR, XAS, etc.[23-25] *In-situ* spectroscopic experiments were very instrumental in examining adsorbed species and for identifying intermediates formed during the reaction. By combining the results of cyclic voltammetry, *in-situ* ellipsometry, XAS, and *in-situ* FTIR experiments, the reaction steps below were proposed. The reaction is thought to initially proceed through a series of dehydrogenation steps to adsorbed CO (Eq 1.6 - 1.9).[18,20-22] Adsorbed CO is a widely accepted intermediate of methanol oxidation, and its presence has been observed with the aid of various in-situ infrared spectroscopy techniques.[26-28] CO and other carbonaceous intermediates can then be oxidized to carbon dioxide and desorbed from the electrode surface by reacting with adsorbed water (Eq 1.10 - 1.12).

The electrochemical oxidation of methanol on Pt is a complicated reaction involving several steps; chemisorption of methanol and water, dehydrogenation of methanol, interaction between adsorbed CO and OH species and the formation of

CO_2.[20,21] At potentials below 0.7 V (the potential region of interest) the rate determining step (RDS) on Pt anodes was shown to be the dissociative chemisorption of water (Eq 1.10).

$$CH_3OH + Pt\ (s) \longrightarrow Pt\text{-}CH_2OH + H^+ + e^- \quad (1.6)$$

$$Pt\text{-}CH_2OH + Pt\ (s) \longrightarrow Pt_2\text{-}CHOH + H^+ + e^- \quad (1.7)$$

$$Pt_2\text{-}CHOH + Pt\ (s) \longrightarrow Pt_3\text{-}CHO + H^+ + e^- \quad (1.8)$$

$$Pt_3\text{-}CHO \longrightarrow Pt\text{-}CO + 2\ Pt\ (s) + H^+ + e^- \quad (1.9)$$

$$H_2O + Pt\ (s) \longrightarrow Pt\text{-}OH + H^+ + e^- \quad (1.10)$$

$$Pt\text{-}CO + Pt\text{-}OH \longrightarrow Pt\text{-}COOH \quad (1.11a)$$

$$Pt\text{-}CO + H_2O \longrightarrow Pt\text{-}COOH + H^+ + e^- \quad (1.11b)$$

$$Pt\text{-}COOH \longrightarrow Pt\ (s) + CO_2 + H^+ + e^- \quad (1.12)$$

Presently DMFCs are faced with a few challenging problems, foremost of which is that the overall reaction is very slow. The electrochemical oxidation of methanol (Eq. 1.5), though thermodynamically favored, is a kinetically sluggish reaction even at high catalyst loading. On the other hand, the electrooxidation of hydrogen (a thermodynamically similar reaction) is very fast at low catalyst loading. The formation of stable intermediates (Eq. 1.6 - 1.9)[29,30] is responsible for the poor kinetics of the methanol oxidation reaction. Adsorbed CO in particular is strongly bound to the surface of Pt requiring a high overpotential (approximately 0.5 V vs NHE) in order to obtain a reasonable current density. Based on these studies it is now accepted that an active surface for methanol electrooxidation must:

- "Activate" water at low potentials
- Be labile to CO chemisorption
- Catalyze the oxidation of CO to CO_2

Binary Electrocatalysts

Although there has been moderate success with Pt anodes,[31-33] the rapid poisoning of the surface with CO has made these electrodes inadequate for use in DMFCs. This decision led to an intensive search for other materials that can improve the performance of the Pt anode during the methanol oxidation process. Several methods have been investigated for promoting the formation of CO_2 (Eq. 1.10 - 1.12). One method involves alloying Pt with a second metal, to accelerate the RDS. Since the dissociative chemisorption of water (Eq. 1.10) is the RDS, Pt was alloyed with oxophilic metals in order to increase the reaction rate. Alloys of Pt and an oxophilic metal have been investigated as electrocatalysts for over 40 years. Beneficial effects have been observed for Pt/Sn,[34,35] Pt/Ir,[36] Pt/W[37-40] and Pt/Ru[28,41-44] electrodes. Studies of Pt alloyed with such metals shows that Ru has by far the largest catalytic effect[18] (Figure 1-1).

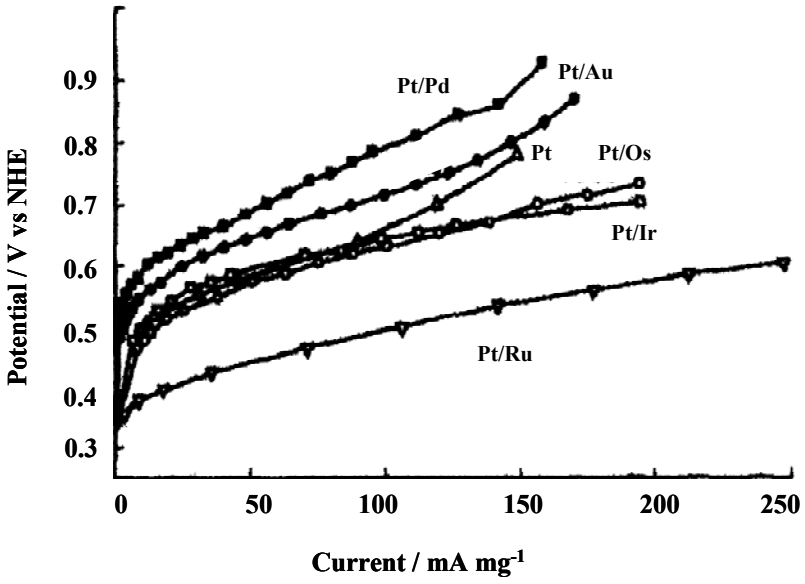

Figure 1-1. Polarization data for Pt/M alloys at 60 °C in 2.5 M H_2SO_4 / 1 M CH_3OH. Adapted from reference 18.

Pt/Ru binary anodes

Considerable effort has been expended to clarify the role of Ru in Pt/Ru binary electrodes. Of the mechanisms proposed, the bifunctional theory has gained general acceptance.[44-46] According to this mechanism, the Pt sites are responsible for the chemisorption and dehydrogenation of methanol, while the Ru sites are responsible for water activation (Eq. 1.13 - 1.14). This is supported by the fact that the discharging of water on Ru occurs at 0.2 V, while the chemisorption of methanol on Pt is favored over Ru.

$$H_2O + Ru\ (s) \longrightarrow Ru\text{-}OH + H^+ + 1e^- \qquad (1.13)$$

$$Pt\text{-}CO + Ru\text{-}OH \longrightarrow Pt\ (s) + Ru\ (s) + CO_2 + H^+ + 1e^- \qquad (1.14)$$

In-situ CO stripping voltammetry was used to evaluate the active surface area, intrinsic catalytic effect and the surface composition of the anode. An anodic shift of the peak potential was observed for the CO stripping voltammograms of the Pt/Ru electrodes. This shift combined with the improved catalytic activity provides clear evidence that on Pt/Ru binary electrodes CO removal is the RDS. The optimal Pt:Ru ratio is still being aggressively investigated, and remains a source of some controversy. At high temperatures (90 – 130 °C) and on a carbon support it has been shown that the optimal Ru content is 50 mole %.[47] It is thought that at 50 % coverage the intrinsic rate constant is maximized.

The alloying of Pt with non-noble metals, most notably Re[48] and Mo, has been reported to result in a strong enhancement of the methanol oxidation reaction. The effectiveness of binary electrodes, especially Pt/Ru, has resulted in the recent investigation of ternary Pt/Ru/Sn,[49] Pt/Ru/Mo[49] and Pt/Ru/W[49,50] as well as quaternary systems Pt/Ru/Os/Ir,[41,51,52] Pt/Ru/Mo/W[53] and Pt/Ru/Sn/W.[54] Only a slight to moderate

improvement in activity was observed for these systems, relative to the Pt/Ru binary electrode.

Combinatorial Screening

After thirty years of research, the Pt/Ru (50/50) binary alloy remains one of the more active electrocatalysts for the methanol oxidation reaction. This lack of a breakthrough and the high cost of the precious metals have made electrocatalysts a prime target for combinatorial screening. Combinatorial chemistry and high-throughput screening have revolutionized drug discovery and the pharmaceutical industry. These complementary technologies are now used for the preparation and evaluation of large numbers of formulations. Combinatorial screening of inorganic material has been used for almost thirty years. This method has been instrumental in characterizing new materials and in the development of new catalysts.

Combinatorial searches for electrocatalysts by current voltage methods are extremely cumbersome, especially for large sample sizes. This obstacle was circumvented in 1998 by Mallouk[52] who monitored the cell reactions via a fluorescence signal. In 1999 Ward[55] expanded on this method and used an automated multi-electrode array to perform the combinatorial screening. These methods have since been applied by other researchers and have led to ternary and quaternary electrode materials that display greater catalytic activity than Pt/Ru electrodes.

Reaction Intermediates

Although the complete oxidation of methanol to carbon dioxide is desired for fuel cell applications, other species are often formed leading to a decrease in the fuel efficiency. Frequently observed by-products of methanol oxidation include formaldehyde (Eq. 1.15)

and formic acid (Eq. 1.16). These products can undergo a condensation reaction to form dimethoxymethane (DMM) (Eq. 1.17) and methyl formate (MF) (Eq. 1.18).

$$CH_3OH \longrightarrow H_2CO + 2\,H^+ + 2\,e^- \quad (1.15)$$

$$H_2CO \longrightarrow HCOOH + 2\,H^+ + 2\,e^- \quad (1.16)$$

$$H_2CO + 2\,CH_3OH \longrightarrow CH_2(OCH_3)_2 + H_2O \quad (1.17)$$

$$HCOOH + CH_3OH \longrightarrow HCOOCH_3 + H_2O \quad (1.18)$$

The current efficiency and product ratio were shown to be dependent on several variables such as temperature, anodic potential, mass transport and the catalyst type.[56,57] For example when the electrolysis of methanol is performed on a smooth Pt electrode at ambient temperature the incomplete oxidation products formaldehyde and formic acid are preferred.[58] However when a high surface area platinized Pt electrode was used the complete oxidation to carbon dioxide was favored.[58] The condensation products DMM and MF were observed in the anode exhaust of DMFCs operating at high temperatures and methanol concentration.

Electrochemical Oxidation of Alcohols by Metal Complexes

The electrochemical oxidation of alcohols using a catalyst in solution is an example of an indirect electrochemical process. It is termed indirect because it is the mediator (metal complex) not the substrate (alcohol) that is oxidized at the electrode surface (Scheme 1-2). After undergoing this activation the mediator reacts in bulk solution with the substrate, regenerating the reduced metal complex and forming the oxidized substrate.

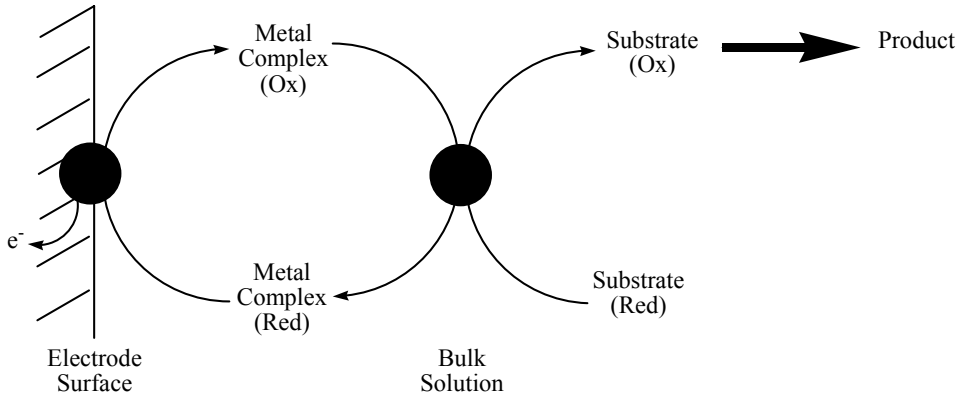

Scheme 1-2. Adapted from reference 59.

There are two means by which the mediator can oxidize the substrate during the homogeneous reaction:

1. "Redox Catalysis"[59] in which the mediator merely plays the role of an electron carrier (Scheme 1-3), transferring electrons to the substrate via an outer sphere process

$$[\,M\,]_{(red)} \longrightarrow [\,M\,]_{(ox)} + n\,e^-$$

$$[\,M\,]_{(ox)} + Substrate_{(red)} \longrightarrow [\,M\,]_{(red)} + Substrate_{(ox)}$$

$$Substrate_{(ox)} \longrightarrow Product$$

Scheme 1-3.

2. "Chemical Catalysis"[59] in which the mediator reacts with the substrate to form an adduct (Scheme 1-4) before electron transfer occurs

$$[\,M\,]_{(red)} \longrightarrow [\,M\,]_{(ox)} + n\,e^-$$

$$[\,M\,]_{(ox)} + Substrate_{(red)} \longrightarrow [\,M\text{—}Substrate\,]_{(ox)}$$

$$[\,M\text{—}Substrate\,]_{(ox)} \longrightarrow Product + [\,M\,]_{(red)}$$

Scheme 1-4.

In this dissertation only the chemical catalysis (often referred to as electrocatalysis) will be considered.

Ruthenium Electrocatalysts

Ruthenium polypyridyl complexes are suited as electrooxidation catalysts due to the high stability and accessibility of multiple oxidation states, tunable redox potentials by varying ligands and the possibility of multiple electron transfers. The electrochemical oxidation of alcohols has been extensively studied with ruthenium polypyridyl catalysts.[60-68] Significant contribution to this area has been made by Meyer, who in 1978 observed the $2e^-$ reduction of a Ru complex accompanied by oxidation of triphenylphosphine to triphenylphosphine oxide (Scheme 1-5).[63] The pyridine ligand however, is not suited to prolonged use and eventually dissociates, leading to an inactive oxo bridged dimer. The instability of the pyridine ligand was eventually overcome by replacing it and a bipyridine with the terpyridine (trpy) ligand.[65] Of all the polypyridyl complexes investigated as electrocatalysts, $[(trpy)(bpy)Ru^{II}(OH_2)]^{2+}$ has attracted the most interest.

$$[(bpy)_2pyRu^{IV}O]^{2+} + PPh_3 \xrightarrow{\text{fast}} [(bpy)_2pyRu^{II}(OPPh_3)]^{2+}$$

$$\xrightarrow[CH_3CN]{\text{slow}} [(bpy)_2pyRu^{II}(CH_3CN)]^{2+} + O=PPh_3$$

Scheme 1-5. Adapted from reference 63.

The Ru(II) aquo complex can undergo two reversible proton coupled 1 e^- oxidation steps to generate the versatile oxidant $[(trpy)(bpy)Ru^{IV}(O)]^{2+}$ (Eq. 1.19 -1.20).

$$[(trpy)(bpy)Ru^{II}(OH_2)]^{2+} \rightleftharpoons [(trpy)(bpy)Ru^{III}(OH)]^{2+} + e^- + H^+ \quad (1.19)$$

$$[(trpy)(bpy)Ru^{III}(OH)]^{2+} \rightleftharpoons [(trpy)(bpy)Ru^{IV}O]^{2+} + e^- + H^+ \quad (1.20)$$

As an oxidant $[(trpy)(bpy)Ru^{IV}(O)]^{2+}$ is very versatile and has been used for the electrocatalytic oxidation of alkenes,[69,70] ketones,[68-70] aldehydes,[68,71] sugars[72,73] and

DNA.[72,74,75] A simplistic view of the catalytic cycle is shown in Scheme 1-6. In this cartoon a potential capable of oxidizing the metal center from Ru(II) to Ru(IV) is applied at the electrode. The Ru complex is first oxidized at the electrode surface before reacting in solution with the substrate regenerating the Ru(II) aquo complex.

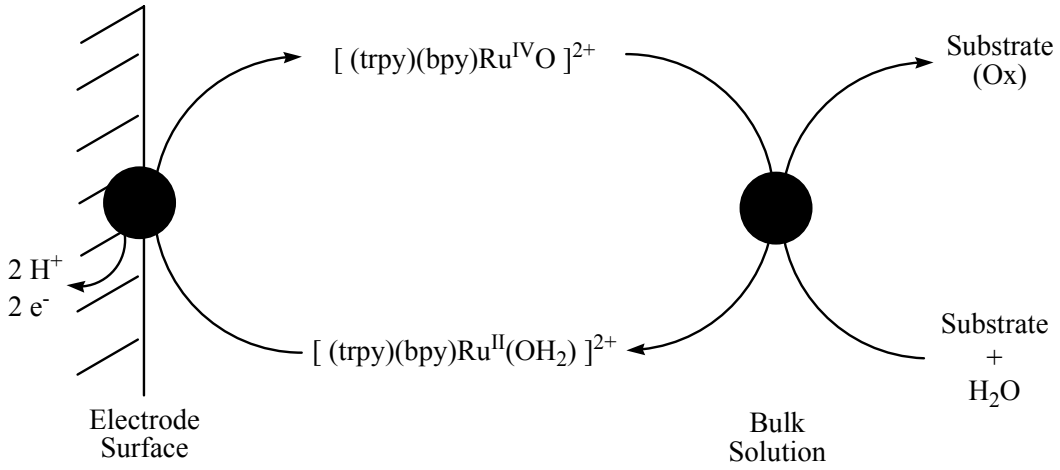

Scheme 1-6. Adapted from reference 76.

Since Meyer's publication[65] in 1980 on the electrocatalytic properties of $[(trpy)(bpy)Ru^{IV}(O)]^{2+}$, the catalytic abilities of several other polypyridyl complexes have been reported. An example of this is $[Ru(4,4'\text{-}Me_2bpy)_2(PPh_3)(H_2O)][(ClO_4)_2]$, an active electrocatalyst that selectively oxidizes primary alcohols to the corresponding aldehyde.[77] Cyclic voltammograms of these solutions exhibit an increase in anodic current when an alcohol is introduced. This increase in current is characteristic of the catalytic electrooxidation of alcohols by Ru^{IV}=O.[78]

Extensive mechanistic studies have been performed on the electrooxidation of aqueous alcoholic solutions with ruthenium complexes. Several mechanisms have since been proposed with each containing a Ru-oxo complex as the catalytically active species. The Ru-oxo bond is either generated *in situ* from water or is present beforehand in the

pre-catalyst. The mechanisms which have been proposed are hydride transfer[79,80] (Scheme 1-7), oxygen insertion[81] (Scheme 1-8) and hydrogen atom abstraction[82] (Scheme 1-9).

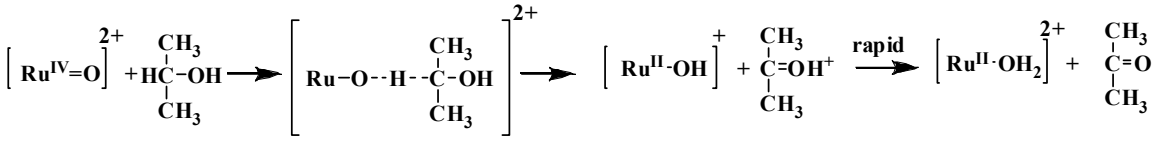

Scheme 1-7. Adapted from reference 79.

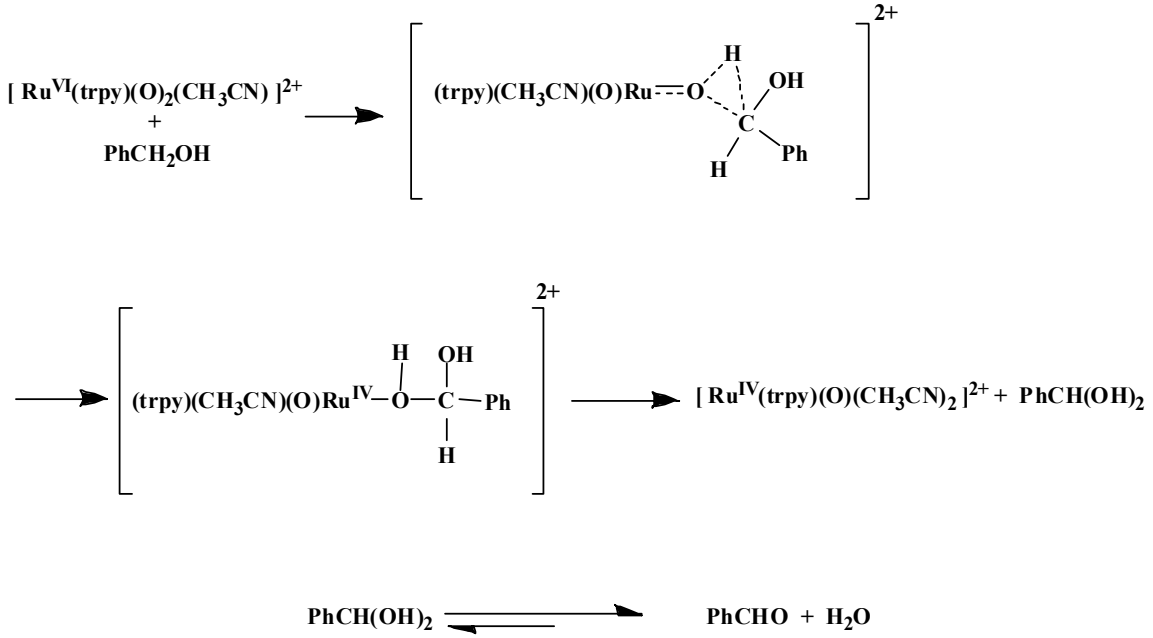

Scheme 1-8 Adapted from reference 81.

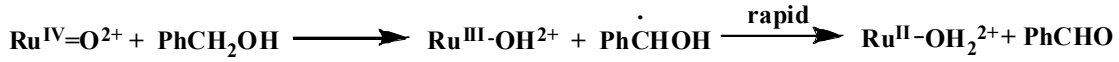

Scheme 1-9 Adapted from reference 82.

Reactivity of Bimetallic Complexes

The term "catalysis" was coined by Berzelius in 1836 to describe a new force other than affinity that can drive a reaction to completion. The modern definition of a catalyst is any substance that accelerates the rate of a chemical reaction without being consumed during the reaction. From an economical and environmental standpoint, catalytic

reactions currently dominate the chemical industry.[83] These reactions have a considerable impact on the production of pharmaceuticals, agrochemicals, polymers, fine chemicals, etc.[84] Catalysis offers the possibility of achieving complex synthetic transformations with high efficiency, chemical and stereochemical control while minimizing, if not eliminating, waste products and solvents.

Because of the distinct advantages gained from being able to catalyze chemical reactions, researchers are constantly trying to improve upon the reactivity and selectivity of current catalysts. It is clear that the catalytic reactions that occur in nature are generally far superior to the reactions developed by chemists. The elucidation of many enzymatic processes has revealed the interaction of two or more reactive centers during some of these catalytic transformations. The multifunctional catalysis observed in nature is rarely exploited in synthetic catalysts which chiefly utilize a single reactive site.

In trying to mimic the hydrolytic cleavage of a phosphate ester bond by a metalloenzyme, Reinhoudt developed **1** a calix[4]arene functionalized with two Zn(II) metal centers. Complex **1** catalyzes the cyclization of the RNA model substrate 2-(hydroxypropyl)-*p*-nitrophenyl phosphate[85] (HPNP, Scheme 1-10) with a 23,000 fold rate increase at pH 7 and 25 °C. The increased activity of **1** was explained via a bifunctional mechanism (Scheme 1-10) in which one zinc center acts as a Lewis acid and activates the phosphate group while the second activates the nucleophilic hydroxyl group.

Bimetallic complexes are now an accepted means to improving the catalytic properties of some mononuclear systems.[87-89] In recent years heterobimetallic complexes have also received a tremendous amount of attention due to the possibility of exploiting the different reactivities of the metal centers during a chemical reaction. An example

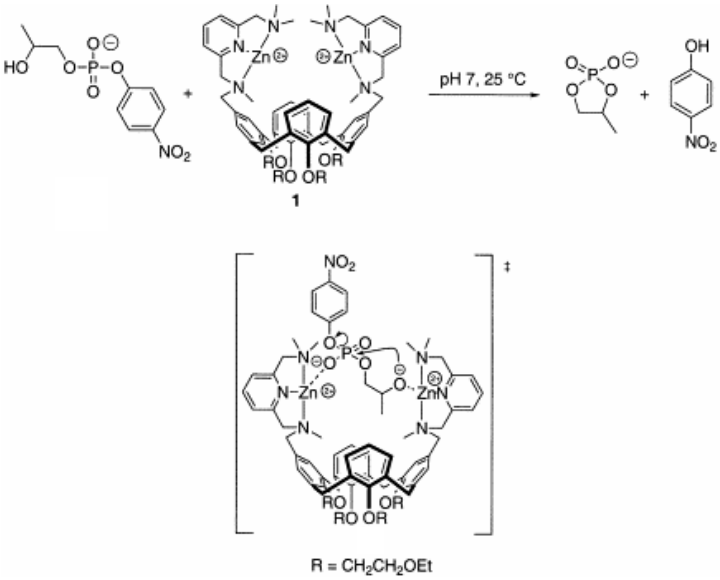

Scheme 1-10. Adapted from reference 86.

relevant to this dissertation is the Oppenauer-type oxidation of primary and secondary alcohols to the corresponding aldehyde and ketone with complex **2** (Table 1-1).[90] Although the mechanism for this catalytic cycle is not entirely clear, it is apparent that both metal fragments are crucial to the performance of the catalyst. This certainty was based on the two key observations made by Severin:

1. Under similar conditions, Ru and Rh homobimetallic complexes displayed no Oppenauer-type oxidative ability (Table 1-1)
2. Ligand modification to the Ru or Rh fragment affects the activity of the complexes

Another example relevant to this dissertation is the heterobimetallic catalyst $[N(n\text{-}Bu_4)][M(N)R_2(\mu\text{-}O)_2CrO_2]$ where M= Ru or Os developed by Shapley.[6,91] When air is used as the co-oxidant, this complex selectively oxidizes benzylic, primary and secondary alcohols at 60 °C to the corresponding carbonyl compounds. A mechanism based on the experimental results is shown in Scheme 1-11. It was proposed that after coordinating to Os there is a proton transfer to one of the bridging oxo ligands, followed

by β–hydride elimination and formation of the carbonyl compound. After the carbonyl compound dissociates, molecular oxygen is activated by the Os-Cr bond, regenerating the starting metal complex.[6]

Table 1-1. Catalytic oxidation of 1-phenylethanol. Adapted from reference 90.

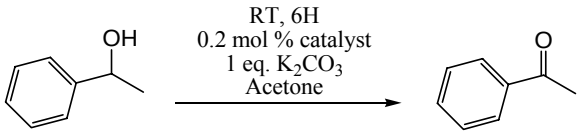

Catalyst	Conversion / %
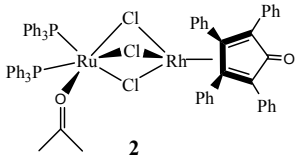 **2**	94
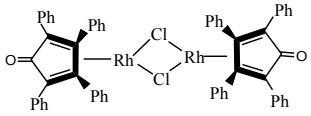	< 1
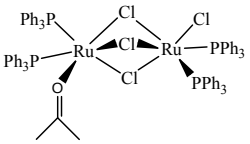	< 1

Heterobimetallic Electrooxidation Catalysts

Previous studies in the McElwee-White research group resulted in the synthesis of three heterobimetallic complexes $CpRu(PPh_3)(\mu\text{-}Cl)(\mu\text{-}dppm)PtCl_2$ (**3**), $CpRu(PPh_3)(\mu\text{-}Cl)(\mu\text{-}dppm)PdCl_2$ (**4**) and $CpRu(PPh_3)(Cl)(\mu\text{-}dppm)AuCl$ (**5**).[92,93] Complexes **3** - **5** were prepared by reacting $CpRu(PPh_3)(Cl)(\eta^1\text{-}dppm)$ (**6**) with $Pt(COD)Cl_2$, $Pd(COD)Cl_2$ or $Au(PPh_3)Cl$ (Scheme 1-12) at room temperature. The molecular structures of **3** - **5** were confirmed via X-ray crystallography and NMR.

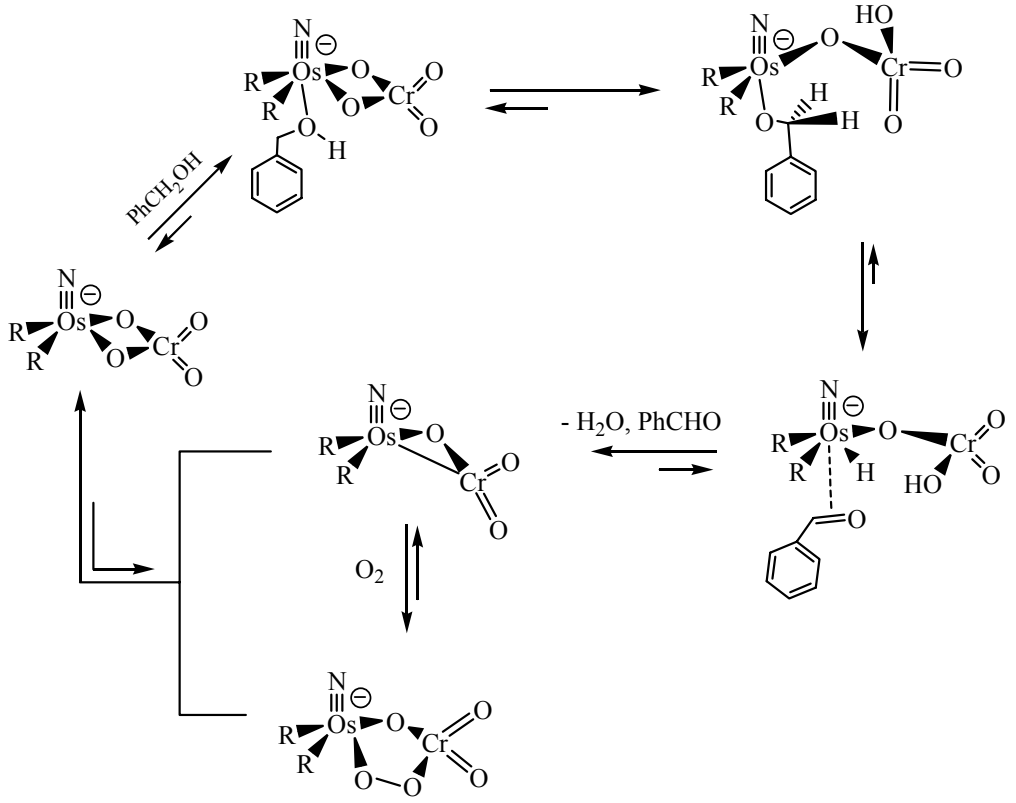

Scheme 1-11. Adapted from reference 6.

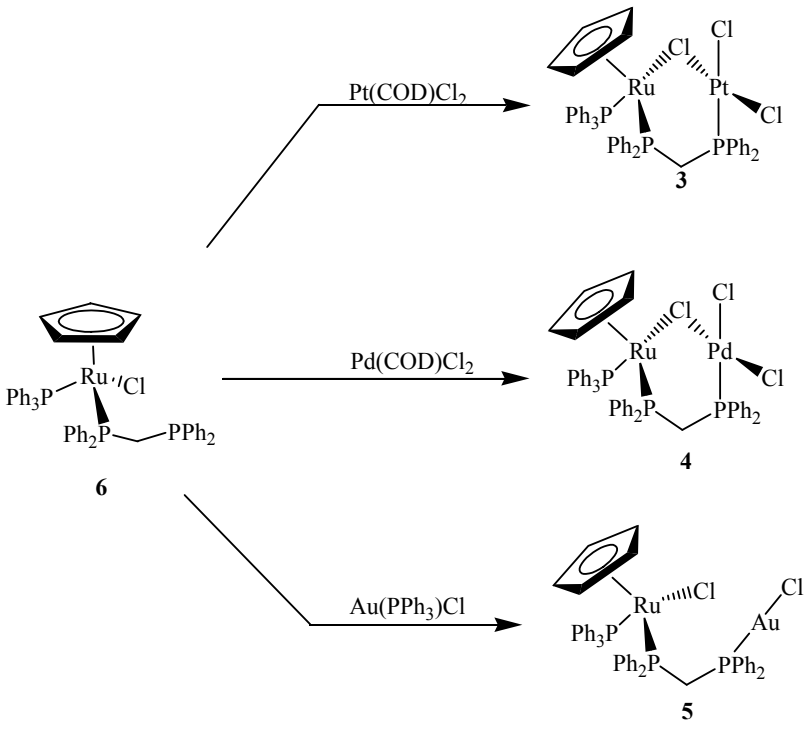

Scheme 1-12.

Cyclic voltammetry (CV) of complexes **3 - 5** was performed in 1,2-dichloroethane (DCE) containing 0.7 M tetrabutyl ammonium trifluoromethane sulfonate (TBAT). All three complexes exhibited three oxidation waves (Table 1-2). The first and third wave are assigned to the Ru(II/III) and Ru(III/IV) couples respectively, while the middle wave is assigned to the redox couple of the second metal.

Table 1-2. Formal potentials for complexes **3, 4, 5** and **7**

Complex[a]	Couple	$E_{1/2}$ (V)	Couple	E_{pa} (V)	Couple	E_{pa} (V)
Ru/Pt (**3**)	$Ru^{II/III}$	1.21	$Pt^{II/IV}$	1.69	$Ru^{III/IV}$	1.91
Ru/Pd (**4**)	$Ru^{II/III}$	1.30	$Pd^{II/IV}$	1.49	$Ru^{III/IV}$	1.92
Ru/Au (**5**)	$Ru^{II/III}$	0.89	$Au^{I/III}$	1.42	$Ru^{III/IV}$	1.81
CpRu(η^2-dppm)Cl (**7**)	$Ru^{II/III}$	0.61			$Ru^{III/IV}$	1.38

[a] All potentials obtained in 0.7 M TBAT / DCE and reported vs NHE. Adapted from reference 92.

Cyclic voltammetry was also used in screening the electrocatalytic properties of $CpRu(PPh_3)(\mu\text{-}Cl)(\mu\text{-}dppm)PtCl_2$ (**3**), $CpRu(PPh_3)(\mu\text{-}Cl)(\mu\text{-}dppm)PdCl_2$ (**4**) and $CpRu(PPh_3)(Cl)(\mu\text{-}dppm)AuCl$ (**5**) towards methanol oxidation. For complex **3**, the introduction of methanol (Figure 1-2) results in a significant increase in current that coincides with the Pt(II/IV) redox wave. This increase in current is typical of an electrocatalytic oxidation process, and is also observed at the Pd(II/IV) redox couple of complex **4**. In contrast, the catalytic current of the Ru/Au complex does not occur at the Au(I/III) couple but at the Ru(III/IV) couple.

Product Formation

As previously described, the surface catalyzed electrooxidation of methanol involves a complicated multistep reaction (Eq. 1.6 – 1.12). When the electrooxidation of methanol is performed with a homogeneous catalyst, the oxidation products are

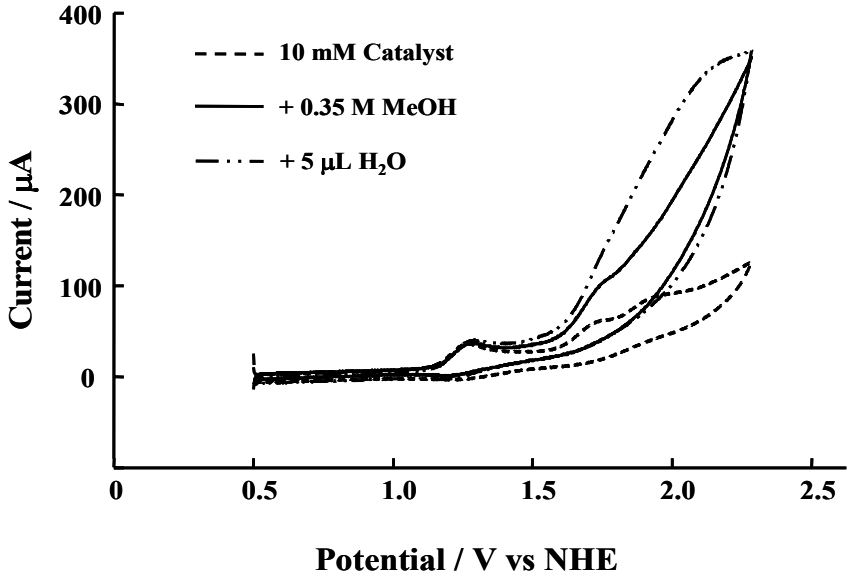

Figure 1-2. Cyclic voltammograms of **3** under nitrogen in 3.5 mL of DCE/0.7 M TBAT; glassy carbon working electrode; Ag/Ag^{+} reference electrode; 50 mV/s solutions as specified. Adapted from reference 93.

formaldehyde (Eq 1.15) and formic acid (Eq 1.16). In the presence of excess methanol both formaldehyde and formic acid undergo condensation reactions to form dimethoxymethane (Eq. 1.17) and methyl formate (Eq. 1.18) respectively. It is important to point out that with the excess of methanol present the equilibria for these reactions should favor the formation of DMM and MF. Therefore when observed, DMM is formed from the incomplete $2e^{-}$ oxidation of methanol. MF is formed from the $4e^{-}$ oxidation of methanol. Current efficiency was calculated based on the yields of DMM, MF and the total charge passed (Eq 1.21).

$$\text{Current efficiency} = \left[\frac{96485\ (\text{C mol}^{-1})}{\text{charge passed (C)}}\right]\left\{[\ 2 \text{ x DMM (mol)}\ ] + [\ 4 \text{ x MF (mol)}\ ]\right\} \text{x } 100\ (\%) \quad (1.21)$$

Bulk Electrolysis of Methanol

The bulk electrolyses of **3** - **5** and the Ru model compound CpRu(η^2-dppm)Cl (**7**) were performed at 1.7 V, the potential at which the catalytic current begins for complex **3**. Oxidation with the Ru/Pd complex **4** was performed between the Pd(II/IV) and Ru(III/IV) waves, while electrolysis with the Ru/Au compound **5** was performed between the Au(I/III) and Ru(III/IV) waves. Oxidation of methanol with the Ru model compound **7** was performed at a potential more positive than the Ru(III/IV) couple.

The organic products of bulk electrolyses of dry methanol were analyzed with a gas chromatograph (GC) and identified as dimethoxymethane and methyl formate. The formation of these products is consistent with the electrooxidation of methanol on Pt/Ru electrodes. A result of this condensation reaction is that water is formed during the electrolysis. Addition of water not only results in an increase in the catalytic currents for compounds **3 - 5** (Figure 1-2) but also favors the formation of methyl formate (Table 1-3).

Table 1-3. Bulk electrolysis data for the oxidation of methanol by **3** - **7**

Complex[a]	Dry Current Efficiency[b] (%)	Dry Product Ratio[b] (DMM / MF)	Wet Current Efficiency[b] (%)	Wet Product Ratio[b] (DMM / MF)
3	18.6	1.20	19.5	0.41
4	24.6	0.87	20.6	0.54
5	25.4	0.46	26.1	0.34
7	3.2	∞	7.2	0.33

[a] Electrolyses were performed at 1.7 V vs NHE. [b] Product ratio and current efficiencies after 130 C of charge passed. Adapted from reference 92.

Current efficiencies for the oxidation of methanol with **3** - **5** and **7** are summarized in Table 1-3. Although the current efficiencies of the heterobimetallic complexes are moderate at best (18 - 26 %), they are still significantly higher than that of the Ru model compound (3 - 7 %). These results indicate that there is a cooperative interaction

between Ru and the second metal center resulting in an enhancement of the catalytic properties of the heterobimetallic complexes relative to their mononuclear components.

Summary

Ruthenium complexes have been studied as alcohol electrooxidation catalysts since the 1970s. Heterobimetallic homogeneous electrocatalysts is a fairly new field, with research being driven by the McElwee-White group. As a result of this research it is evident that the non-Ru metal center of **3** – **5** has a profound effect on the catalytic activity of the heterobimetallic complexes. The remainder of this dissertation will focus on the role of the non-Ru metal center during the electrooxidation of methanol with ruthenium heterobimetallic complexes.

CHAPTER 2
SYNTHESIS AND ELECTROCHEMICAL PROPERTIES OF A RUTHENIUM / MERCURY HETEROBIMETALLIC COMPLEX

Introduction

Interest in heterobimetallic complexes has grown significantly in the last twenty years, mainly due to the potential catalytic application of interacting metal centers.[94-97] Cooperative interaction between metal centers has been shown to generate catalysts with greater reactivity and selectivity than their mononuclear components.[98-100] A similar cooperative effect was observed during the electrooxidation of methanol on Pt/Ru binary anodes. A cooperative effect was also observed during the oxidation of alcohols with Ru/Rh (Table 1-1) and Os/Cr (Scheme 1-11) homogeneous catalysts. Interest in this cooperative effect led to the synthesis, and investigation of the electrocatalytic properties of $CpRu(PPh_3)(\mu\text{-}Cl)(\mu\text{-}dppm)PtCl_2$ (**3**), $CpRu(PPh_3)(\mu\text{-}Cl)(\mu\text{-}dppm)PdCl_2$ (**4**) and $CpRu(PPh_3)(Cl)(\mu\text{-}dppm)AuCl$ (**5**).[92,93] Complexes **3** - **5** were used as catalyst during the electrooxidation of methanol and resulted in significantly better current efficiencies (Table 1-2) than the mononuclear model complex $CpRu(\eta^2\text{-}dppm)Cl$.[92]

The increased activity displayed by complexes **3** - **5** during the methanol oxidation reaction inspired further study and led to the synthesis of **8** – **14**. In complexes **8** – **14** the structures of **3** - **5** were altered by varying the ligands.[101] The CVs of **8** - **14** (Table 2-1) are similar to those observed for **3** – **5**, and the assignment of the redox waves were made from comparison to these complexes. Electronic interaction between the metal centers of complexes **8** - **12** is observed in their CVs. The presence of a bridging halide promotes

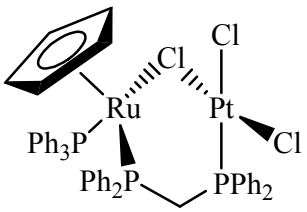

3

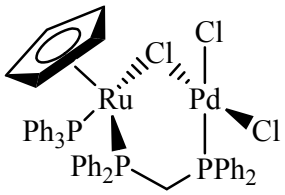

4

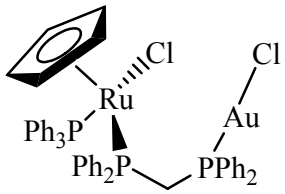

5

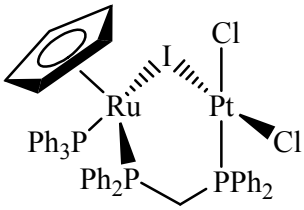

8

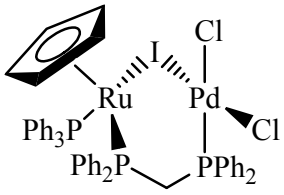

11

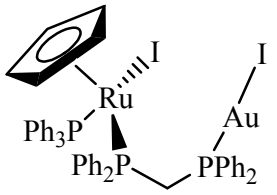

13

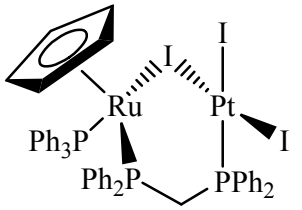

9

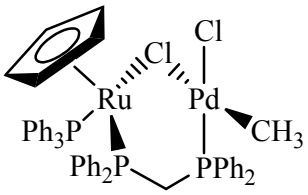

12

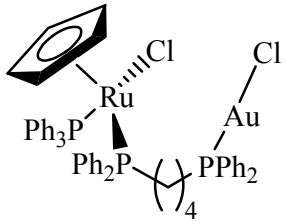

14

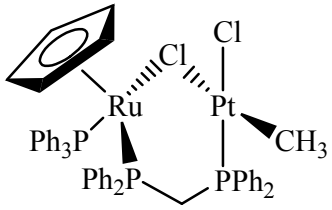

10

Figure 2-1. Structure of compounds **3** - **5** and **8** - **14**

this interaction, and the donation of electron density from Ru to Pd or Pt is reflected in the Ru(II/III) oxidation potential. Due to the considerable loss of electron density, the Ru(II/III) oxidation wave for complexes **8** – **12** occurs at a much higher potential than $CpRu(PPh_3)(Cl)(\eta^1\text{-dppm})$ (Table 2-1). The lack of electronic interactionbetween the Ru

and Au metal centers can also be observed by examining the CV data (Table 2-1). The Ru(II/III) and Au(I/III) oxidation waves of **13** and **14** are shifted only slightly relative to their monometallic model compounds.

Table 2-1. Formal potentials for complexes **8** - **14**

Complex[a]	Couple	$E_{1/2}$ (V)	Couple	E_{pa} (V)	Couple	E_{pa} (V)
8	$Ru^{II/III}$	1.25	$Pt^{II/IV}$	1.54	$Ru^{III/IV}$	1.90
9	$Ru^{II/III}$	1.10	$Pt^{II/IV}$	1.49	$Ru^{III/IV}$	1.98
10	$Ru^{II/III}$	1.08	$Pt^{II/IV}$	1.53	$Ru^{III/IV}$	1.95
11	$Ru^{II/III}$	1.29	$Pd^{II/IV}$	1.55	$Ru^{III/IV}$	1.98
12	$Ru^{II/III}$	1.10	$Pd^{II/IV}$	1.50	$Ru^{III/IV}$	1.95
13	$Ru^{II/III}$	0.89	$Au^{I/III}$	1.54	$Ru^{III/IV}$	1.80
14	$Ru^{II/III}$	0.75	$Au^{I/III}$	-	$Ru^{III/IV}$	1.76
$CpRu(PPh_3)(Cl)(\eta^1\text{-dppm})$ (**6**)	$Ru^{II/III}$	0.72				
$CpRu(PPh_3)_2Cl$	$Ru^{II/III}$	0.87				

[a] All potentials obtained in 0.7 M TBAT / DCE and reported vs NHE. Adapted from reference 101.

The electrooxidation of methanol was performed with complexes **8** - **14** at 1.7 V in 0.7 M TBAT / DCE, forming DMM and MF (Table 2-2) as the only oxidation products. By expanding the Ru/M series of complexes, it is apparent that the Ru/Au complexes are less active during this reaction, than the Ru/Pd and Ru/Pt complexes (Table 2-2). In fact the current efficiency of the Ru/Au complexes are more comparable to the Ru model compound $CpRu(PPh_3)_2Cl$ than to the Ru/Pt and Ru/Pd complexes.

Role of the Non-Ru Metal Center

From the current efficiencies in Table 2-2 it is evident that the non-Ru metal center is critical to the improved catalytic ability exhibited by the heterobimetallic complexes. Possible roles of the non-Ru metal include:

- Oxidant
- Activation of the Ru metal center
- Methanol binding site

Table 2-2. Bulk electrolysis data for the oxidation of methanol by **8 - 14**

Complex[a]	Current Efficiency (%)	Product Ratio (DMM / MF)
3[b]	18.6	1.20
8	43	0.98
9	39	1.26
10	32	3.02
4[b]	24.6	0.87
11	42	0.91
12	23	2.94
5[b]	25.4	0.46
13	16	2.10
14	12	2.32
$CpRu(PPh_3)_2Cl$	12	2.87
$CpRu(\eta^2\text{-dppm})Cl$	3.2	∞

[a] Electrolyses performed at 1.7 V vs NHE. Product ratio and current efficiencies after 130 C of charge passed. Adapted from reference 92. [b] Adapted from reference 101.

The oxidation of alcohols by Pt,[102] Pd[103-106] and Au[107] complexes have literature precedent and are still being actively investigated. Recent examples of these transformations with molecular oxygen as the co-oxidant are shown in Schemes 2-1 and 2-2.

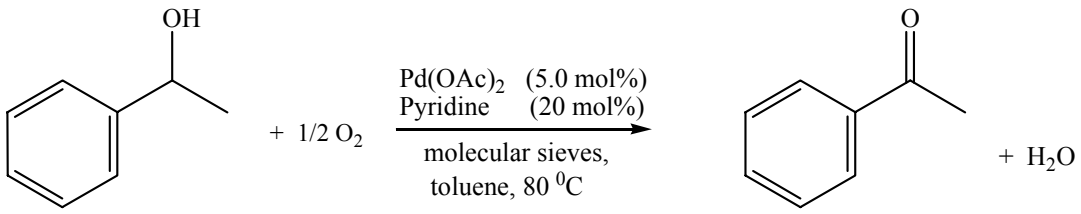

Scheme 2-1. Adapted from reference 105

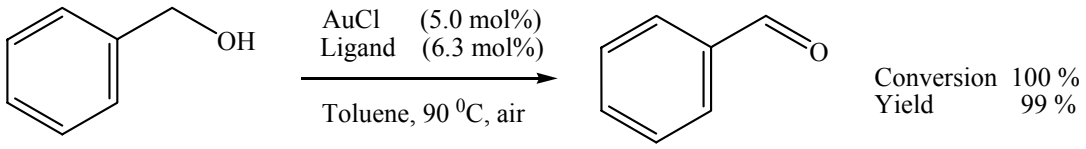

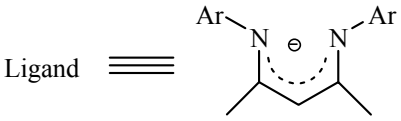

Scheme 2-2. Adapted from reference 107.

The Pt, Pd or Au center could also activate the Ru by mediating the electron density around it. The mediation of the Ru(II/III) couple of complexes **8** – **12** (Table 2-1) is an example of this. The bridging halide of complexes **8** – **12** facilitates the electronic interaction between Ru and Pt or Pd. As a result of this interaction the Ru metal center of complexes **8** – **12** will be more electrophilic than complex **6**. The increased electrophilicity (Lewis acidity) of Ru would then favor the interaction / coordination with the nucleophilic methanol substrate.

The third possibility that exists is a site for methanol binding. In this role the Pt, Pd or Au metal center would bind and activate the methanol before oxidation is performed

by the Ru metal center. A similar bifunctional mechanism[44-46] was proposed for the oxidation of methanol by PtRu binary anodes in DMFCs.

The second and third roles are closely related and could possibly be performed by a Lewis acid metal center. To investigate the role of the second metal a Ru/Hg complex similar to the Ru/Pt and Ru/Pd complexes (Figure 2-1) was synthesized. Mercury was selected because it is of moderate Lewis acidity and non-redox active within the potential window used.

Lewis Acid Catalysts

Lewis defined an acid in 1923 as an electron pair acceptor while a Lewis base is an electron pair donor. The term "Lewis acid" is now used to differentiate this interaction from the Brønsted-Lowry acid (proton donor). Lewis acid catalyzed reactions have a rich history in organic synthesis and continue to be extensively studied (Figure 2-2).

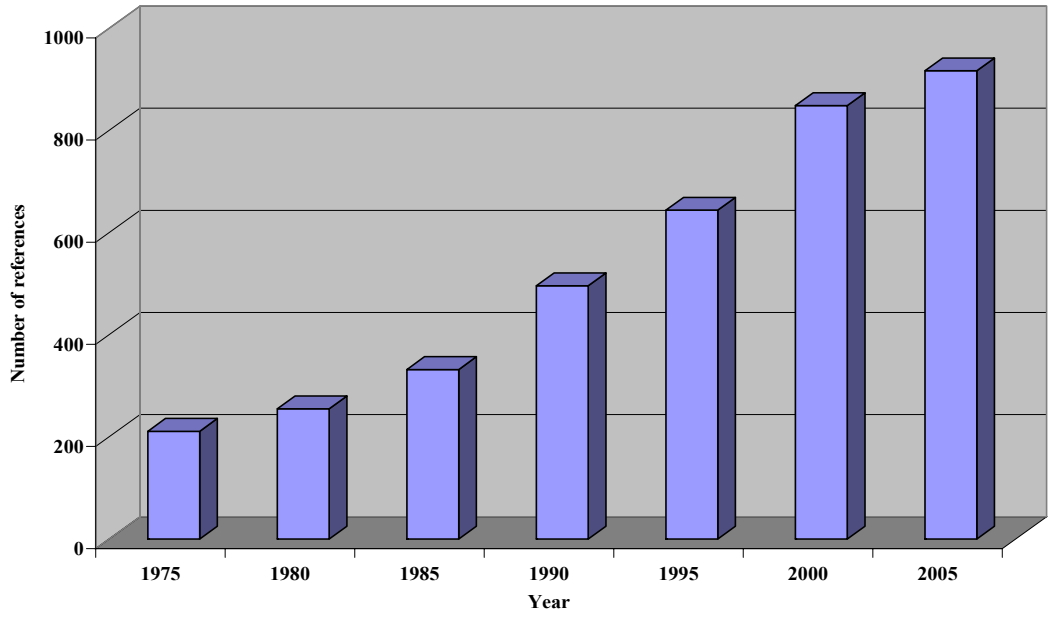

Figure 2-2. References to "Lewis acid" in the scientific literature (SciFinder Scholar).

Carbon-carbon bond formation via the Friedel-Crafts reaction (Eq. 2.1), Mukaiyama aldol synthesis, the Diels-Alder and ene reactions are classic organic reactions catalyzed by conventional Lewis acids such as $AlCl_3$, $SnCl_4$ or $TiCl_4$.[108] These simple Lewis acids, although very moisture sensitive, are capable of catalyzing a large number of reactions but with limited stereo-, regio- and chemo- selectivity.

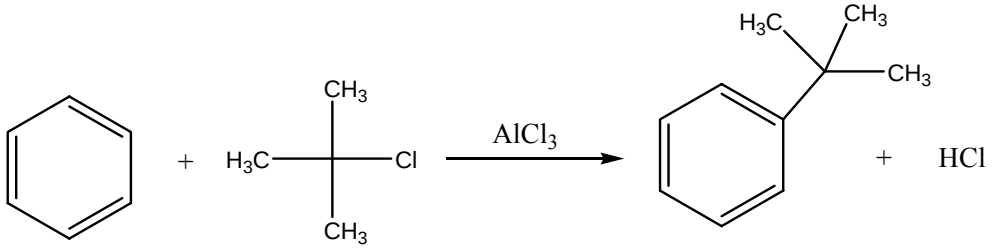

(2.1)

In this modern age of organic synthesis, selectivity is as important a factor to the viability of a catalyst, as is its reactivity. Due to continuing research in the field of Lewis acid catalyzed reactions, two key goals have been met.

1 The number of metals widely used in Lewis acid reagents has grown significantly. Currently more than 28 metals are used in Lewis acid catalyzed reactions each with its own attributes. The expansion of the Lewis acid reagents has led to reactivity previously unavailable to conventional Lewis acids (Eq 2.2).[109]

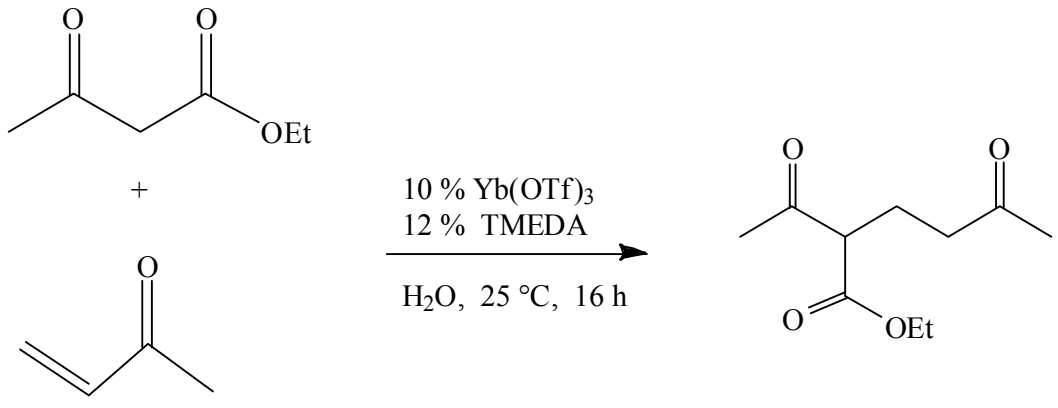

71 %

(2.2)

2 Design of novel ligands capable of stabilizing and promoting unique reactivity of Lewis acid metal centers. An example of this is the enantioselective Diels-Alder reaction (Eq. 2.3) reported by Kelly[110] in 1986. In this reaction the C2 symmetric ligand (a derivative of binaphthol) leads to one enantiomer being favored.

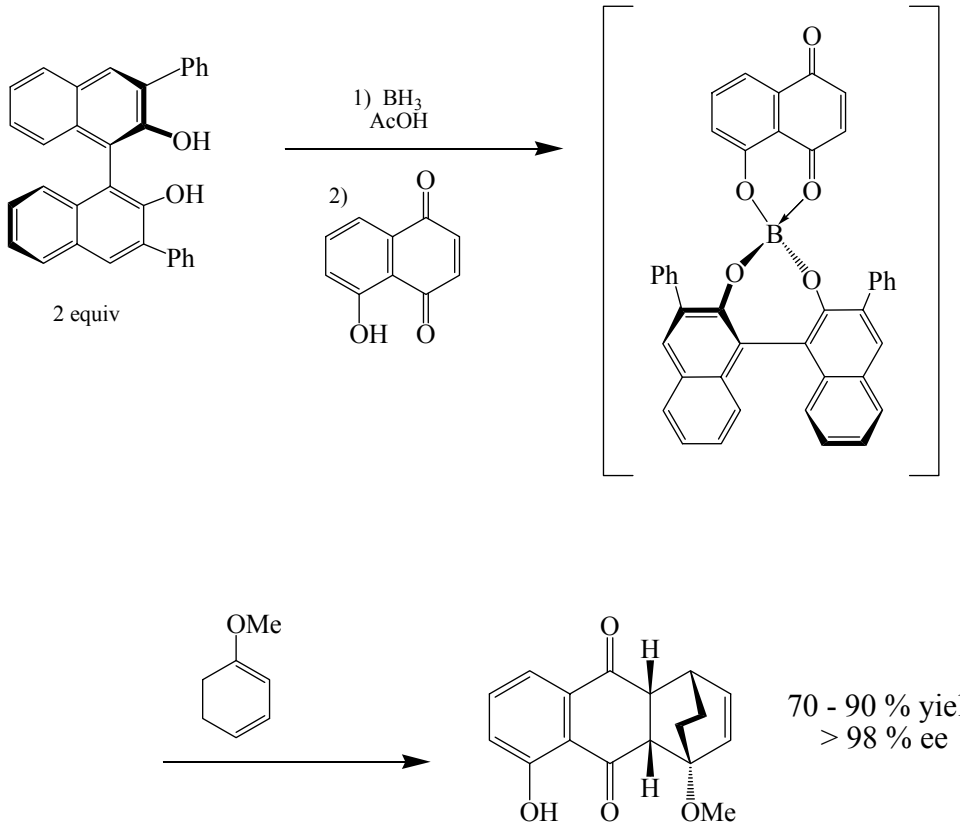

(2.3)

With the use of non-traditional Lewis acids and the design of some novel ligands, the limitations of conventional Lewis acids have been to a large part surmounted. It is now possible to do Lewis acid catalyzed reactions under less stringent conditions, with high stereo-, regio- and chemo- selectivity.

Classification of Lewis Acids

Even though a large number of metal reagents have been used as Lewis acids during catalytic organic transformations, most of these reagents are chosen only after experimental trial and error. Trial and error is necessary because scientists currently only

have a crude understanding of Lewis acidic character. There have been a few attempts at classifying Lewis acidic reagents. These classifications have been made using one of the following methods:

- Reactivity of a Lewis acid
- NMR data
- Theoretical calculations

In 1972 Olah arranged over 130 Lewis acids based on their activity during a Friedel-Crafts reaction (Scheme 2-3).[111] The Lewis acids were then placed in one of four categories: very active, moderately active, weak or very weak (Scheme 2-3) based on the amount of products formed during the benzylation and subsequent isomerization.

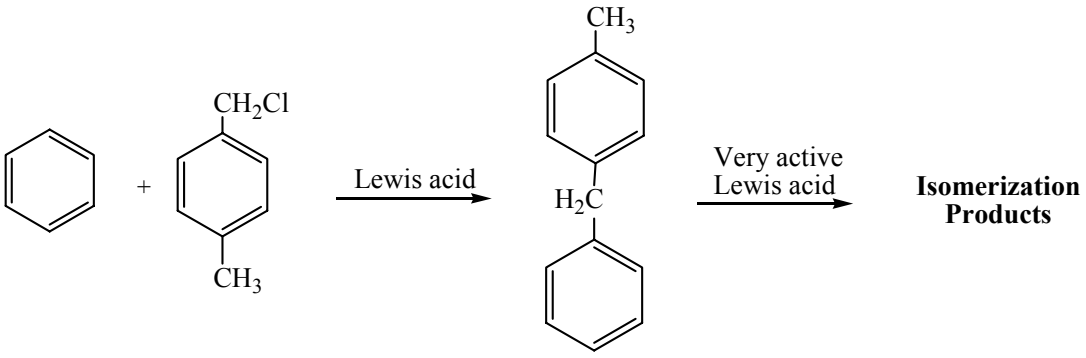

Lewis Acid Classification

Very active: High conversion, large amount of isomerization products = $AlCl_3$, $GaCl_3$, $NbCl_5$, $TaCl_5$

Moderately active: High conversion, very little isomerization = $InCl_3$, WCl_6, $ReCl_5$, $SbCl_5$

Weak: Low yield, no isomerization = $SnCl_4$, BBr_3, $TiCl_4$, $FeCl_2$, $PtCl_4$

Very weak: No Products = $SbCl_3$, $BeCl_2$, $CuCl_2$, $IrCl_3$, $HgCl_2$, $AuCl_3$

Scheme 2-3. Adapted from reference 111.

Kobayashi grouped Lewis acids based on the activity and selectivity during the addition reaction of a silyl enolate to an aldehyde and an aldimine (Scheme 2-4).[112] Based on the experimental results the Lewis acids were classified as: active, weak or inactive (Scheme 2-4).

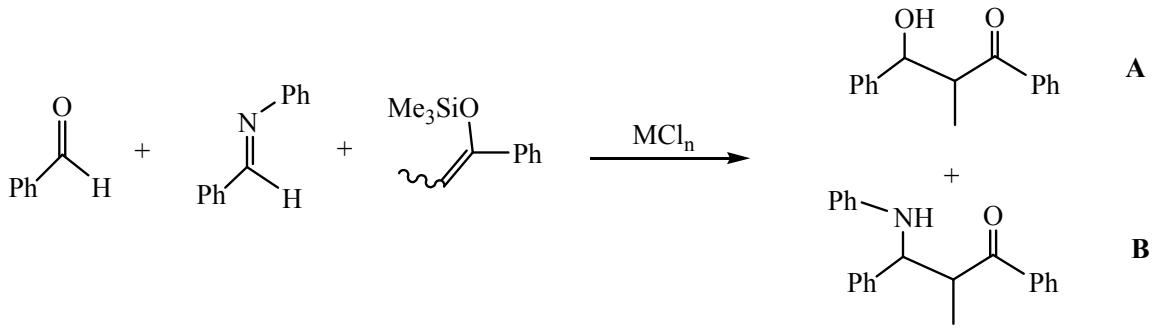

Lewis Acid Classification
Active: Yields greater than 40 % = $AlCl_3$, $GaCl_3$, $NbCl_5$, $TaCl_5$
Weak: Yields less than 40 % = $FeCl_2$, $PtCl_2$, $RuCl_3$, $SiCl_4$
Inactive: No Products = HgCl, $HgCl_2$,$PdCl_2$, AuCl

Scheme 2-4. Adapted from reference 112.

Lewis Acidic Properties of Mercury Complexes

In both classification schemes by Olah[111] and Kobayashi[112] the mercury halides HgCl and $HgCl_2$ are listed as inactive and therefore are very weak Lewis acids. As with most metal complexes, the Lewis acidity of mercury is greatly affected by the ligands coordinated to it. Experiments designed at tuning the Lewis acidity through ligand variation have been performed with mercury organometallic complexes.[113-116] The aim of these experiments is to investigate the mechanism by which polyfunctional Lewis acids activate carbonyl groups during organic reactions. It has been proposed that chelation of the carbonyl group by Lewis acids plays an important role in the enhanced catalytic activity. The Lewis acidity of mercury halides can be increased by coordinating with an electron withdrawing ligand (Scheme 2-5).[113] Complex **15** exhibits strong Lewis acidic character readily forming an adduct with acetone. The bidentate coordination was confirmed with a crystal structure of the solvent adduct.

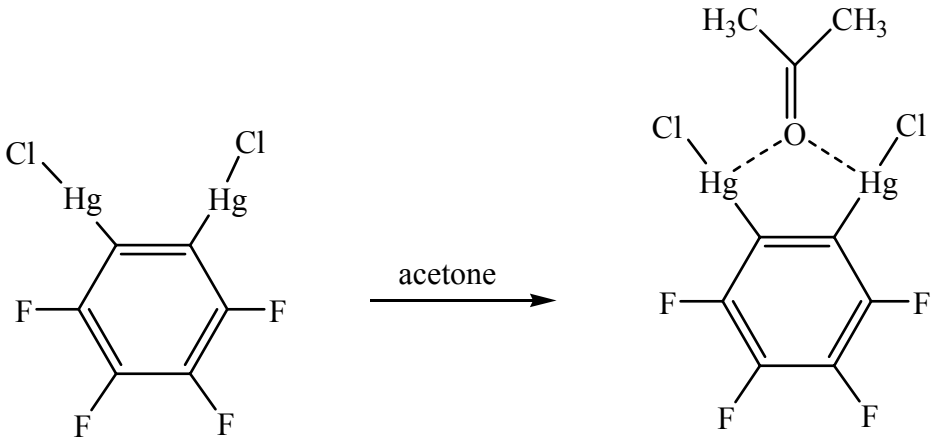

15

Scheme 2-5.

The Lewis acidity of the Hg metal center can be increased even more by expanding the fluorinated backbone. This strategy led to the isolation of the trimeric perfluoro-*ortho*-phenylene mercury complex (Figure 2-3).[115] This complex has a strong affinity for aromatic compounds and has formed isolable 1:1 adducts with biphenyl, naphthalene, pyrene and triphenylene. The π stacking of trimeric perfluoro-*ortho*-phenylene mercury and aromatic hydrocarbons result in phosphorescence being observed for the aromatic substrate. It is thought that the phosphorescence is due to a heavy atom effect of mercury promoting intersystem spin crossing from the S_1 to the T_1 state.[115]

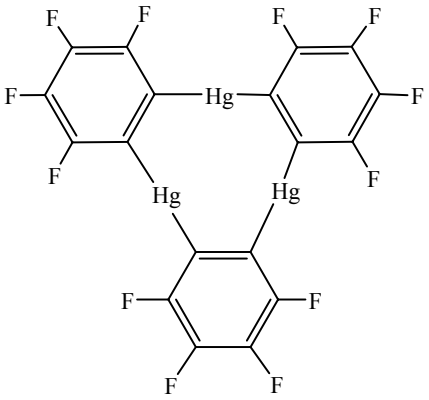

Figure 2-3. Structure of trimeric perfluoro-*ortho*-phenylene mercury

Chemistry of Mercury

Organometallic chemistry effectively started in 1849 when Frankland observed that metallic zinc reacts with methyl iodide. Frankland later extended this reaction to other metals and prepared several new organometallic compounds, one of which was methylmercuric iodide. During characterization of methylmercuric iodide he recorded the nauseous taste, totally unaware of its extraordinary toxicity. Mercury compounds are extremely toxic and exposure can occur through inhalation, ingestion or dermal absorption. The amount of mercury absorbed by the body is dependent upon the chemical form. Only 0.01 % of elemental mercury is absorbed when ingested but methyl mercury is almost totally absorbed. In the human body mercury accumulates in the liver, kidney, blood and brain. Due to decreased handling of mercury acute health effects such as cardiovascular collapse or kidney failure (both of which are fatal) are not as common today. Chronic health effects include central nervous system effects, kidney damage and birth defects. Genetic damage is also suspected. Due to the high toxicity of mercury it cannot be overstated how important it is to follow proper lab procedures when handling any material containing this element.

Mercury Catalyzed Reactions

There are limited examples in the literature for mercury catalyzed reactions. A recent example of this includes the reaction between alkynes and phosphonic acid monoesters (Eq. 2.4) to yield vinyl phosphonates.[117]

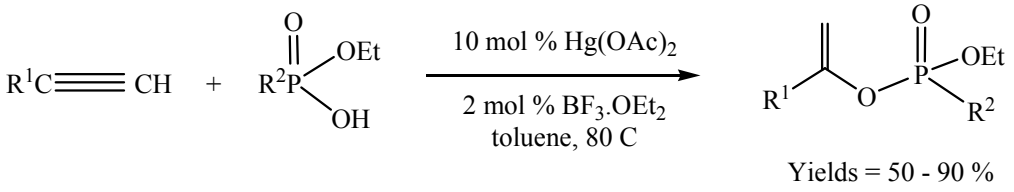

Yields = 50 - 90 % (2.4)

Mercury acetate is essential to the reaction, forming the corresponding Markovnikov adducts in moderate to good yields with high regioselectivity. Little to no vinyl phosphonates were formed when other addition catalysts such as $RuCl_3$, $PdCl_2(PPh_3)_2$ and $Pd(PPh_3)_4$ were used.

Another Hg(II) catalyzed reaction is the homogeneous oxidation of methane to methanol (Eq. 2.5 – 2.8).[118] This transformation is extremely selective (85 %) with high yields (43 %) in the presence of Hg(II) ions.

$$CH_4 + 2\,H_2SO_4 \xrightarrow{HgSO_4} CH_3OSO_3H + 2\,H_2O + SO_2 \quad (2.5)$$

$$CH_3OSO_3H + H_2O \longrightarrow CH_3OH + H_2SO_4 \quad (2.6)$$

$$SO_2 + 1/_2\,O_2 + H_2O \longrightarrow H_2SO_4 \quad (2.7)$$

$$CH_4 + 1/_2\,O_2 \longrightarrow CH_3OH \quad (2.8)$$

Synthesis and Characterization of $CpRu(PPh_3)(\mu\text{-}Cl)(\mu\text{-}dppm)HgCl_2$

Attempted Synthesis of $CpRu(PPh_3)(\mu\text{-}Cl)(\mu\text{-}dppm)HgCl_2$ (16)

Initial attempts at preparing **16** involved reacting $CpRu(PPh_3)Cl(\eta^1\text{-}dppm)$ with $HgCl_2$. A similar method was used during the synthesis of complexes **3** – **5** (Scheme 1-12) and for the preparation of $(CO)_3Ru(\mu\text{-}Ph_2PCH_2NC_4H_8O)_2HgI_2$ (Eq. 2.9).[119] Instead of the desired dppm bridged complex the reaction between $CpRu(PPh_3)Cl(\eta^1\text{-}dppm)$ (**6**) and $HgCl_2$ led to the formation of $[CpRu(PPh_3)(\eta^2\text{-}dppm)]^+$ (**17**) (Eq 2.10) as confirmed by $^{31}P\{^1H\}$ NMR (Table 2-3). The phosphorus NMR of **17** displayed a triplet at 50.2 ppm for the Ru bound PPh_3 and a doublet at 2.2 ppm for the chelated dppm. $ZnCl_2$ and $CdCl_2$ also reacted in a similar manner and an unrefined X-ray crystal structure of the resulting Zn complex can be seen in Figure 2-4.

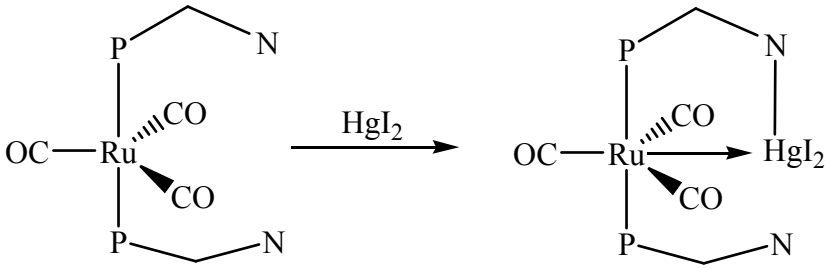

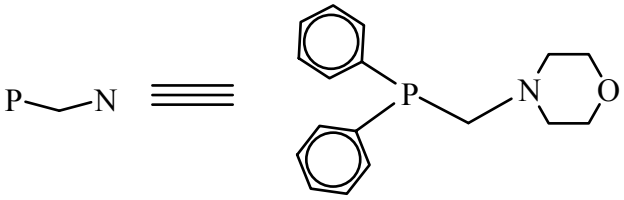

(2.9)

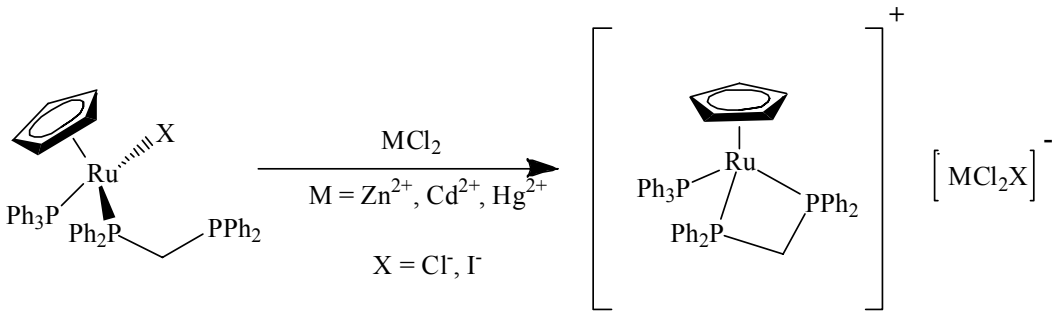

(2.10)

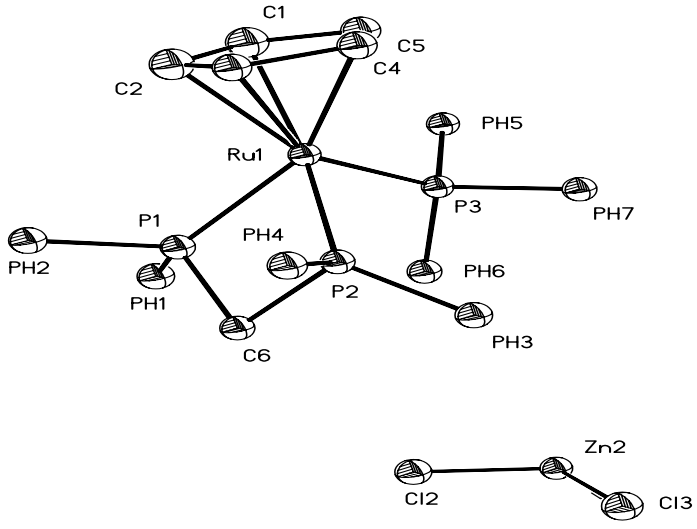

Figure 2-4. Unrefined crystal structure of $[CpRu(PPh_3)(\eta^2\text{-dppm})]^+ [ZnCl_3]^-$ (**17**).

Synthesis of CpRu(PPh$_3$)(μ-Cl)(μ-dppm)HgCl$_2$ (16)

An alternative route to **16** was found by first reacting CpRu(PPh$_3$)Cl(η^1-dppm) (**6**) with Hg(OAc)$_2$ followed by acetyl chloride (Eq. 2.11). CpRu(PPh$_3$)(μ-Cl)(μ-dppm)HgCl$_2$ is a yellow air and moisture stable solid. Solutions of **16** are also very stable when stored in an inert atmosphere; they however decompose upon prolonged exposed to air. The $^{31}P\{^1H\}$ NMR spectrum of complex **16** displays the expected resonances (Table 2-3). The Ru bound phosphorus signals appear as a doublet for PPh$_3$ at 40.0 ppm (J_{PP} = 41 Hz) and a doublet of doublets for dppm at 35.1 ppm (J_{PP} = 41 Hz and 11 Hz). The Hg bound phosphorus appears as a doublet at 29.7 ppm (J_{PP} = 11 Hz).

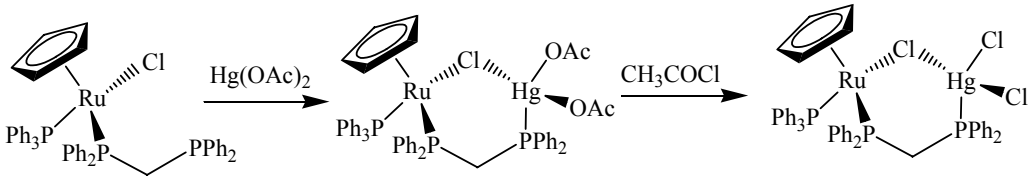

6 **18** **16** (2.11)

Synthesis of CpRu(PPh$_3$)(μ-Cl)(μ-dppm)Hg(OAc)$_2$ (18)

The Hg acetate intermediate CpRu(PPh$_3$)(μ-Cl)(μ-dppm)Hg(OAc)$_2$ (**18**) that is formed during the synthesis of **16** (Eq. 2.11), can be isolated cleanly and in high yields if acetyl chloride is not added to the reaction mixture. The stability of complex **18** is very similar to **16**, and it is isolated as an air and moisture stable yellow solid with moderate stability in solution. Complex **18** displays the expected $^{31}P\{^1H\}$ NMR spectrum, which is analogous to that of compound **16** (Table 2-3). The Ru bound phosphorus signals are shifted downfield relative to the analogous signals in **16**, appearing as a doublet for PPh$_3$ at 41.9 ppm (J_{PP} = 43 Hz) and a doublet of doublets for dppm at 36.9 ppm (J_{PP} = 43 Hz

and 28 Hz). The Hg bound phosphorus signal is shifted upfield relative to **16**, appearing as a doublet at 24.1 ppm (J_{PP} = 28 Hz).

Table 2-3. Selected NMR data for complexes **16 - 18**

Complex	Ru-PPh_3	Ru-dppm	Hg-dppm
16	39.9 (d, J_{PP} = 40 Hz)	35.0 (dd, J_{PP} = 40, 10 Hz)	30.1 (d, J_{PP} = 10 Hz)
17	48.0 (t, J_{PP} = 35 Hz)	1.9 (d, J_{PP} = 35 Hz)	
18	41.9 (d, J_{PP} = 43 Hz)	36.9 (dd, J_{PP} = 43, 28 Hz)	24.1 (d, J_{PP} = 28 Hz)

Analysis of $CpRu(PPh_3)(\mu\text{-}Cl)(\mu\text{-}dppm)HgCl_2$ Structure

Selected bond lengths and angles for **16** are shown in Table 2-4; crystallographic data and structure refinement are provided in Table 2-5. In the solid state, the crystal structure of $CpRu(PPh_3)(\mu\text{-}Cl)(\mu\text{-}dppm)HgCl_2$ contains the complex and two disordered DCE solvent molecules with no unusual contacts between any of these species. Complex **16** (Figure 2-5) contains a bridging chloride and dppm moiety as do the structurally similar $CpRu(PPh_3)(\mu\text{-}Cl)(\mu\text{-}dppm)PtCl_2$ (**3**) and $CpRu(PPh_3)(\mu\text{-}Cl)(\mu\text{-}dppm)PdCl_2$ (**4**)**.** The metal centers and bridging ligands form a distorted six-membered ring consisting of Ru, Cl3, Hg, P1, C6 and P2.

The Cp ligand is bound to Ru in a η^5 mode resulting in the typical three legged piano stool conformation about the Ru center. The Ru-Cl bond length of 2.4577(8) Å in **16** is longer than distance of 2.4403(7) Å reported for the Ru-Cl bond in complex **4**. The Ru-Cl bond in **16** is comparable to that of complex **5**, [2.4598(11) Å] whose chloride is not bridging. The Hg metal center is four coordinate and forms bonds with three chlorides and a phosphorus atom to give the expected tetrahedral geometry. The Hg-Cl3 bond length of 2.7372(8) Å is shorter than the bridging chloride [2.763(9) Å] reported for the Hg dimer $[Hg_2(Cl)_2(\mu\text{-}Cl)(\mu\text{-}dppm)_2]^+$ in which the Hg centers are also bridged by two dppm ligands. The bridging chloride exerts a strong trans effect on the Hg-Cl1 bond

[2.4901(11) Å] making it much longer than the Hg-Cl2 bond [2.3993(9) Å]. The bond lengths of both terminal chlorides are shorter than the terminal Hg-Cl bonds reported for $Rh_2Cp_2(\mu\text{-}CO)(\mu\text{-}dppm)(\mu\text{-}HgCl_2)$ [2.534(3) Å and 2.581(3) Å] and within the typical range of four coordinate Hg species (2.28 – 2.68 Å).

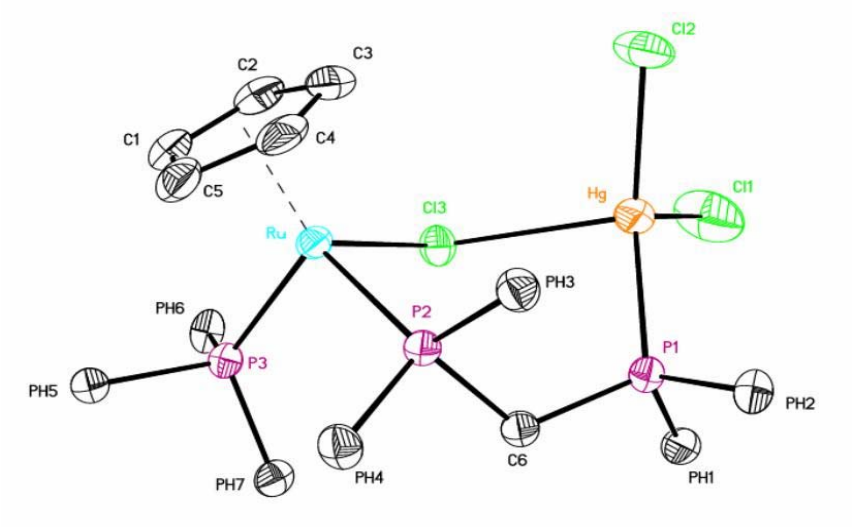

Figure 2-5. Thermal ellipsoids drawing of the molecular structure of $CpRu(PPh_3)(\mu\text{-}Cl)(\mu\text{-}dppm)HgCl_2$ (**16**). Thermal ellipsoids are plotted at 50 % probability. Phenyl rings and hydrogen atoms are omitted for clarity.

Table 2-4. Selected bond distances (Å) and angles (deg) for $CpRu(PPh_3)(\mu\text{-}Cl)(\mu\text{-}dppm)HgCl_2$ (**16**).

Bond Length (Å)		Bond Angle (deg)	
Hg-P1	2.4143(8)	P1-Hg-Cl3	90.44(2)
Hg-Cl1	2.4901(11)	P1-Hg-Cl1	111.24(4)
Hg-Cl2	2.3993(9)	Cl1-Hg-Cl3	102.94(4)
Hg-Cl3	2.7372(8)	Cl3-Hg-Cl2	104.67(3)
Ru-P2	2.3193(8)	Cl1-Hg-Cl2	102.66(5)
Ru-P3	2.3387(8)	Hg-Cl3-Ru	110.87(3)
Ru-Cl3	2.4577(8)	P2-Ru-Cl3	92.69(3)
Ru-C1	2.217(3)	P3-Ru-Cl3	88.32(3)
Ru-C2	2.230(3)	P1-C6-P2	117.71(16)
Ru-C3	2.232(3)		
Ru-C4	2.186(3)		
Ru-C5	2.178(3)		

Table 2-5. Crystal data and structure refinement for $CpRu(PPh_3)(\mu\text{-}Cl)(\mu\text{-}dppm)HgCl_2$ (**16**)

Formula	$C_{52}H_{50}Cl_7HgP_3Ru$	
Formula weight	1317.64	
Temperature	193(2) K	
Wavelength	0.71073 Å	
Crystal system	Monoclinic	
Space group	Cc	
Unit cell dimensions	a = 23.384(2) Å	α = 90°
	b = 11.5264(7) Å	β = 94.875(2)°
	c = 19.295(2) Å	γ = 90°
Volume ($Å^3$)	5182.2(6)	
Z	4	
Density (calcd) (Mg/m^3)	1.689	
Absorption coefficient (mm^{-1})	3.739	
F_{000}	2600	
Crystal size (mm^3)	0.27 x 0.23 x 0.20	
θ range (deg)	1.75 to 27.50	
Index ranges	-30≤h≤29, -14≤k≤14, -25≤l≤25	
Reflections collected	22341	
Independent reflections	11134[R(int) = 0.0160]	
Completeness to theta = 27.50°	99.1 %	
Absorption correction	Analytical	
Max. and min. transmission	0.5328 and 0.3680	
Refinement method	Full matrix least squares on F^2	
Data / restraints / parameters	11134 / 2 / 581	
Goodness-of-fit on F^2	1.023	
Final R indices [I >2sigma(I)]	[a]R1 = 0.0207	[b]wR2 = 0.0523 [10968]
R indices (all data)	[a]R1 = 0.0211	[b]wR2 = 0.526
Absolute structure parameter	-0.0063(17)	
Largest diff. peak and hole ($e.Å^3$)	0.893 and -0.607	

[a]$R1 = \Sigma(||Fo| - |Fc||) / \Sigma|Fo|$, [b]$wR2 = [\Sigma[w(Fo^2 - Fc^2)^2] / \Sigma w[Fo]^2]^{1/2}$, $S = [\Sigma[w(Fo^2 - Fc^2)^2] / (n-p)]^{1/2}$ $w = 1/[\sigma^2(Fo^2)+(0.027*p)^2+8.56*p]$, $p = [\max(Fo^2,0)+ 2* Fc^2]/3$

Cyclic Voltammetry

The first three ionization potentials for mercury are 10.43, 18.65 and 34.4 eV respectively. The large difference between the second and third ionization potentials is one reason why the formation of Hg(III) species is so difficult if not impossible to attain. There is only one report of a Hg(III) species, a short lived $[Hg(cyclam)]^{3+}$ which was electrochemically generated and observed in 1976.[120] Unfortunately, this experiment has

never been independently confirmed. Based on this and the absence of any oxidation waves for the model compound $HgCl_2(PPh_3)_2$ (0 – 2.0 V), it was assumed that Hg(II) is non-redox active within the potential window used for these studies.

During the CV studies of complex **16**, three irreversible redox waves at 0.70, 1.02 and 1.50 V were observed (Figure 2-6). Three oxidation waves were unexpected since the only redox active species in the solution is the Ru(II) metal center. During previous studies on complexes **3** – **14** (Table 1-1 and Table 2-1) only two Ru based redox processes, the Ru(II/III) and Ru(III/IV) oxidation waves were observed. Since Hg(II) is not redox active within the potential window used in these experiments there should only be two oxidation processes. With subsequent scans the first and third wave diminish in intensity, until only the second oxidation wave, now shifted to 1.14 V (Figure 2-6) was observed. Analysis of the resulting solution after the CV experiments confirmed that $CpRu(PPh_3)(\mu\text{-}Cl)(\mu\text{-}dppm)HgCl_2$ (**16**) had decomposed during the CV experiments. The decomposition of **16** resulted in the formation of $[CpRu(PPh_3)(\eta^2\text{-}dppm)]^+$ (**17**). A comparison of the CVs for $[CpRu(PPh_3)(\eta^2\text{-}dppm)]^+[PF_6]^-$ and **16** after decomposition allowed the assignment of the oxidation wave at 1.14 V (Figure 2-6) to the Ru(II/III) couple of $[CpRu(PPh_3)(\eta^2\text{-}dppm)]^+$. The first oxidation wave at 0.70 V is much lower than any observed for the halide bridged complexes **8** -**12** (Table 2-1). The oxidation wave at 0.70 V is instead closer to the Ru(II/III) couple of $CpRu(PPh_3)(Cl)(\eta^1\text{-}dppm)$ (**6**) and $CpRu(PPh_3)(Cl)(\mu\text{-}dppb)AuCl$ (**14**) (Table 2-1), complexes containing no halide bridge. The stability of **16**, in 0.7 M TBAT / DCE was monitored via $^{31}P\{^1H\}$ NMR. Complete decomposition to **17** occurred after only 5 hours, without the passage of any current. A similar result was observed at lower electrolyte concentration

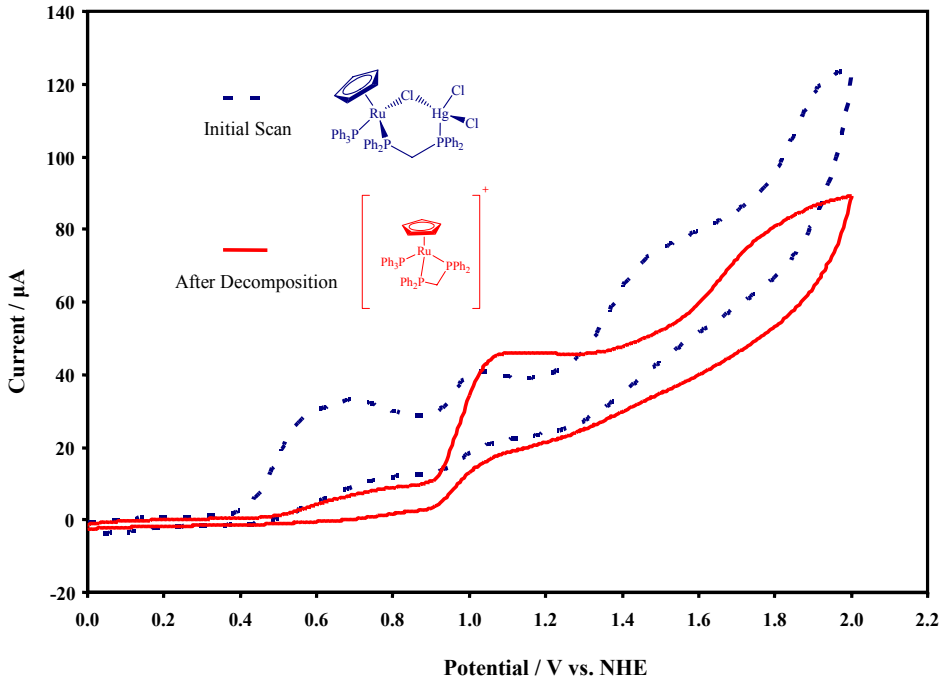

Figure 2-6. Cyclic voltammograms of **16** under nitrogen in 3.5 mL of DCE / 0.7 M TBAT; glassy carbon working electrode; Ag/Ag^+ reference electrode; 50 mV/s scan rate.

(0.1 M TBAT / DCE). The supporting electrolyte was also changed to the weakly coordinating electrolyte tetra-n-butylammonium tetrakis(pentafluorophenyl)borate. Changing the supporting electrolyte had no effect, and $CpRu(PPh_3)(\mu\text{-}Cl)(\mu\text{-}dppm)HgCl_2$ (**16**) still decomposed to $[CpRu(PPh_3)(\eta^2\text{-}dppm)]^+$ (**17**). These results indicate that the decomposition is not only due to the passage of current but also to the interaction of the supporting electrolyte with the complex.

Summary

A novel Ru/Hg complex $CpRu(PPh_3)(\mu\text{-}Cl)(\mu\text{-}dppm)HgCl_2$ (**16**) was synthesized and characterized. The metal centers are connected with a bridging chloride and dppm

ligands. This is the first reported Ru/Hg complex bridged in this manner. $CpRu(PPh_3)(\mu\text{-}Cl)(\mu\text{-}dppm)HgCl_2$ is unstable in solutions containing electrolyte, and rapidly decomposes to $[CpRu(PPh_3)(\eta^2\text{-}dppm)]^+$ (**17**) during cyclic voltammetry. Due to the instability of **16** during the CV experiments, the electrocatalytic properties of $CpRu(PPh_3)(\mu\text{-}Cl)(\mu\text{-}dppm)HgCl_2$ were not studied

CHAPTER 3
THE SELECTIVE PARTIAL ELECTROOXIDATION OF METHANOL TO DIMETHOXYMETHANE WITH RUTHENIUM/TIN HETEROBIMETALLIC COMPLEXES

Introduction

The cooperative interaction between Ru/Pt, Ru/Pd and Ru/Au complexes has been shown to improve the catalytic ability of the heterobimetallic complexes relative to the monometallic components.[92,121] As mentioned before one possible role of the non-Ru metal center could be as a Lewis acid. To continue the study of this interaction, a series of Ru/Sn complexes was synthesized and characterized.

Chemistry of Tin

As a group 14 element, tin has the ability to form stable and relatively strong bonds with most elements in the periodic table.[122] Except for the bonds formed to the heavier alkali and alkaline earth metals, most of the bonds formed to tin are covalent in character. The first and second ionization potentials for tin are similar to those of elements that readily form divalent cations (Table 3-1). Hence it is not surprising that tin is able to form stable Sn(II) compounds. The more stable oxidation state is Sn(IV), but the energy difference between it and Sn(II) is very small (Eq 3.1). Due to the stability of the two

$$Sn^{2+} \longrightarrow Sn^{4+} + 2\,e^- \quad E^o = 0.1364\ V \qquad (3.1)$$

oxidation states, there are extensive and varied chemistries for both states. Kinetically stable trivalent complexes have been isolated but generally Sn(III) is considered unstable and is thought to readily disproportionate.

Table 3-1. Selected ionization potentials

	Ionization Potential (eV)			
Element	1st	2nd	3rd	4th
C	11.260	24.383	47.887	64.492
Sn	7.344	14.632	30.502	40.734
Mg	7.464	15.035		
Ca	6.113	11.871		
Mn	7.435	15.640		
Fe	7.870	16.18		

Bonding in Heterobimetallic Tin (II) Complexes

Tin is known to form heterobimetallic complexes containing metal-metal bonds to transition metals, lanthanides, actinides and group 12 metals. In bonding to transition metals, stannylenes donate two of the available p electrons to the transition metal. Stannylenes can also act as Lewis acids, forming adducts with both hard and soft Lewis bases. These adducts are better Lewis bases than the stannylenes (eg. $SnCl_3^-$ is a better Lewis base than $SnCl_2$). There are empty low lying p and d orbitals on tin, which when hybridized are capable of accepting electron density from the transition metal. Due to these factors the bonds between tin and a transition metal contain both σ and π components.

Synthesis of Ruthenium / Tin (II) Complexes

There are several synthetic routes available for the preparation of M-Sn complexes, such as salt elimination, elimination of small molecules, oxidative addition, insertion of tin (II) and transmetalation. For the group VIII metals (Fe, Ru and Os), the synthesis is often accomplished via the following methods:

Salt elimination:[123] $Na_2Ru(CO)_4 + 2\ Ph_3SnCl \rightarrow (Ph_3Sn)_2Ru(CO)_4 + 2\ NaCl$ (3.2)

Oxidative addition:[124] $Fe(CO)_4(PPh_3) + SnCl_4 \rightarrow (SnCl_3)Fe(CO)_3(PPh_3)Cl + CO$ (3.3)

Insertion of $SnCl_2$:[125] $CpRu(PPh_3)_2Cl + SnCl_2 \rightarrow CpRu(PPh_3)_2(SnCl_3)$ (3.4)

Mechanistic information on the formation of M-Sn complexes is limited. The insertion of tin (II) halides however, has been the subject of much discussion. Though not proven conclusively, there is evidence for the mechanism in Scheme 3-1. It has been proposed that the tin (II) halide first coordinates to the halide ligand of the transition metal before rearranging intramolecularly to the three centered intermediate.

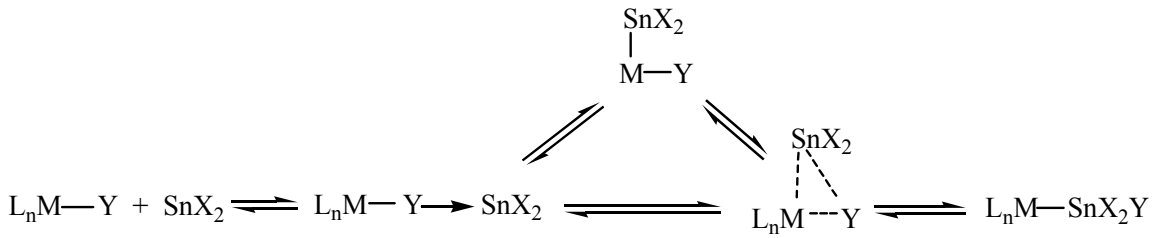

Scheme 3-1. Adapted from reference 126.

Evidence to support this mechanism includes the isolation of a bridging halide complex $Ir(\mu\text{-}Cl)(SnCl_2)(CO)(PPh_3)_2$.[127] The reaction between $CpRu[Ph_2PCH(CH_3)CH_2PPh_2]Cl$ and $SnCl_2$ (Scheme 3-2) also provides evidence for the intramolecular rearrangement, since the reaction proceeds with retention of configuration at Ru.[128] The diastereomers formed during the reaction are configurationally stable and therefore do not interconvert as a solid or in solution.

Heterobimetallic Tin (II) Catalysts

Stannylene complexes are often utilized as catalysts or co-catalysts due to the two following properties:

1. As a ligand, tin exerts a strong trans effect hence facilitating the establishment of a vacant coordination site on the transition metal.
2. Tin (II) compounds readily undergo oxidative addition and subsequent reductive elimination.

Heterobimetallic tin complexes have been used in hydrogenation,[126,129] dehydrogenation,[125,126,130-132] Friedel-Crafts alkylation,[133] polymerization[134,135] and

hydroformylation.[136-138] Of relevance to this dissertation is the thermal dehydrogenation of methanol by Ru/Sn heterobimetallic catalysts.

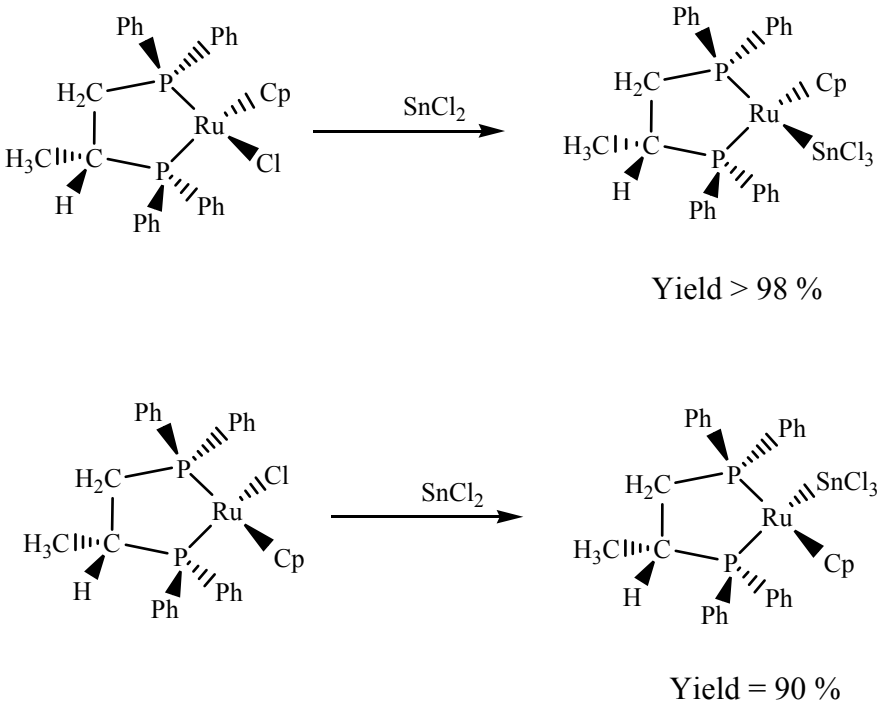

Scheme 3-2. Adapted from reference 128.

A series of Ru/Sn heterobimetallic complexes has been investigated as catalysts for the thermal dehydrogenation of methanol.[132] A comparison of $[RuCl_2\{P(OMe)_3\}_4]$, $[RuCl(SnCl_3)\{P(OMe)_3\}_4]$ and $[Ru(SnCl_3)_2\{P(OMe)_3\}_3]$ reveals that the $SnCl_3^-$ ligand is vital to the catalytic activity. $[Ru(SnCl_3)_2\{P(OMe)_3\}_3]$ is the only complex that catalyzed the conversion of methanol to acetic acid or methyl acetate (due to the esterification of acetic acid).[132]

The mechanism for the thermal dehydrogenation of methanol has been studied but is not yet fully understood.[125,130,132,139] Carbonylation was ruled out as a possible route to methyl acetate since isotopically labeled ^{13}CO was not incorporated into the product. The reaction path in Scheme 3-3 was then suggested based on previously observed

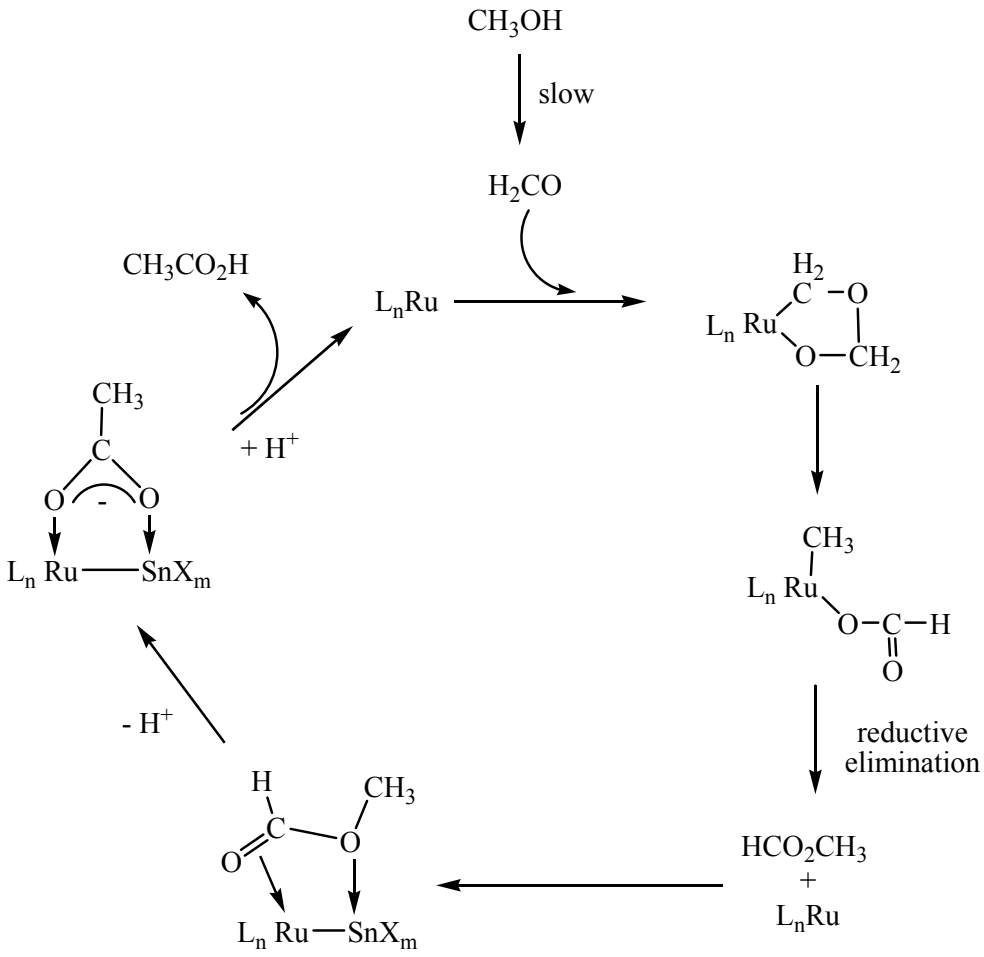

Scheme 3-3. Adapted from reference 139.

transformations. Dehydrogenation of methanol to formaldehyde is known to occur for Ru complexes.[140] It has also been reported that H_2CO can react with metals to give a methyl-formato complex which upon reductive elimination yields methyl formate.[141] It is then suggested by Shinoda that methyl formate (which is observed in the reaction mixture) is isomerized to acetic acid.[139] The isomerization is thought to go through a four center interaction (Scheme 3-3) which is favored by the soft and hard nature of Ru(II) and Sn(II) respectively. The methyl migration step is not evident, but would be stabilized

by the resulting acetate bridge. Other evidence to support methyl migration is that ethyl and isopropyl formates also react to form propionic and isobutyric acids (or their esters) respectively.[132]

The Ru/Sn complexes investigated as catalysts for the dehydrogenation of methanol include $CpRuP_2X$ where X = SnF_3, $SnCl_3$ and $SnBr_3$ and P_2 = PPh_3, PPh_2Me and dppe.[125] These catalysts were very selective during the dehydrogenation of methanol, forming only methyl acetate. For these catalysts Gusevskaya suggested that the Lewis acidic tin halide ligand rendered Ru more electrophilic. The increased electrophilicity of Ru will favor the β–hydride interaction and subsequent elimination (Eq 3.5) proposed as the rate determining step (Scheme 3-3).

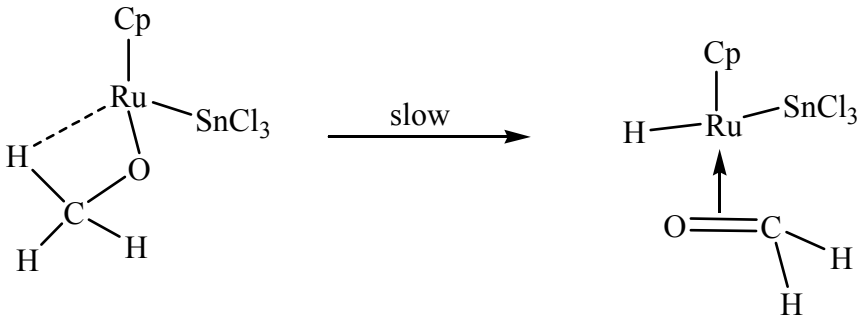

(3.5)

Methanol as a Chemical Feedstock

Due to the ease of transportation, storage and reactivity, methanol has been utilized as a chemical feedstock in several industrial processes. Examples of these include the carbonylation of methanol to acetic acid, a chemical reagent used in the production of polymers, aspirin and solvents. The Monsanto process,[142] commercialized in 1970, is based on the use of homogeneous Rh catalysts, while the Cativa process,[143] commercialized in 1996, uses Ir catalysts. Combined, both catalytic cycles account for approximately 80 % of the acetic acid produced worldwide.[143]

Another industrial example is the methanol to olefin or methanol to gasoline process patented in 1975 by Mobil. In this reaction methanol is converted to ethylene (Scheme 3-4) or propylene over solid acid catalysts. The light olefins can then be used to produce longer chain hydrocarbons. Because of increasing demands for light olefins as a chemical feedstock, this reaction continues to be an industrially interesting process.

$$n\ CH_3OH \xrightarrow{-\ n\ H_2O} (CH_2)_n \longrightarrow \text{gasoline}$$

Scheme 3-4. Adapted from reference 144.

The selective oxidation of methanol has also been of interest as a route to several important organic chemicals such as formaldehyde,[145] methyl formate[146] (MF) and dimethoxymethane[147-150] (DMM). Due to the low toxicity, good solvent power, amphiphilic nature, low viscosity, low surface tension and high evaporation rate DMM has many industrial applications. DMM is utilized as a solvent in the cosmetic, pharmaceutical and paint industries as well as a chain length regulator during the preparation of ion exchange resins. Another recent application of DMM is that of an additive to diesel fuel.

Current Environmental Protection Agency (EPA) regulations require a 95 % reduction in harmful emissions from diesel engines.[151] When fully implemented in 2010 it is estimated that 2.6 million tons of smog-causing nitrogen oxide (NO_x) emissions and 110,000 tons of particulate matter (PM) will be reduced each year. It is proposed that these reductions in smog and particulate matter will have a profound effect on our quality of life. An estimated 8,300 premature deaths, 5,500 cases of chronic bronchitis and 17,600 cases of acute bronchitis in children will also be prevented annually. It is also estimated that more than 360,000 asthma attacks and 386,000 cases of respiratory

symptoms in asthmatic children will be avoided every year. In addition, 1.5 million lost work days, 7,100 hospital visits and 2,400 emergency room visits for asthma will be prevented.[151]

NO_x species are generated from nitrogen and oxygen under the high pressure and temperature conditions in the engine. Diesel PM is a complex aggregate of solid and liquid material, the formation of which is not exactly understood. Currently pre- and post-combustion methods are being examined for reducing NO_x and PM emissions. One pre-combustion method uses reformulated diesel fuels containing oxygen rich additives such as certain alcohols, esters, glycol ethers and carbonates. DMM is one additive that has been investigated and shown to reduce PM and soot emission from diesel engines.

The commercial synthesis of DMM is performed using a two-step process involving oxidation of methanol to formaldehyde followed by the condensation of the methanol/formaldehyde mixtures to yield DMM. Due to increasing demands for DMM the direct conversion of methanol[147-150] to DMM has been recently investigated as a possible replacement for the two step process. Rhenium oxides[147,148] and heteropolyacids with Keggin structures[149,150] have been reported to catalyze the selective oxidation of methanol vapor to DMM, typically at temperatures above 400K. Among these catalysts, $SbRe_2O_6$[147,148] has the highest selectivity for DMM, converting 6.5 % of the methanol feed at 573K with a selectivity as high as 92.5 %.

Electrooxidation of methanol typically yields a complex mixture of products (Scheme 3-5), with the major product and selectivity dependent upon the reaction conditions.[153-156] Product distributions have been determined in conjunction with studies on direct methanol fuel cells,[22,30,153,155-160] using Pt black,[153,157,158] Pt/Ru[157,158] and

Pt/Nafion (Pt-SPE)[155,156,159] anodes. The general trend is that the absence of water and lower methanol concentrations favor formaldehyde formation, with yields of DMM rising as the concentration of methanol increases. The presence of water favors formation of MF and/or complete oxidation to CO_2.

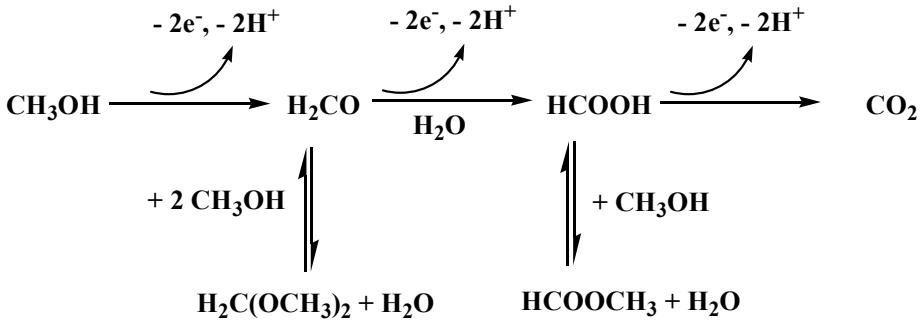

Scheme 3-5. Adapted from reference 152.

Electrochemical Synthesis of Organic Molecules

Electrochemistry is a powerful technique capable of performing versatile and unique organic transformations. During electrochemical reactions, organic substrates can be activated by adding (reducing) or removing (oxidizing) electrons. The result of this process is the generation of radical anions or cations. Since these electrons are generated from the electrode, there is no reagent waste. Because of this electroorganic synthesis is often considered environmentally friendly.

The advantages of this technique are:

- The selectivity of the reaction can be influenced by the applied potential
- Reaction rate is influenced by the current density
- Reaction conditions are typically very mild
- Environmentally friendly, no need for chemical oxidizing or reducing agents

Disadvantages associated with electroorganic synthesis include:

- Special reactors and equipment, fortunately most of these are now commercially available

- Electron transfer is a heterogeneous process, therefore electrodes with large surface area must be used so as to accelerate the reaction rate
- Recovery of supporting electrolyte is often difficult and can be expensive

The first notable application of electrochemistry to organic synthesis was reported in 1843 by Kolbe.[161] During this reaction carboxylic acids are decarboxylated to give an acyloxy radical intermediate that rapidly dimerizes to form a hydrocarbon. Yields for Kolbe type electrolysis typically range from 50 – 90 %, remarkably high for a reaction generating an alkyl radical. Since the work of Kolbe was published, research into electrochemical synthetic transformations has been extensively studied. As a result of these studies some interesting reactions have been developed. Selected examples are shown in Eq. 3.6 – 3.9.[162] It should be pointed out that the fluorination and reduction reactions (Eq 3.7 and 3.8) are unique to electrosynthesis.

Oxidation:

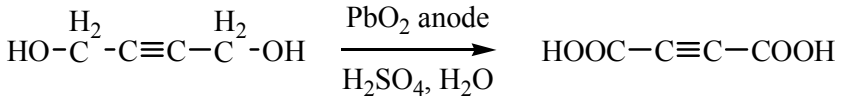

(3.6)

Fluorination:

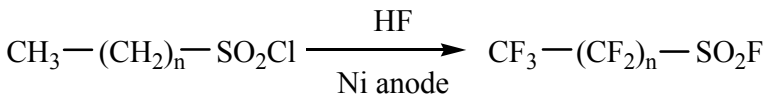

(3.7)

Reduction:

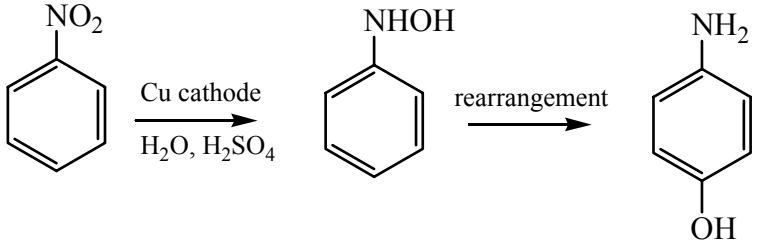

(3.8)

Hydrogenation:

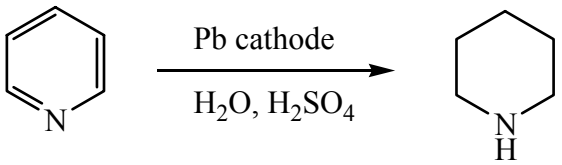

(3.9)

Electrosynthesis of organic compounds is not limited to only laboratory scale preparations, but is also widely used for industrial applications. One example is the reduction of acrylonitrile to adiponitrile (Eq. 3.10), a chemical feedstock used in the synthesis of nylon. The actual reaction is very complicated, involving parallel pathways and competing products. The major side reactions can be limited, to yield adiponitrile selectively (90 %).

$$2\ CH_2{=}CHCN\ +\ 2\ H_2O\ +\ 2\ e^- \longrightarrow NC(CH_2)_4CN\ +\ 2\ OH^- \qquad (3.10)$$

Table 3-2. TEMPO mediated electrooxidation of carbohydrates

Substrate[a]	Product	Yield (%)
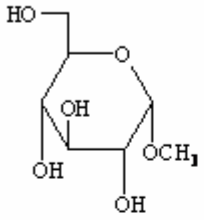	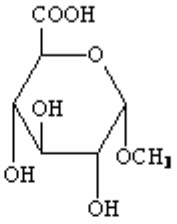	96
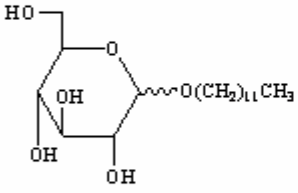	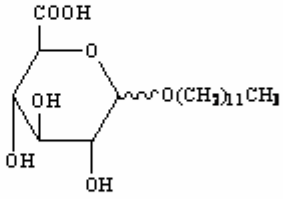	89
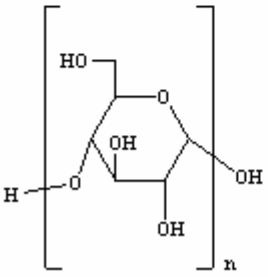	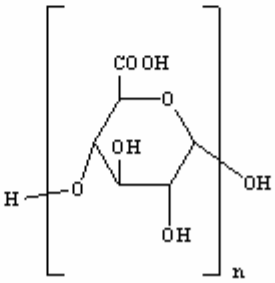	63

[a] Electrolyses performed at 0.53 V vs SCE. Adapted from reference 163.

Apart from the direct electrochemical processes described above indirect electrochemical transformations are also used during the synthesis of organic compounds. An example relevant to this dissertation is the selective oxidation of carbohydrates with 2,2,6,6-tetramethylpiperidin-1-oxyl (TEMPO) (Table 3-2).[163] Secondary hydroxyl groups are in most cases inert during the electrolysis. This selectivity allows the oxidation of carbohydrates to the corresponding carboxylic acids in moderate to excellent yields. The catalytically active species is the nitrosonium ion formed after the one-electron oxidation of TEMPO (Scheme 3-6). The mechanism proposed for the

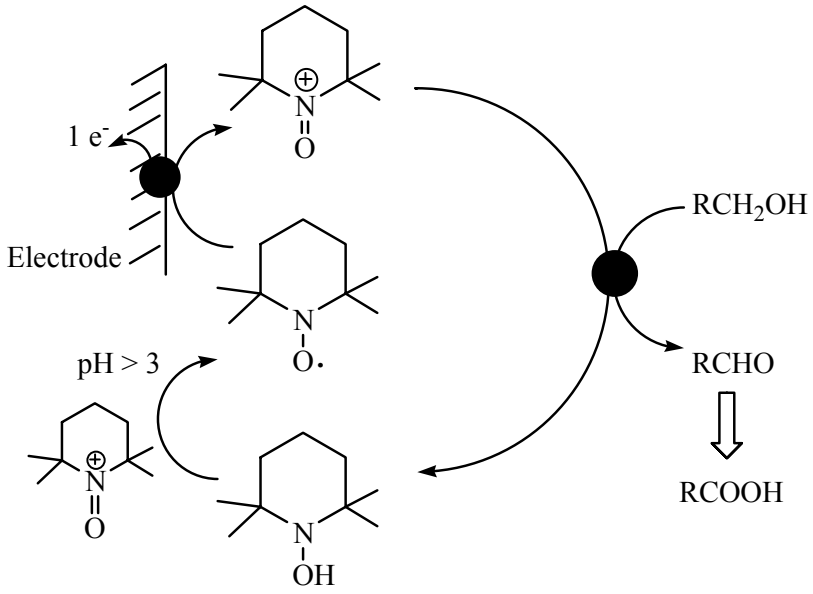

Scheme 3-6. Adapted from reference 163.

electrooxidation of carbohydrates, is the same mechanism proposed by de Nooy[164] for the oxidation of alcohols under basic conditions. The initial step is the coordination of the alkoxy to the nitroso group. After β-hydride elimination the corresponding aldehyde is formed, the hydrate of which can be further oxidized to the carboxylic acid.

The electrochemical oxidation of organic molecules with TEMPO is of interest for industrial applications because:

1. TEMPO and its derivatives are cheap and easily prepared
2. TEMPO is easily recovered in quantitative yields after oxidation of polysaccharides
3. As an oxidant TEMPO is very selective
4. Reaction work up is easily performed

In 2002 and 2003 the McElwee-White group reported that Ru/Pt, Ru/Pd and Ru/Au heterobimetallic complexes can act as catalysts during the electrochemical oxidation of methanol.[92,93,101] For these complexes the non-Ru metal center was shown to improve the catalytic properties as compared to the mononuclear model compounds $CpRu(\eta^2\text{-dppm})Cl$ and $CpRu(PPh_3)_2Cl$. Related beneficial effects of a Lewis acidic tin center in a thermal reaction had previously been reported for $CpRu(PPh_3)_2(SnCl_3)$ (**20**), which selectively oxidizes methanol to methyl acetate at elevated temperatures.[125,165]

In order to continue the study of Lewis acidic interactions during the electrochemical oxidation of methanol the catalytic properties of Ru/Sn complexes **19** – **26** (Figure 3-1) were studied. This chapter also describes the selective partial oxidation of methanol to dimethoxymethane using the Ru/Sn complexes $CpRu(PPh_3)_2(SnCl_3)$ (**20**), $(Ind)Ru(PPh_3)_2(SnCl_3)$ (**21**) and $CpRu(TPPMS)_2(SnCl_3)$ (**23**).

Synthesis

Synthesis of $CpRu(TPPMS)_2Cl$ (22)

The literature procedure for the synthesis of $CpRu(TPPMS)_2Cl$[166] yielded a complex reaction mixture in which unreacted triphenylphosphine monosulfonate (TPPMS) and TPPMS oxide were the only identifiable compounds. Samples of **22** were instead prepared by an alternate route involving substitution of PPh_3 in $CpRu(PPh_3)_2Cl$

(**19**) with TPPMS (Eq 3.11). The reaction of TPPMS with a slight excess of $CpRu(PPh_3)_2Cl$ was performed in refluxing toluene. Complex **22** was isolated in excellent yields (90 %) as an orange, moderately air stable solid. The $^{31}P\{^1H\}$ NMR spectrum of $CpRu(TPPMS)_2Cl$ is very similar to that of $CpRu(PPh_3)_2Cl$, consisting of a singlet at 40 ppm.

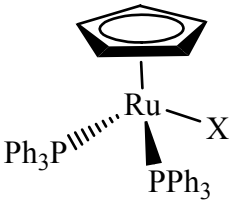

(19) X = Cl

(20) X = $SnCl_3$

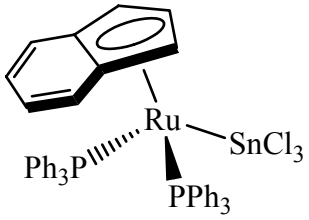

(21)

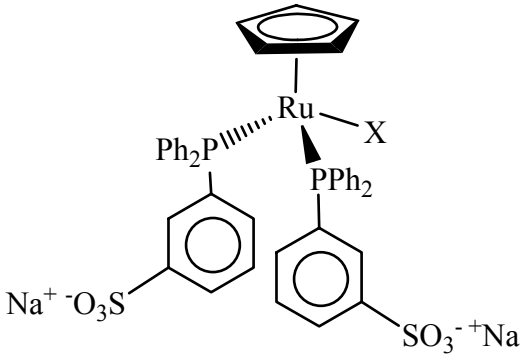

(22) X = Cl

(23) X = $SnCl_3$

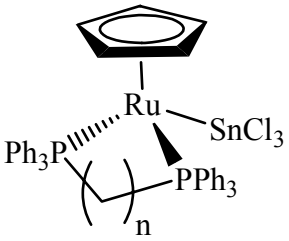

(24) n = 1, dppm

(25) n = 2, dppe

(26) n = 3, dppp

Figure 3-1. Structure of compounds **19 - 26**

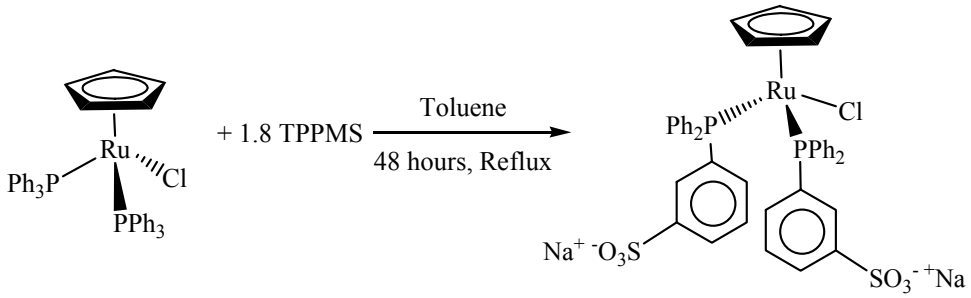

19 **22** (3.11)

Synthesis of CpRu(TPPMS)$_2$(SnCl$_3$) (23)

The Ru/Sn complex CpRu(TPPMS)$_2$(SnCl$_3$) was prepared in an analogous manner to CpRu(PPh$_3$)$_2$(SnCl$_3$)[125] by reacting **22** with a slight excess of SnCl$_2$ (Eq. 3.12) in ethanol. The insertion of Sn into the Ru-Cl bond is facile and the reaction is complete after one hour. The resulting bright yellow solid is moderately stable in air and in solutions of methanol and acetonitrile, but decomposes rapidly when dissolved in water. As expected from the NMR spectrum of CpRu(PPh$_3$)$_2$(SnCl$_3$),[125] the $^{31}P\{^1H\}$ NMR spectrum of CpRu(TPPMS)$_2$(SnCl$_3$) consists of a singlet at 46 ppm with $^2J_{P\text{-}Sn}$ = 422 Hz.

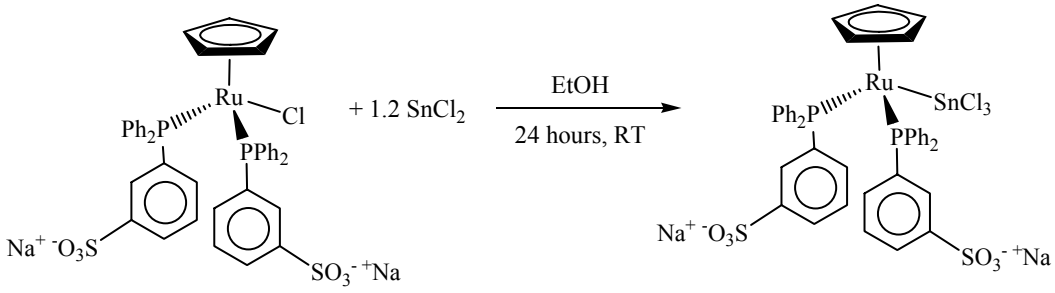

22 **23** (3.12)

Before the synthesis of CpRu(TPPMS)$_2$Cl (**22**) and CpRu(TPPMS)$_2$(SnCl$_3$) (**23**) all electrochemical experiments in the McElwee-White lab were performed in the

chlorinated solvents CH_2Cl_2 or DCE. CH_2Cl_2 or DCE had to be used because of the organic nature of the ligands used in complexes **3** – **5** and **8** – **14**. These solvents have a low dielectric constant, and therefore a high ohmic resistance. Because of the resistance, a high concentration of supporting electrolyte has to be used in order to get a reasonable conductivity and electron transfer rate. In order to improve the electron transfer properties of the reactions being studied there has been a concerted effort to use more polar solvents such as methanol and water. As a result of this $CpRu(TPPMS)_2Cl$ (**22**) and $CpRu(TPPMS)_2(SnCl_3)$ (**23**) have been synthesized. Another reason for performing the electrochemical studies in water is to be able to compare these catalysts to the widely studied $[(trpy)(bpy)Ru^{II}(OH_2)]^{2+}$. As mentioned before the aquo ligand plays a crucial role in the catalytic cycle of $[(trpy)(bpy)Ru^{II}(OH_2)]^{2+}$, being deprotonated (Eq. 1.19 and 1.20) to form the catalytically active oxidant $[(trpy)(bpy)Ru^{IV}(O)]^{2+}$.

Synthesis of $CpRu(\eta^2\text{-dppm})(SnCl_3)$ (24)

Complex **24** was prepared in an analogous manner to $CpRu(\eta^2\text{-dppe})(SnCl_3)$ in high yields (85 %), by reacting $CpRu(\eta^2\text{-dppm})Cl$ with $SnCl_2$ (Eq. 3.13). The $^{31}P\{^1H\}$ NMR spectrum consists of a singlet at 8.3 ppm with tin satellites ($^2J_{P\text{-}Sn}$ = 385 Hz). This singlet is shifted upfield by approximately 6 ppm relative to $CpRu(\eta^2\text{-dppm})Cl$. The ^1H NMR spectrum exhibits a shift downfield for the methylene and cyclopentadienyl protons of approximately 0.3 ppm.

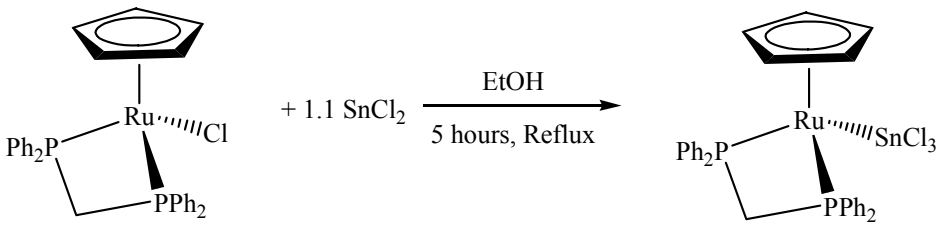

24 (3.13)

Synthesis of CpRu(η^2-dppp)($SnCl_3$) (26)

CpRu(η^2-dppp)($SnCl_3$) (**26**) was prepared in an analogous manner to CpRu(η^2-dppe)($SnCl_3$) in high yields (85 %), by reacting CpRu(η^2-dppm)Cl with $SnCl_2$ (Eq. 3.14). The $^{31}P\{^1H\}$ NMR spectrum consists of a singlet at 33.9 ppm, shifted upfield by approximately 5 ppm relative to CpRu(η^2-dppp)Cl. Complex **26** has a low solubility in the NMR solvents used; because of this no tin satellites were observed. The ^1H NMR spectrum exhibits a shift downfield of approximately 0.4 ppm for the cyclopentadienyl protons. A similar shift downfield was observed for CpRu(η^2-dppm)($SnCl_3$) (**24**).

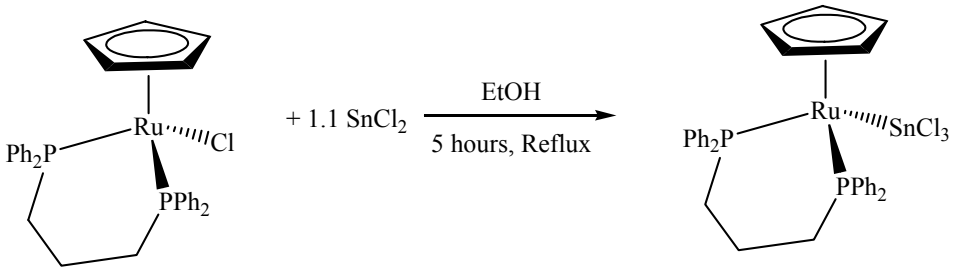

26 (3.14)

The Ru/Sn complexes CpRu(PPh_3)$_2$($SnCl_3$) (**20**), (Ind)Ru(PPh_3)$_2$($SnCl_3$) (**21**) and CpRu(TPPMS)$_2$($SnCl_3$) (**23**) are coordinatively saturated. Before the methanol oxidation reaction can occur, there has to be ligand dissociation and methanol coordination. Phosphine dissociation has been invoked in numerous mechanisms, and it is this reason why phosphine ligands are often used in metal catalysts. Gusevskaya proposed that phosphine dissociation is a key step during the thermal dehydrogenation of methanol with CpRu(PPh_3)$_2$($SnCl_3$) (**20**). To probe if a vacant coordination site on Ru is needed, a series of Ru/Sn complexes containing the bidentate phosphines dppm, dppe and dppp was synthesized. If phosphine dissociation occurs during the catalysis the chelate effect of the

bidentate phosphines should result in a decrease in the reaction rate of **24** – **26** relative to **20**.

NMR Data

^{1}H and $^{31}P\{^{1}H\}$ NMR spectroscopies were utilized to determine the ligand arrangement about the Ru center. Selected NMR data are presented in Table 3-3. Only one singlet is observed in the $^{31}P\{^{1}H\}$ NMR spectra of these complexes suggesting that the phosphine ligands are in similar chemical environments. The proton NMR spectra of the complexes exhibit characteristic peaks for the phenyl, indenyl and cyclopentadienyl groups.

The electron density at the Ru metal center can be varied by changing the peripheral ligands. The chemical shifts of the cyclopentadienyl protons were predictable based on the Lewis acidity of the additional ligands. When the Lewis acidity of the ligands is increased, the Ru metal center will become electron poor and the Cp protons will become deshielded. By being deshielded the Cp protons now experience more of the applied magnetic field and shift to a higher frequency. Hence for $CpRu(PPh_3)_2(X)$ the Cp resonance of X = $SnCl_3$ (4.54 ppm) > Cl (4.10 ppm)

Table 3-3. Selected NMR data for complexes **19** – **26**

Complex[a]	Solvent	Cp ^{1}H NMR (ppm)	$^{31}P\{^{1}H\}$ NMR (ppm)	$^{2}J_{P,Sn}$ (Hz)
$CpRu(PPh_3)_2Cl$ (**19**)	$CDCl_3$	4.10	39.9	
$CpRu(PPh_3)_2(SnCl_3)$ (**20**)	$CDCl_3$	4.54	45.2	435
$(Ind)Ru(PPh_3)_2(SnCl_3)$ (**21**)	$CDCl_3$		48.8	363
$CpRu(TPPMS)_2Cl$ (**22**)	DMSO-d_6	4.07	40.1	
$CpRu(TPPMS)_2(SnCl_3)$ (**23**)	CD_3OD	4.65	46.0	422
$CpRu(\eta^2\text{-dppm})(SnCl_3)$ (**24**)	$CDCl_3$	5.08	8.3	385
$CpRu(\eta^2\text{-dppe})(SnCl_3)$ (**25**)	$CDCl_3$	4.89	77.5	397
$CpRu(\eta^2\text{-dppp})(SnCl_3)$ (**26**)[b]	$CDCl_3$	4.84	33.9	

[a] All NMR data obtained at room temperature. [b)] Low solubility no $^{2}J_{P\text{-}Sn}$ satellites observed.

Cyclic Voltammetry

Since Sn(II) is not redox active within the solvent window of these experiments, it is assumed that any observed redox processes would be due to oxidation of the Ru metal center. Cyclic voltammograms of complexes **19 - 26** in solutions of methanol (0.50 to 1.40 V) or DCE (0.50 to 1.60 V) each display a single oxidation wave in the potential range of the experiments. This oxidation process has previously been assigned for the monometallic complexes $CpRu(PPh_3)_2Cl$[167] and $(Ind)Ru(PPh_3)_2Cl$[168] (Table 3-4) as the reversible one-electron oxidation of the Ru metal center. Based on this assignment the oxidation waves observed for complexes **19 - 26** have been assigned to the Ru(II/III) couple.

Table 3-4. Formal potentials of complexes **19** – **26**

Complex[a]	E_{pa} (V)	$E_{1/2}$[b] (V)	ΔE_p (mV)	i_{pa} / i_{pc}
$CpRu(PPh_3)_2Cl$ (**19**)	0.87	0.82	90	1.03
$CpRu(PPh_3)_2(SnCl_3)$ (**20**)	1.48	1.44	85	0.92
$(Ind)Ru(PPh_3)_2(SnCl_3)$ (**21**)	1.39	1.34	106	0.95
$CpRu(TPPMS)_2Cl$ (**22**)	0.93	0.89	104	1.06
$CpRu(TPPMS)_2Cl$ (**22**)[c]	0.79	0.73	90	0.94
$CpRu(TPPMS)_2(SnCl_3)$ (**23**)	1.58			
$CpRu(TPPMS)_2(SnCl_3)$ (**23**)[c]	1.29			
$CpRu(\eta^2\text{-dppm})(SnCl_3)$ (**24**)[d]	1.54			
$CpRu(\eta^2\text{-dppe})(SnCl_3)$ (**25**)[d]	1.53			
$CpRu(\eta^2\text{-dppp})(SnCl_3)$ (**26**)[d]	1.52			
$CpRu(PPh_3)_2Cl$[e]	0.929	0.869	120	1.00
$(Ind)Ru(PPh_3)_2Cl$[f]		0.69	66	

[a] All potentials obtained in 0.7 M TBAT / DCE unless otherwise specified.
[b] $E_{1/2}$ reported for reversible waves. [c] Potential obtained in 0.1 M TBAT/MeOH.
[d] Potential obtained in 0.7 M TBAT/CH_2Cl_2. [e] Reference 167, potential originally reported vs SCE. [f] Reference 168, potential originally reported vs SCE.

When analyzed in DCE, the one-electron oxidation of $CpRu(PPh_3)_2Cl$ (Figure 3-2) at 0.82 V and $CpRu(TPPMS)_2Cl$ at 0.89 V are chemically reversible with $i_{pa} / i_{pc} \approx 1$ (Table 3-4). When small amounts of methanol are added to the DCE solutions, no

significant change is observed in the cyclic voltammograms of **19** and **22** at potentials less than 1.60 V.

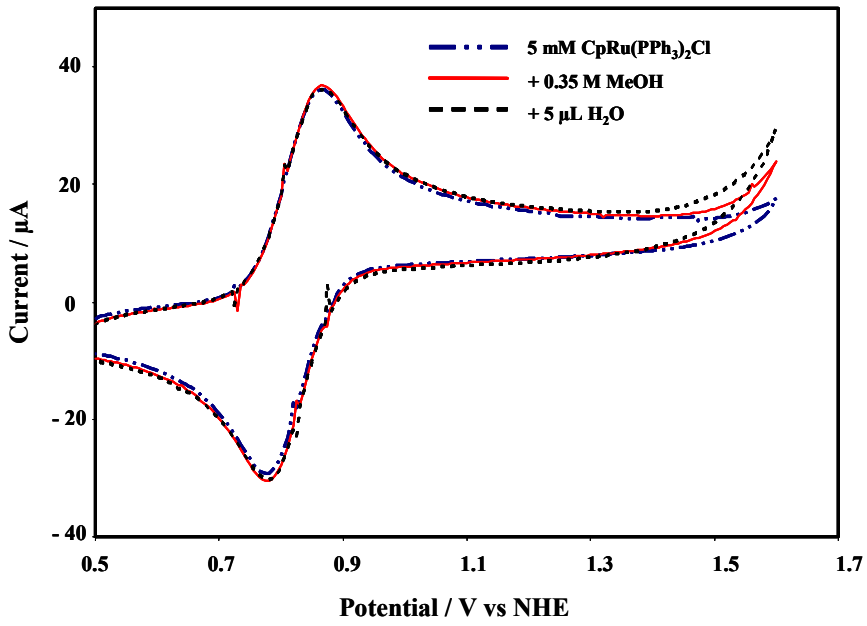

Figure 3-2. Cyclic voltammograms of **19** under nitrogen in 3.5 mL of DCE / 0.7 M TBAT; glassy carbon working electrode; Ag/Ag^{+} reference electrode; 50 mV/s scan rate, solutions as specified in figure. Adapted from reference 169.

The CV of $CpRu(PPh_3)_2(SnCl_3)$ (**20**) in DCE exhibits a reversible Ru(II/III) couple at 1.44 V (Figure 3-3). The Ru(II/III) couple is shifted by approximately 600 mV positive with respect to the corresponding Ru(II/III) wave of $CpRu(PPh_3)_2Cl$ (**19**). This positive shift is consistent with the electron withdrawing $SnCl_3^-$ ligand rendering the Ru in complex **20** electron-poor relative to that of complex **19**. Sn(II) is not redox active within the solvent window (-0.50 – 2.5 V vs. NHE) for these experiments. In the presence of methanol, there is a significant increase in the current that coincides with the oxidation of the Ru metal center (Figure 3-3). This effect is indicative of an electrocatalytic oxidation process.

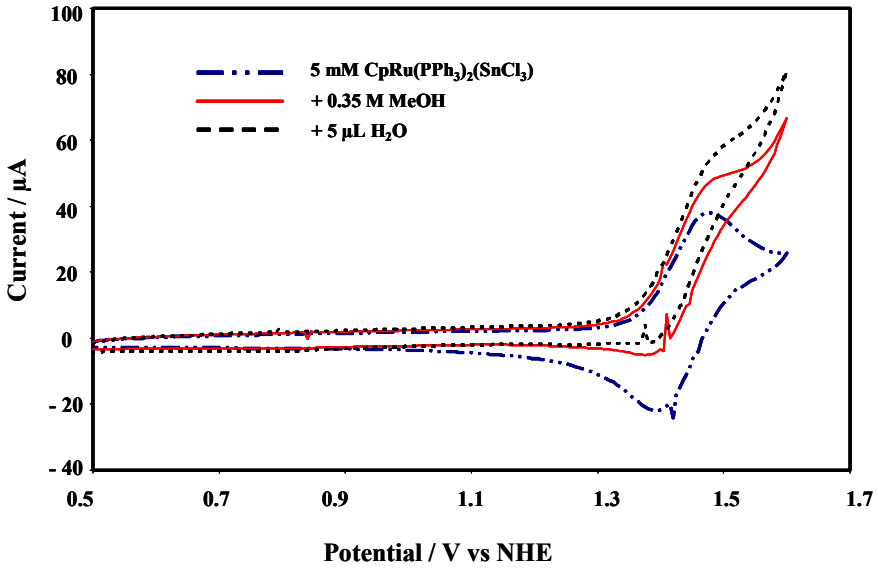

Figure 3-3. Cyclic voltammograms of **20** under nitrogen in 3.5 mL of DCE / 0.7 M TBAT; glassy carbon working electrode; Ag/Ag^{+} reference electrode; 50 mV/s scan rate, solutions as specified in figure. Adapted from reference 169.

The CV of **21** is very similar to that of complex **20**, exhibiting a reversible Ru(II/III) couple in DCE (Table 3-4). The Ru(II/III) couple however, at 1.34 V is 100 mV negative with respect to the analogous Ru(II/III) couple of complex **20**. This shifting of the II/III couple[168] is due to additional electron density associated with the indenyl ligand. The current rise from electrooxidation of methanol by **21** also coincides with its Ru(II/III) redox wave, as evidenced by a increase in the current at 1.34 V in the presence of methanol.

The CV of **23** exhibits a single irreversible wave in DCE at 1.58 V (Table 3-4). This irreversible redox wave has been assigned to the oxidation of the metal center from Ru(II) to Ru(III). The single irreversible Ru(II/III) wave is also observed in methanol at 1.29 V, shifted by approximately 290 mV relative to the redox potential in DCE. Cyclic voltammetry of **23** in DCE exhibits a significant increase in the catalytic current at the

Ru(II/III) wave when methanol is introduced. A similar catalytic effect was observed for **20** and **21**.

Methylene chloride solutions of CpRu(η^2-dppm)($SnCl_3$) (**24**), CpRu(η^2-dppe)($SnCl_3$) (**25**) and CpRu(η^2-dppp)($SnCl_3$) (**26**) each exhibit a single irreversible oxidation wave at 1.54, 1.53 and 1.52 V respectively. When methanol is introduced the expected catalytic current is observed at the Ru(II/III) oxidation wave. The oxidation waves for **24, 25** and **26** (Table 3-4) are only 20 mV apart. This indicates that the structurally similar complexes also have similar electronic configuration.

Electrochemical Oxidation of Methanol

The cyclic voltammograms of the Ru-$SnCl_3$ complexes all exhibit a significant current increase in the presence of methanol. As mentioned before, this increase in anodic current in the presence of an alcohol is characteristic of the catalytic electrooxidation of alcohols. The onset of this electrocatalytic current for the heterobimetallic complexes coincides with the oxidation of the metal center from Ru(II) to Ru(III). A similar current increase was observed in the CVs of the dppm bridged complexes CpRu(PPh_3)(μ-Cl)(μ-dppm)$PtCl_2$ (**3**), CpRu(PPh_3)(μ-Cl)(μ-dppm)$PdCl_2$ (**4**) and CpRu(PPh_3)(Cl)(μ-dppm)AuCl (**5**) when methanol was introduced. For complexes **3** and **4** the increase in the anodic current coincides with the oxidation of the Pt and Pd metal center. For the Ru/Au complex the onset of the catalytic current coincides with the Ru(III/IV) redox wave. In contrast to the CVs for the heterobimetallic complexes above, the CV of the Ru model compound CpRu(PPh_3)$_2$Cl (**19**) (Figure 3-2) exhibits no significant current increase when methanol is introduced.

In order to assess the electrocatalytic ability of the Ru-$SnCl_3$ complexes, the electrochemical oxidation of methanol was performed at 1.7 V in 0.7 M TBAT / DCE

(Table 3-5). The anodic potential of 1.7 V was chosen during the catalytic studies of **3**, and is the potential at which the catalytic current begins for complex **3**. For comparison purposes initial catalytic studies of **19 – 21** and **24 – 26** were performed at 1.7 V. At 1.7 V, the Ru in all complexes studied will be in the +3 oxidation state and within the catalytic current region.

Bulk electrolysis data for the oxidation of methanol with $CpRu(PPh_3)_2Cl$ (**19**), $CpRu(PPh_3)_2(SnCl_3)$ (**20**), $(Ind)Ru(PPh_3)_2(SnCl_3)$ (**21**), $CpRu(\eta^2\text{-dppm})(SnCl_3)$ (**22**), $CpRu(\eta^2\text{-dppe})(SnCl_3)$ (**23**) and $CpRu(\eta^2\text{-dppp})(SnCl_3)$ (**24**) are presented in Table 3-5. Differences between the activities of the complexes can be seen in the turnover numbers, current efficiencies and product ratios. The chelating phosphines significantly inhibited the catalytic activity of the complexes. At an anodic potential of 1.7 V, $CpRu(\eta^2\text{-dppm})(SnCl_3)$ (**22**), $CpRu(\eta^2\text{-dppe})(SnCl_3)$ (**23**) and $CpRu(\eta^2\text{-dppp})(SnCl_3)$ (**24**) exhibited little to no activity for the methanol oxidation reaction. The heterobimetallic complexes **22** – **24** are less active than the Ru model compound $CpRu(PPh_3)_2Cl$ (**19**). The Ru model compound $CpRu(PPh_3)_2Cl$ was more active, forming significantly more oxidation products. The inactivity of the complexes with bidentate phosphine suggests that a vacant coordination site on the Ru metal center is critical in the oxidation reaction.

Table 3-5. Bulk electrolysis data for the oxidation of methanol by **19 - 21** and **24 - 26**

Complex[a]	Anodic Potential (V)	TON[b]	Current Efficiency[c] (%)	DMM (10^{-5} moles)	MF (10^{-5} moles)	Product Ratio (DMM/MF)
$CpRu(PPh_3)_2Cl$ (**19**)	1.70	2.60 ± 0.15	7.3 ± 0.5	6.84 ± 0.34	2.26 ± 0.11	3.0 ± 1.0
$CpRu(PPh_3)_2(SnCl_3)$ (**20**)	1.70	3.37 ± 0.20	13.1 ± 0.7	8.65 ± 0.43	3.15 ± 0.16	2.7 ± 1.0
$(Ind)Ru(PPh_3)_2(SnCl_3)$ (**21**)	1.70	4.69 ± 0.28	17.9 ± 1.0	12.1 ± 0.60	4.34 ± 0.22	2.8 ± 1.0
$CpRu(\eta^2\text{-dppm})(SnCl_3)$ (**24**)	1.70	0	0	0	0	-
$CpRu(\eta^2\text{-dppe})(SnCl_3)$ (**25**)	1.70	0.53 ± 0.03	0.78 ± 0.09	1.85 ± 0.09	0	∞
$CpRu(\eta^2\text{-dppp})(SnCl_3)$ (**26**)	1.70	0	0	0	0	-
$CpRu(PPh_3)_2Cl$ (**19**)	1.55	1.00 ± 0.06	5.6 ± 0.2	2.69 ± 0.13	0.81 ± 0.04	3.3 ± 1.0
$CpRu(PPh_3)_2(SnCl_3)$ (**20**)	1.55	3.00 ± 0.20	18.2 ± 0.5	9.98 ± 0.50	0.52 ± 0.03	19.2 ± 1.1
$(Ind)Ru(PPh_3)_2(SnCl_3)$ (**21**)	1.55	2.80 ± 0.18	16.3 ± 0.5	9.07 ± 0.45	0.73 ± 0.04	12.4 ± 1.1

[a] All electrolyses performed in 0.7 M TBAT / DCE with 10 mM catalyst, 0.35 M methanol for 5 hours unless otherwise specified.
[b] Moles of product formed per mole of catalyst. [c] Calculated using Eq. 1.21.

For the complexes **19** – **21** with the monodentate phosphines the heterobimetallic complexes are more active toward methanol oxidation. $CpRu(PPh_3)_2(SnCl_3)$ (**20**) and $(Ind)Ru(PPh_3)_2(SnCl_3)$ (**21**) form greater quantities of oxidation products than the Ru model compound $CpRu(PPh_3)_2Cl$ (**19**). The greater reactivity is also observed in the current efficiency of these complexes during the reaction. The Ru-$SnCl_3$ complexes have a higher current efficiency and therefore convert a larger portion of the charge passed into products.

To probe the effect of the anodic potential on the electrochemical reaction, the oxidation of methanol with $CpRu(PPh_3)_2Cl$ (**19**), $CpRu(PPh_3)_2(SnCl_3)$ (**20**) and $(Ind)Ru(PPh_3)_2(SnCl_3)$ (**21**) was also investigated at 1.55 V (Table 3-5). At 1.55 V, the Ru metal center in all three catalysts will be in the Ru(III) oxidation state during the catalysis (Table 3-4). As expected, decreasing the anodic potential has a profound effect on the amounts of products and the TON (Table 3-5). Significantly less products are formed at the lower potential when the electrolysis is performed with **19**, **20** and **21**.

All three complexes $CpRu(PPh_3)_2Cl$ (**19**), $CpRu(PPh_3)_2(SnCl_3)$ (**20**) and $(Ind)Ru(PPh_3)_2(SnCl_3)$ (**21**) produce more DMM than MF as evidenced by the large product ratios (Table 3-5). Reducing the anodic potential has a significant effect on the selectivity (product ratio) of the reaction when the heterobimetallic complexes are used as catalysts. For $CpRu(PPh_3)_2(SnCl_3)$ (**20**) the product ratio increases from 2.07 to 19.2 when the potential is decreased from 1.70 to 1.55 V. A similar effect is observed for $(Ind)Ru(PPh_3)_2(SnCl_3)$ (**21**); when the potential is decreased the product ratio is increased from 2.79 to 12.4. When the Ru model compound is used as the catalyst, the ratio of

DMM:MF is independent of the anodic potential, remaining virtually unchanged when the potential is decreased.

Bulk electrolyses of the sulfonated complexes **22** and **23** were performed in methanol as the solvent. The electrolysis in methanol was also studied at two anodic potentials. Due to the limited anodic range of methanol, the anodic potentials used during these experiments are 1.40 V and 1.25 V. Similar to the catalysis in DCE and CH_2Cl_2, the electrooxidation of neat methanol resulted in the formation of DMM and MF. The same trends observed during the electrooxidation of methanol in DCE are also observed in neat methanol (Table 3-6):

- DMM formation is favored over MF, by both complexes
- The heterobimetallic complex is much more active than the Ru model compound
- When $CpRu(TPPMS)_2(SnCl_3)$ is used as the catalyst, lowering the anodic potential increases the ratio of DMM:MF

When the electrolysis is performed in methanol instead of the less polar DCE or CH_2Cl_2, there is a significant increase in the current efficiency, amounts of products formed and TON (Table 3-6). This increase in catalytic activity has been attributed to the improved

Table 3-6. Bulk electrolysis data for the oxidation of methanol by **22** and **23**

Complex[a]	Anodic Potential (V)	TON[b]	Current Efficiency[c] (%)	DMM (10^{-5} moles)	MF (10^{-5} moles)	Product Ratio (DMM/MF)
$CpRu(TPPMS)_2Cl$ (**22**)	1.25	13.4 ± 0.9	63.2 ± 2.3	46.9 ± 2.34	0	∞
$CpRu(TPPMS)_2(SnCl_3)$ (**23**)	1.25	33.4 ± 2.3	89.4 ± 5.6	117 ± 5.85	0	∞
$CpRu(TPPMS)_2Cl$ (**22**)	1.40	15.1 ± 1.0	76.9 ± 2.6	52.1 ± 2.60	0.75 ± 0.04	69.5 ± 1.1
$CpRu(TPPMS)_2(SnCl_3)$ (**23**)	1.40	40.0 ± 2.6	90.1 ± 6.7	127 ± 6.35	13.0 ± 0.65	9.8 ± 1.0

[a] All electrolyses performed in 0.1 M TBAT / MeOH with 10mM catalyst for 5 hours.
[b] Moles of product formed per mole of catalyst. [c] Calculated using Eq. 1.21.

electron transfer kinetics and to the higher concentration of substrate. The electrooxidation of methanol with $CpRu(TPPMS)_2Cl$ (**22**) and $CpRu(TPPMS)_2(SnCl_3)$ (**23**) at 1.25 V resulted in the selective formation of DMM.

As mentioned before, the electrochemical oxidation of methanol is a complicated reaction (Scheme 3-5) that often forms multiple stable products (eg. H_2CO, HCOOH, CO, $H_2C(OCH_3)_2$ and $HCOOCH_3$). To the best of my knowledge this is the first time that the electrooxidation of methanol resulted in a single oxidation product. When compared to the high temperature synthesis of DMM (Table 3-7), the electrochemical oxidation of methanol is a promising alternative for the synthesis of DMM.

Table 3-7. Selective partial oxidation of methanol.

Catalyst	Reaction Conditions	DMM Selectivity (%)	Conversion
$H_4PVMo_{11}O_{40}$ / SiO_2[a]	493 K, 4 kPa CH_3OH, 9 kPa O_2	58.1	68
$SbRe_2O_6$[b]	573 K, MeOH / O_2 = 4.0 / 9.7 (mol %)	92.5	6.5
$CpRu(TPPMS)_2Cl$ (**22**)	1.25 V, 0.1 M TBAT / MeOH	100	63.2[c]
$CpRu(TPPMS)_2(SnCl_3)$ (**23**)	1.25 V, 0.1 M TBAT / MeOH	100	89.4[c]

[a] Reference 150. [b] Reference 148. [c] Current efficiency (Eq. 1.21).

Electrochemical Oxidation of Wet Methanol

The CVs of the heterobimetallic complexes **20** (Figure 3-3), **21** and **23** all display a slight increase in the catalytic current when small amounts of water are added to the reaction mixtures. It should be noted that all of the samples contain some water due to the condensation of methanol with formaldehyde to generate DMM (Scheme 3-5). The effect of additional water on the electrocatalytic reaction was probed by introducing 5 μL of water before starting the electrolysis. In DCE the addition of water has a profound

effect on the selectivity of the reaction. The product ratio for the oxidation of "wet" methanol is lower than the corresponding electrolysis in "dry" methanol (Table 3-8). The addition of water therefore favors the formation of MF. A similar effect was previously described for heterogenous[148] and similar ruthenium[92,93] catalysts.

Table 3-8. Bulk electrolysis data for the oxidation of wet methanol by **20**, **21** and **23**

Complex[a]	Anodic Potential (V)	TON[b]	Current Efficiency[c] (%)	DMM (10^{-5} moles)	MF (10^{-5} moles)	Product Ratio (DMM / MF)
$CpRu(PPh_3)_2(SnCl_3)$ (**20**)	1.55	2.50 ± 0.14	17.2 ± 0.5	6.45 ± 0.32	2.30 ± 0.11	2.8 ± 1.0
$(Ind)Ru(PPh_3)_2(SnCl_3)$ (**21**)	1.55	2.90 ± 0.16	20.7 ± 0.6	6.67 ± 0.33	3.48 ± 0.17	1.9 ± 1.0
$CpRu(TPPMS)_2(SnCl_3)$ (**23**)[d]	1.25	15.3 ± 0.9	74.2 ± 3.1	42.1 ± 2.10	11.5 ± 0.57	3.7 ± 1.0

[a] All electrolyses performed in 0.7 M TBAT / DCE with 0.35 M methanol and 5.0 μL H_2O for 5 hours unless otherwise specified. [b] Moles of product formed per mole of catalyst. [c] Calculated using Eq. 1.21. [d] Electrolyses performed in 0.1 M TBAT/MeOH with 5.0 μL H_2O for 5 hours.

Methyl formate formation is also favored in "wet" vs "dry" methanol when the electrolysis is performed in methanol with $CpRu(TPPMS)_2(SnCl_3)$ (**23**). There is however a significant decrease in the TON and current efficiency of the catalyst (Table 3-8). During the synthesis of $CpRu(TPPMS)_2(SnCl_3)$, it was observed that this complex was very unstable in aqueous solutions. The decrease in TON and current efficiency is probably due to a shorter catalyst lifetime in aqueous solutions. This premise is supported by $^{31}P\{^1H\}$ NMR that revealed more TPPMS oxide in the "wet" solutions than in the "dry" solutions. $CpRu(PPh_3)_2(SnCl_3)$ and $(Ind)Ru(PPh_3)_2(SnCl_3)$ are also unstable in solutions containing water. The low solubility of water in DCE probably

accounts for why no significant change in the TON and current efficiency of $CpRu(PPh_3)_2(SnCl_3)$ and $(Ind)Ru(PPh_3)_2(SnCl_3)$ was observed.

Electrochemical Oxidation of Dimethoxymethane

The electrooxidation of DMM was studied in order to test the competency of DMM as an intermediate on the pathway to methyl formate. Control experiments have established that the electrooxidation of DMM in DCE does not proceed in the absence of catalyst at a potential of 1.70 V. The CV of $CpRu(PPh_3)_2(SnCl_3)$ (**20**) exhibits no catalytic current in the presence of DMM. After 5 hours of electrolysis at 1.7 V complex **20** formed 6.64×10^{-5} moles of MF with a current efficiency of 14.3 %. These results indicate that DMM could be an intermediate during the oxidation of methanol to MF

Summary

A series of heterobimetallic complexes containing a Ru-Sn metal bond were synthesized and characterized. The catalytic activity of these complexes was then investigated during the electrochemical oxidation of methanol. The catalytic activity of these complexes is sensitive to the ligands coordinated to ruthenium. Complexes containing a bidentate phosphine (**24** – **26**), display little to no catalytic activity (at an anodic potential of 1.7 V) during the electrolysis of methanol. This supports the premise that a vacant coordination site on Ru is critical to the electrooxidation reaction.

Complexes containing a monodentate phosphine (**19** – **23**), catalyze the electrochemical oxidation of methanol to DMM and MF. The Ru/Sn catalysts **20**, **21** and **23** favor the formation of DMM; this selectivity can be increased by lowering the anodic potential. The electrooxidation of methanol is more efficient and selective for the TPPMS complexes **22** and **23**, which allow the oxidation to be performed in methanol.

The partial oxidation of methanol to DMM was achieved selectively (100 %) and efficiently (89.4 %) with $CpRu(TPPMS)_2(SnCl_3)$ (**23**).

The addition of water to the DCE and methanol solutions favors the formation of MF. In methanol, the presence of water increases the decomposition rate of the catalyst. With a shorter catalyst lifetime there is a significant decrease in the current efficiency and amount of products when water is added to the methanol solutions. Due to the low solubility of water in DCE, the catalyst lifetime is not affected by the addition of water to the DCE solutions.

CHAPTER 4
CHEMICALLY MODIFIED ELECTRODES CONTAINING IMMOBILIZED RUTHENIUM/TIN HETEROBIMETALLIC COMPLEXES

Introduction

Electrochemistry is a powerful and versatile method for the synthesis of organic molecules. Transition metals are often used as catalysts / mediators to increase the reaction rates of these electrochemical reactions. As with most catalytic cycles involving transition metals, for commercial applications there is a desire to recycle the catalyst. One method of achieving this is by attaching the catalyst to the electrode surface. These chemically modified electrodes (CME) have an extensive history, and excellent reviews on their application have been published.[170-172] In this chapter, electrodes modified with cationic ruthenium complexes will be prepared and studied.

Nafion®

Nafion® is a fluorinated polymer (Figure 4-1) consisting of a fluorocarbon backbone and side chains that terminate in an anionic sulfonate site. In the commercially available membranes, the charge is typically balanced with proton or sodium ions.

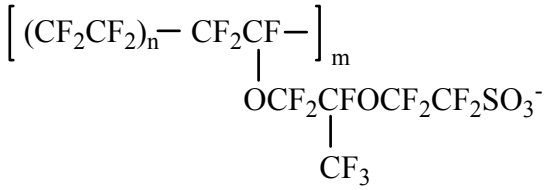

Figure 4-1. Structure of Nafion® where $5 \leq n \leq 7$ and m is approximately 1000. Adapted from reference 173.

Nafion® was developed by DuPont in the early 1960s for use in chlor-alkali cells and was the first ionomer (synthetic polymer with ionic properties) ever synthesized.[174] Other

applications of Nafion® include as a solid polymer electrolyte in fuel cells and batteries and a selective drying or humidifying agent for gases. Nafion® is also used as a super-acid catalyst in the production of fine chemicals.

As an ionic derivative of Teflon®, Nafion® has some unique properties:

- Mechanically stable and very resistant to chemical attack.
- High working temperatures, stable up to 230 °C.
- Ion-conductive, able to function as a cation exchange resin.
- Super-acid catalyst, readily donating protons due to the stabilizing effect of the electron withdrawing fluorinated backbone on the sulfonic acid.
- Nafion® is very selectively and highly permeable to water. The sulfonic acid groups in Nafion® have a very high water of hydration, so they very efficiently absorb water.

Extensive research has been performed on the structure of Nafion® membranes.[175] As a result of this research Nafion® membranes are commonly considered as segregated domains containing hydrophobic (fluorocarbon) and hydrophilic (hydrated sulfonate) regions (Figure 4-2). When hydrated the SO_3^- headgroups are thought to form water containing clusters approximately 40 Å in diameter. These clusters are then connected within the hydrophobic matrix by short channels 10 Å in diameter. It is from this 'inverted micelle' structure that Nafion® derives the exceptional ion selectivity and cation transport properties.

Nafion® Supported Metal Catalysts

Because of its stability and cation exchange properties, Nafion® has also been studied as a support for metal catalysts. Supported complexes are formed by covalently or electrostatically immobilizing metal species into a heterogeneous matrix. Typically the heterogeneous materials that are used as supports can be placed into three categories:

1. Inorganic matrix containing surface active hydroxyl groups such as Al_2O_3 and SiO_2
2. Organic polymers containing a pendant ligand such as polystyrene
3. Ion exchange membranes such as Nafion® and polyaniline

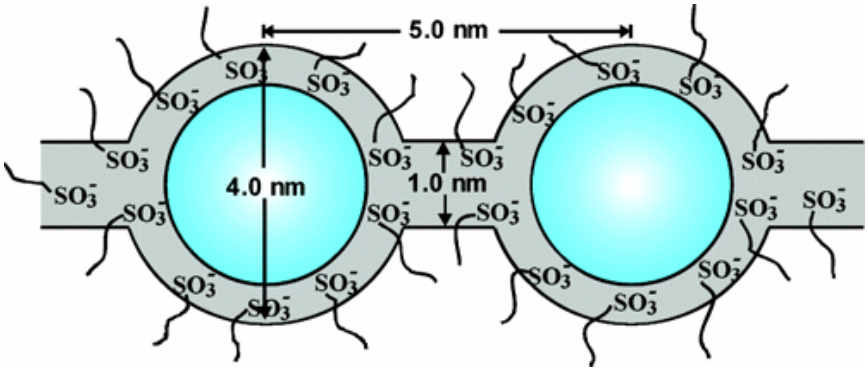

Figure 4-2. Cluster-network model for hydrated Nafion®. Adapted from reference 176.

The concept of immobilizing a soluble metal complex by attaching it to solid support was first introduced over thirty years ago. Even so this methodology still attracts considerable interest from the scientific community. The sustained interest in supported metal complexes is due to the distinct advantages of "heterogenized" complexes over traditional homogeneous species. Advantages of supported metal complexes include an increased reactivity and selectivity along with recyclability, stability and an ease of separation, inherent to heterogeneous systems.

As a result of the advantages listed above, supported metal complexes have been investigated for possible applications in numerous fields. Of these applications catalysis has received the most attention, especially for the synthesis of fine chemicals. The first example of a Nafion® supported metal catalyst was published in 1978 by Meidar,[177] who demonstrated that a Hg impregnated Nafion® membrane could catalyze the hydration of alkynes. This catalyst was easily separated from the mixture but upon reuse there was some loss of activity.[177] Since this report there have been several attempts at designing active Nafion® supported metal species as catalysts for organic synthesis.

With properties of an excellent support, a few cationic metal complexes have been successfully immobilized onto Nafion. In several instances catalytic activities comparable to homogeneous conditions have been observed for the Nafion® supported catalysts. In 1999 Seen reported the increased catalytic activity exhibited by a Nafion® supported Pd(II) complex during the methoxycarbonylation of ethene.[178] Because this catalyst is limited by diffusion, a combination of low catalyst loading and high dispersion of Nafion® was used in order to increase the activity. When this Nafion® supported catalyst was used in water it was significantly more active than the unsupported catalyst, having a turnover frequency comparable to commercial applications.

Chemically Modified Electrodes

Chemically modified electrodes (CME) result from the modification of a conductive substrate to produce an electrode with properties that differ from that of the unmodified substrate. These electrodes have been studied from the mid-1960s when French investigated the behavior of a ferrocene modified carbon paste electrode (CPE).[179] The composite nature of CPE makes these electrodes among the easiest to modify by simply admixing a third component with the graphite and binder. Other methods of preparing modified electrodes include adsorption, covalent attachment and coating the electrode with multi-layer films. CME are typically designed for applications such as catalysis or a sensitive sensor. An excellent review on the analytical application of sensors containing CME was published in 2003.[180] Sensor applications of CME are beyond the scope of this dissertation and will not be reviewed further.

Catalysis can be performed with CME if favorable conditions are present for the flow of electrons between the electrode and the species to be oxidized or reduced.[170] Scheme 4-1 shows a diagram of the reduction of A by the reduced form of the catalyst Q.

The reduction can occur within the film or at the film/solution interface by means of the reaction paths shown.

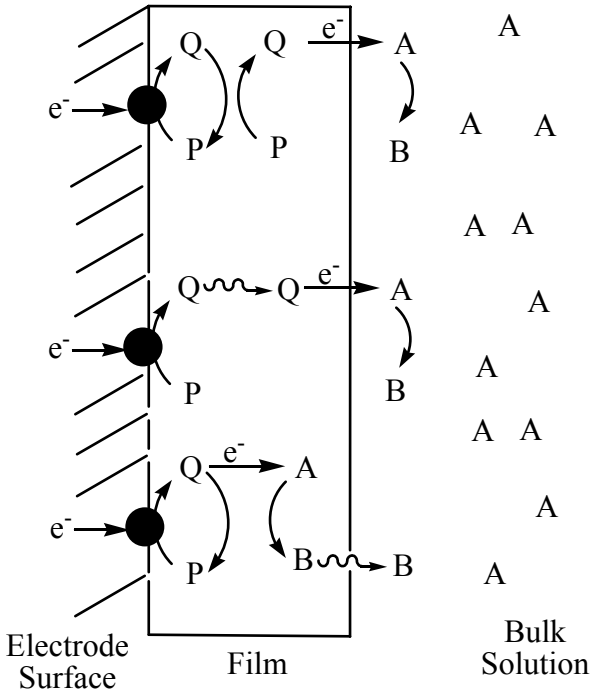

Scheme 4-1. Adapted from reference 181.

Electrodes Modified with Ruthenium Complexes

CME can be used to catalyze several reactions such as CO reduction, Cr(VI) reduction, NADH oxidation, the oxidation of small organic molecules such as methanol, formic acid, propene, ascorbic acid etc. These reactions were recently reviewed by Malinauskas,[182] Andreev[183] and Rolison.[184] The first example of a ruthenium complex attached to an electrode is $[(bpy)_2(H_2O)Ru(P4VP)_n^{2+}]$ where P4VP is poly-4-vinylpyridine.[64] This ruthenium metallopolymer was covalently attached to the electrode surface and used as a catalyst during the electrooxidation of isopropanol to acetone. This complex was not very stable during the catalysis and slowly decomposed to an unidentified species.

Since the CME containing a ruthenium complex was published, several other electrodes modified with ruthenium complexes have been prepared.[185-189] The methods of preparation have been varied and include encapsulation of the catalyst into ion-exchange membranes[190-192] such as Nafion® and sulfonated polystyrene. Meyer reported that the dimer $[Ru(bpy)_2(H_2O)]_2O^{4+}$ in solution is an active catalyst for the electrooxidation of water.[193] When supported on polystyrene sulfonate this complex has no catalytic activity.[194] Meyer proposed that the catalyst deactivation was due to the displacement of the aquo ligand and formation of a sulfonate complex. The loss of water will deactivate the catalytic reaction, by inhibiting the formation of the catalytically active oxo species.

The ruthenium bound CME can also be prepared by attaching the metal complex to a polymer film.[64,187,195,196] The stability of electrodes prepared in this manner has been studied, and is dependent on the polymer and the method of preparation. In 2000 Meyer reported that the surface bound poly-*cis*-$[Ru(vbpy)_2(O)_2]^{2+}$ (vbpy is 4-methyl-4'-vinyl-2,2'-bipyridine) is catalytically active during the electrooxidation of alkyl and aryl alcohols.[194] In solution this complex is very unstable readily losing bipyridine to form the inactive *trans*-dioxo complex. The rigid nature of the polymer film retards ligand loss and increases the stability of the catalytically active *cis*-dioxo Ru(VI) species.

Preparation of CME

Typically the modified layer is assembled upon a very stable reproducible surface. This material is normally used as an electrode even when unmodified due to good

mechanical and chemical stability. Examples of typical materials include platinum, gold, tin oxide and carbon.

As classified by Murray,[197] CME can be grouped into four categories based on the method used to modify them:

- Sorption
- Covalently modified electrodes
- Polymer coatings
- Heterogeneous multi-layer

CME prepared using sorption methods rely on chemical and physical interactions to form and maintain the monolayer.[198] These electrodes have the advantage of being easily prepared but are not as stable as electrodes modified by other methods. Covalent modification of electrodes is another method for anchoring molecules to an electrode surface.[198] Functional groups which have been employed include >C=O, >C-OH, ≡Pt-OH and ≡Sn-OH. As with the adsorption method, these electrodes are limited to monolayer coverage, severely restricting the amount of modifier on the surface. The monolayer limitation can be overcome by preparing multi-layer CMEs. Multi-layer CME are prepared from uniform polymer coatings of ionomers, redox polymers, inorganic polymers, polymerization of mediators bearing monomers, etc.[198] Another method of preparing multi-layer CME is the incorporation of mediators in a non-uniform matrix such as carbon paste, epoxy resin, clay, zeolite and other polymeric systems.[198]

Electrodes Modified with Bimetallic Complexes

CME have been aggressively studied for the last 20 years (Figure 4-3). The modification of electrodes with bimetallic complexes however is one field that is still in its infancy, with only a handful of electrodes studied.[192,199-203] The only reference to a

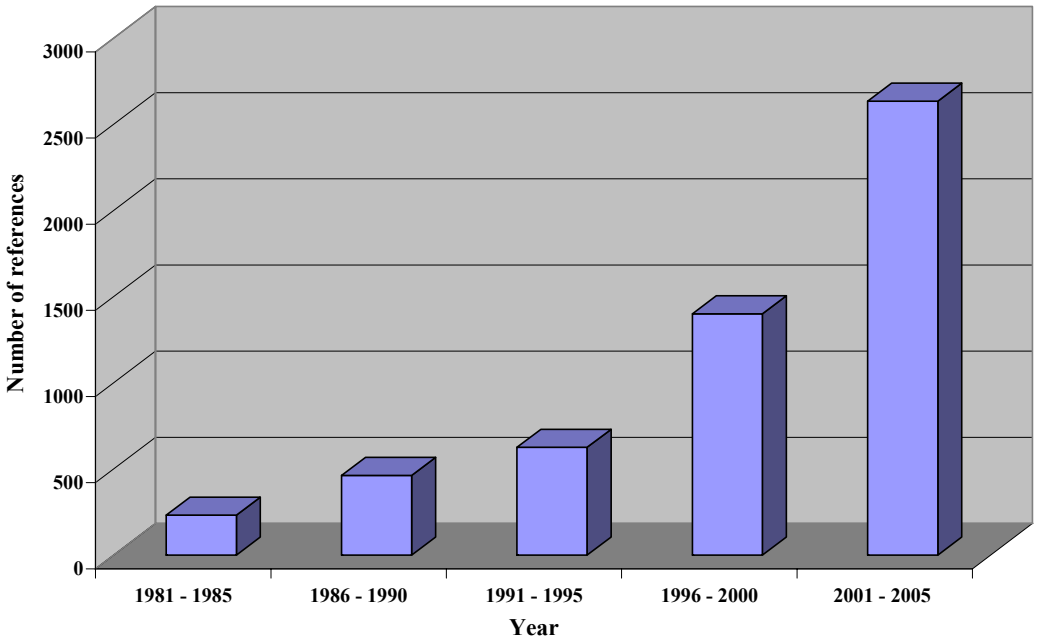

Figure 4-3. References to "chemically modified electrodes" in the scientific literature (SciFinder Scholar).

heterobimetallic complex immobilized on an electrode is the Co(II)-Pt(II) porphyrin reported by Srour in 2005.[204] When adsorbed to the surface of an edge plane graphite electrode a significant shift (600 mV) in the reduction potential of molecular oxygen was observed. This CME can act as a catalyst reducing all of the oxygen present to water (50 %) and hydrogen peroxide (50 %).

The electrochemical oxidation of methanol with Ru/Sn catalysts in solution was previously reported from this research group.[169] The activity of the Ru/Sn heterobimetallic catalysts is dependent on the ancillary phosphine ligands. It was shown that bidentate phosphines greatly inhibited the catalytic activity of the complexes. The Ru/Sn complexes with monodentate phosphines are very efficient (90 % current efficiency) and selective (100 % DMM) when the electrooxidation is performed in neat

methanol. In order to continue the study of Ru/Sn Lewis acidic interactions, the synthesis and study of a series of Nafion® supported Ru/Sn complexes (Figure 4-4) was performed.

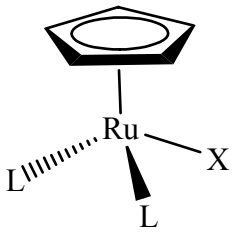

(27) L = PPh_3, X = $SnPh_3$

(28) L = $Ph_2PCH_2CH_2NMe_2$, X = Cl

(29) L = $Ph_2PCH_2CH_2NMe_2$, X = $SnCl_3$

(30) L = $Ph_2PCH_2CH_2NMe_2$, X = $SnPh_3$

(31) L = $Ph_2PCH_2CH_2NMe_3BF_4$, X = Cl

(32) L = $Ph_2PCH_2CH_2NMe_3BF_4$, X = $SnCl_3$

Figure 4-4. Structure of compounds **27** – **32**.

Synthesis

Synthesis of $CpRu(PPh_3)_2(SnPh_3)$ (27)

The Ru-$SnPh_3$ complex **27** was prepared by reacting $CpRu(PPh_3)_2(SnCl_3)$ (**20**) in benzene with an excess of phenyl lithium (Eq 4.1) at room temperature. $CpRu(PPh_3)_2(SnPh_3)$ was isolated as an air and moisture stable dark yellow solid in 90 % yield. Replacing the chlorides in $CpRu(PPh_3)_2(SnCl_3)$ with phenyl anions has a profound effect on the $^{31}P\{^1H\}$ NMR data. The singlet for the equivalent phosphorus atoms is shifted downfield relative to $CpRu(PPh_3)_2(SnCl_3)$ by approximately 8 ppm to 53 ppm. The P-Sn coupling is also affected; decreasing by 165 Hz to 270 Hz.

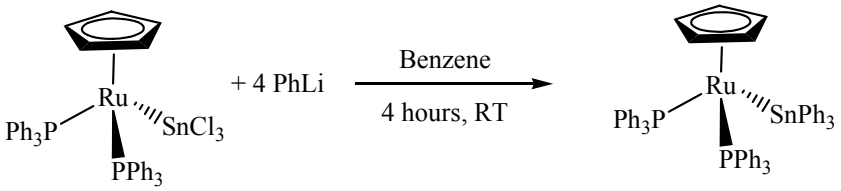

20 **27** (4.1)

Synthesis of $CpRu(Ph_2PCH_2CH_2NMe_2)_2Cl$ (28)

Attempts at synthesizing complex **28** through ligand displacement from $CpRu(PPh_3)_2Cl$ led to product mixtures containing the monosubstituted complex. These product mixtures were difficult to separate and therefore an alternative route to **28** was needed. Complex **28** was instead synthesized by reacting $Ru(\eta^2\text{-}Ph_2PCH_2CH_2NMe_2)_2Cl_2$ with an excess of cyclopentadiene in refluxing ethanol (Eq. 4.2). After 3 days $CpRu(Ph_2PCH_2CH_2NMe_2)_2Cl$ was isolated in high yield (74 %) as a yellow solid. Complex **28** is very stable as a solid or in solution even upon prolonged exposure to air and moisture. The $^{31}P\{^1H\}$ NMR spectrum of $CpRu(Ph_2PCH_2CH_2NMe_2)_2Cl$ is very similar to that of $CpRu(PPh_3)_2Cl$, consisting of a singlet at 37 ppm.

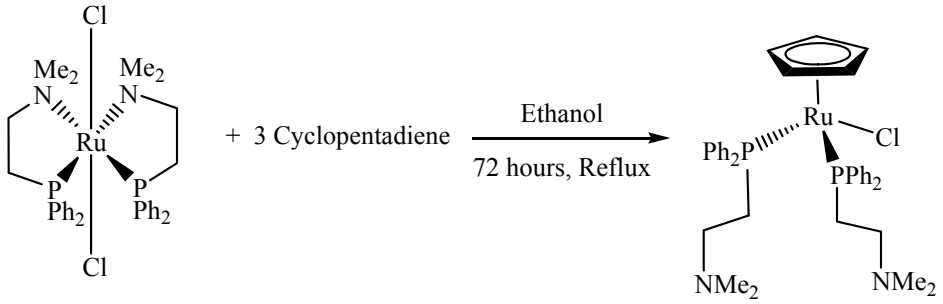

28 (4.2)

Synthesis of $CpRu(Ph_2PCH_2CH_2NMe_2)_2(SnCl_3)$ (29)

The reaction between $CpRu(Ph_2PCH_2CH_2NMe_2)_2Cl$ and $SnCl_2$ in DCE (Eq 4.3) produced $CpRu(Ph_2PCH_2CH_2NMe_2)_2(SnCl_3)$ in near quantitative yield. Complex **29** was isolated as a yellow solid that was stable to air and moisture not only in the solid state but also in solution. The $^{31}P\{^1H\}$ NMR spectrum is very similar to the previously synthesized Ru-$SnCl_3$ complexes, displaying only one singlet at 39 ppm with tin satellite couplings of 412 Hz.

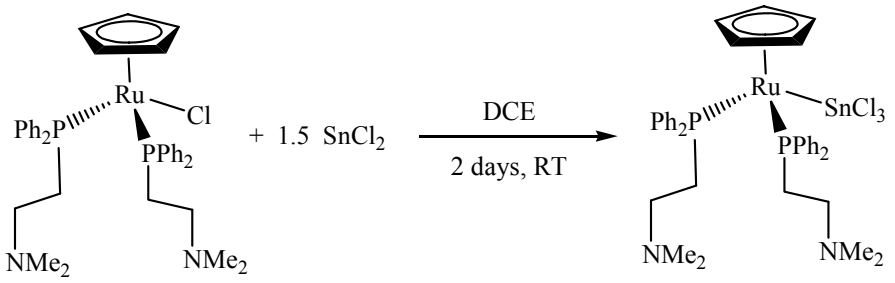

28 **29** (4.3)

Synthesis of CpRu($Ph_2PCH_2CH_2NMe_2$)$_2$($SnPh_3$) (30)

Complex 30 was prepared in a similar manner to CpRu(PPh_3)$_2$($SnPh_3$), by reacting CpRu($Ph_2PCH_2CH_2NMe_2$)$_2$($SnCl_3$) with phenyl lithium (Eq 4.4). After workup CpRu($Ph_2PCH_2CH_2NMe_2$)$_2$($SnPh_3$) was isolated in 64 % yield as a yellow solid. Complex **30** is stable in the presence of air and moisture, not only as a solid but also in solution. The singlet for the equivalent phosphorus atoms is shifted upfield relative to CpRu(PPh_3)$_2$($SnPh_3$) by approximately 9 ppm to 44 ppm. The P-Sn coupling ($^2J_{P\text{-}Sn}$ = 262 Hz) of **30** is unaffected by the change in ligand environment.

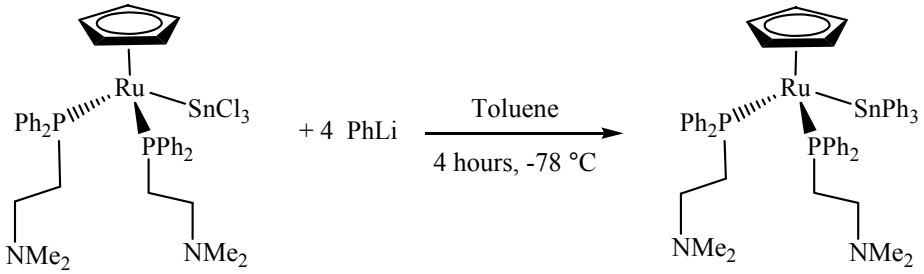

29 **30** (4.4)

Synthesis of CpRu(amphos)$_2$Cl (31)

CpRu(amphos)$_2$Cl was prepared in a similar manner to CpRu(TPPMS)$_2$Cl, by substitution of triphenylphosphine with amphos. The ligand substitution reaction was performed in refluxing toluene (Eq. 4.5). After four days of reflux **31** was isolated in 76

% yield as an orange solid. The stability of complex **31** is very similar to that of complex **28**, showing no signs of decomposition even after prolonged exposure to air and moisture. The $^{31}P\{^{1}H\}$NMR spectrum of **31** is very similar to that of **28** consisting of a singlet at 36 ppm.

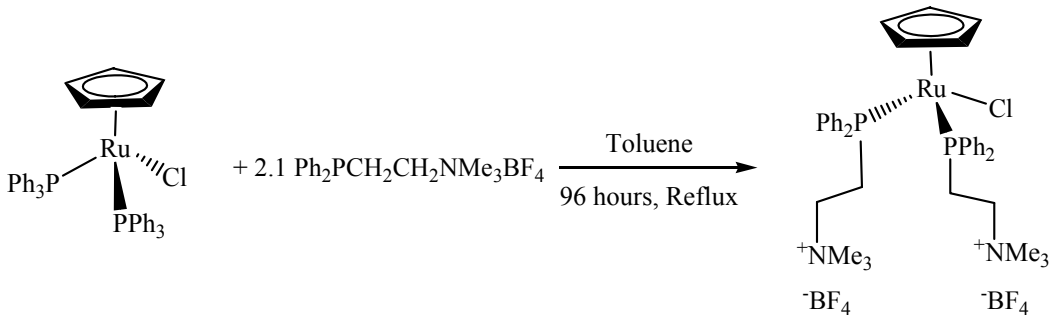

19 **31** (4.5)

Synthesis of CpRu(amphos)$_2$(SnCl$_3$) (32)

The Ru/Sn complex CpRu(amphos)$_2$(SnCl$_3$) was prepared in an analogous manner to CpRu(PPh$_3$)$_2$(SnCl$_3$)[125] by reacting **31** with a slight excess of SnCl$_2$ (Eq. 4.6) in refluxing ethanol. The resulting yellow solid is stable in air and in solutions exposed to air and moisture. As expected from the NMR spectrum of CpRu(Ph$_2$PCH$_2$CH$_2$NMe$_2$)$_2$(SnCl$_3$) (**29**), the $^{31}P\{^{1}H\}$ NMR spectrum of CpRu(amphos)$_2$(SnCl$_3$) consists of a singlet at 40 ppm with $^{2}J_{P\text{-}Sn}$ = 405 Hz.

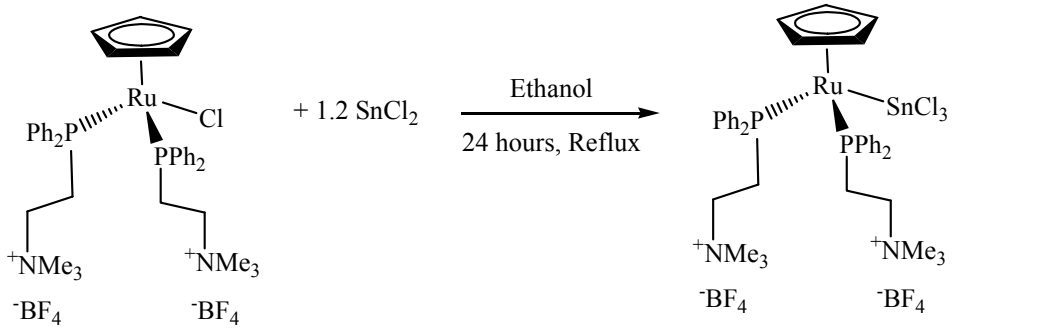

31 **32** (4.6)

As mentioned above, Nafion® is a cation exchange polymer capable of acting as a solid support for positively charged species. Because of this, cationic complexes analogous to $CpRu(TPPMS)_2Cl$ (**22**) and $CpRu(TPPMS)_2(SnCl_3)$ (**23**) were prepared. The cationic phosphine amphos, was selected as the ligand to replace TPPMS, forming $CpRu(Ph_2PCH_2CH_2NMe_3BF_4)_2Cl$ (**31**) and $CpRu(Ph_2PCH_2CH_2NMe_3BF_4)_2(SnCl_3)$ (**32**). The neutral complexes $CpRu(Ph_2PCH_2CH_2NMe_2)_2Cl$ (**28**) and $CpRu(Ph_2PCH_2CH_2NMe_2)_2(SnCl_3)$ (**29**) were also synthesized; these complexes will be readily protonated by Nafion® to form positively charged species.

NMR Data

^1H and $^{31}P\{^1H\}$ NMR spectroscopies were utilized to determine the ligand arrangement about the Ru center. Selected NMR data are presented in Table 4-1. The ^1H and $^{31}P\{^1H\}$ NMR spectral data are very similar to the previously reported complexes (Table 3-3). Only one singlet is observed in the $^{31}P\{^1H\}$ NMR spectra for complexes **27** – **32**. The chemical shifts of the cyclopentadienyl protons are a good indication of the electron density located on the Ru metal center. As observed in the ^1H NMR of compounds **19** – **23** (Table 3-3), the Cp protons shift downfield as the electron density on Ru decreases. Hence for $CpRuL_2Cl$, the chemical shift of the Cp protons for

Table 4-1. Selected NMR data for complexes **27** – **32**

Complex[a]	Solvent	Cp ^1H NMR (ppm)	$^{31}P\{^1H\}$ NMR (ppm)	$^2J_{P,Sn}$ (Hz)
$CpRu(PPh_3)_2(SnPh_3)$ (**27**)	$CDCl_3$	4.27	53.0	270
$CpRu(Ph_2PCH_2CH_2NMe_2)_2Cl$ (**28**)	$CDCl_3$	4.29	36.6	
$CpRu(Ph_2PCH_2CH_2NMe_2)_2(SnCl_3)$ (**29**)	$CDCl_3$	4.71	39.4	412
$CpRu(Ph_2PCH_2CH_2NMe_2)_2(SnPh_3)$ (**30**)	$CDCl_3$	4.21	43.8	262
$CpRu(amphos)_2Cl$ (**31**)	DMSO-d_6	4.48	35.9	
$CpRu(amphos)_2(SnCl_3)$ (**32**)	acetone-d_6	5.00	39.5	405

[a] All NMR data obtained at room temperature.

L = amphos > $Ph_2PCH_2CH_2NMe_2$ > PPh_3 ≈ TPPMS. The same trend was observed for the complexes containing the $SnCl_3$ ligand.

Homogeneous Studies

Cyclic Voltammetry

Cyclic voltammograms of complexes **27 - 32** each display a single oxidation wave (Table 4-2). This oxidation process has previously been assigned to the Ru(II/III) couple for the monometallic [$CpRu(PPh_3)_2Cl$,[167] $(Ind)Ru(PPh_3)_2Cl$,[168] $CpRu(TPPMS)_2Cl$] and heterobimetallic [$CpRu(PPh_3)_2(SnCl_3)$, $CpRu(TPPMS)_2(SnCl_3)$] complexes (Table 3-3). Based on this assignment, the oxidation waves observed for complexes **27 - 32** have been assigned to the one-electron oxidation of Ru(II) to Ru(III).

The amphiphilic nature of the amino-phosphine ligands allow the electrochemical study of the Ru complexes **28 - 32** in polar and non-polar solvents. These ligands also stabilize complexes **28 - 32** in water. This increased stability was observed during the characterization of these molecules, and during the CV studies in aqueous solutions (Table 4-2). This contrasts to $CpRu(TPPMS)_2Cl$ (**22**) and $CpRu(TPPMS)_2(SnCl_3)$ (**23**), both of which are soluble but decompose quickly in water. Due to an inductive effect, the positive charge on the amphos ligand pulls electrons density away from the Ru metal center. Because of this the Ru(II/III) oxidation waves of complexes **31** and **32** occur at a slightly higher potential than **28** and **29**, respectively.

The oxidation of the Ru/Cl complex $CpRu(amphos)_2Cl$ (**31**) is chemically reversible ($i_{pa} / i_{pc} \approx 1$), when analyzed in methylene chloride, methanol, water and acetonitrile (Table 4-2). The other monometallic complex $CpRu(Ph_2PCH_2CH_2NMe_2)_2Cl$ (**28**) is also reversible when oxidized in methylene chloride, methanol and water.

Table 4-2. Formal potentials of complexes **27** – **32**

Complex[a]	Electrolyte	E_{pa} (V)	$E_{1/2}$ (V)	ΔE_p (mV)	i_{pa} / i_{pc}
$CpRu(PPh_3)_2(SnCl_3)$ (**20**)[b]	0.7 M TBAT / DCE	1.48	1.44	85	0.92
$CpRu(PPh_3)_2(SnCl_3)$ (**20**)	0.1 M TBAT / $MeNO_2$	1.42	1.35	139	1.13
$CpRu(PPh_3)_2(SnCl_3)$ (**20**)	0.1 M TBAT / CH_3CN	1.32, 1.50			
$CpRu(PPh_3)_2(SnPh_3)$ (**27**)	0.7 M TBAT / CH_2Cl_2	1.19	1.13	116	1.21
$CpRu(PPh_3)_2(SnPh_3)$ (**27**)	0.1 M TBAT / MeOH	1.18			
$CpRu(Ph_2PCH_2CH_2NMe_2)_2Cl$ (**28**)	0.7 M TBAT / CH_2Cl_2	1.13	1.05	134	1.04
$CpRu(Ph_2PCH_2CH_2NMe_2)_2Cl$ (**28**)	0.1 M TBAT / MeOH	0.97	0.90	142	1.13
$CpRu(Ph_2PCH_2CH_2NMe_2)_2Cl$ (**28**)	0.1 M KCl / H_2O	0.86	0.80	125	1.07
$CpRu(Ph_2PCH_2CH_2NMe_2)_2Cl$ (**28**)	0.1 M TBAT / CH_3CN	0.82, 1.14			
$CpRu(amphos)_2Cl$ (**31**)	0.7 M TBAT / CH_2Cl_2	1.18	1.12	124	1.10
$CpRu(amphos)_2Cl$ (**31**)	0.1 M TBAT / MeOH	1.00	0.93	114	0.99
$CpRu(amphos)_2Cl$ (**31**)	0.1 M TBAT / $MeNO_2$	0.92	0.88	90	1.06
$CpRu(amphos)_2Cl$ (**31**)	0.1 M KCl / H_2O	0.85	0.80	108	0.95
$CpRu(amphos)_2Cl$ (**31**)	0.1 M TBAT / CH_3CN	0.86	0.80	113	1.03
$CpRu(Ph_2PCH_2CH_2NMe_2)_2(SnCl_3)$ (**29**)	0.1 M TBAT / $MeNO_2$	1.65			
$CpRu(Ph_2PCH_2CH_2NMe_2)_2(SnCl_3)$ (**29**)	0.7 M TBAT / CH_2Cl_2	1.62			
$CpRu(Ph_2PCH_2CH_2NMe_2)_2(SnCl_3)$ (**29**)	0.1 M TBAT / CH_3CN	1.52			
$CpRu(Ph_2PCH_2CH_2NMe_2)_2(SnPh_3)$ (**30**)	0.1 M TBAT / MeOH	1.15			
$CpRu(amphos)_2(SnCl_3)$ (**32**)	0.1 M TBAT / $MeNO_2$	1.64			
$CpRu(amphos)_2(SnCl_3)$ (**32**)	0.7 M TBAT / CH_2Cl_2	1.70			
$CpRu(amphos)_2(SnCl_3)$ (**32**)	0.1M TBAT / PC	1.73			
$CpRu(amphos)_2(SnCl_3)$ (**32**)	0.1 M TBAT / CH_3CN	1.59			

[a] All potentials reported vs NHE. [b] Reference 169.

When analyzed in acetonitrile, the CV of **28** exhibits two irreversible peaks at 0.82 and 1.14 V. The first peak at 0.82 V was assigned to the one-electron oxidation of the Ru metal center in complex **28**. This assignment was made by comparing the CV of **28** to that of **31**. The second irreversible oxidation wave has not been conclusively assigned but is probably due to the oxidation of an acetonitrile adduct.

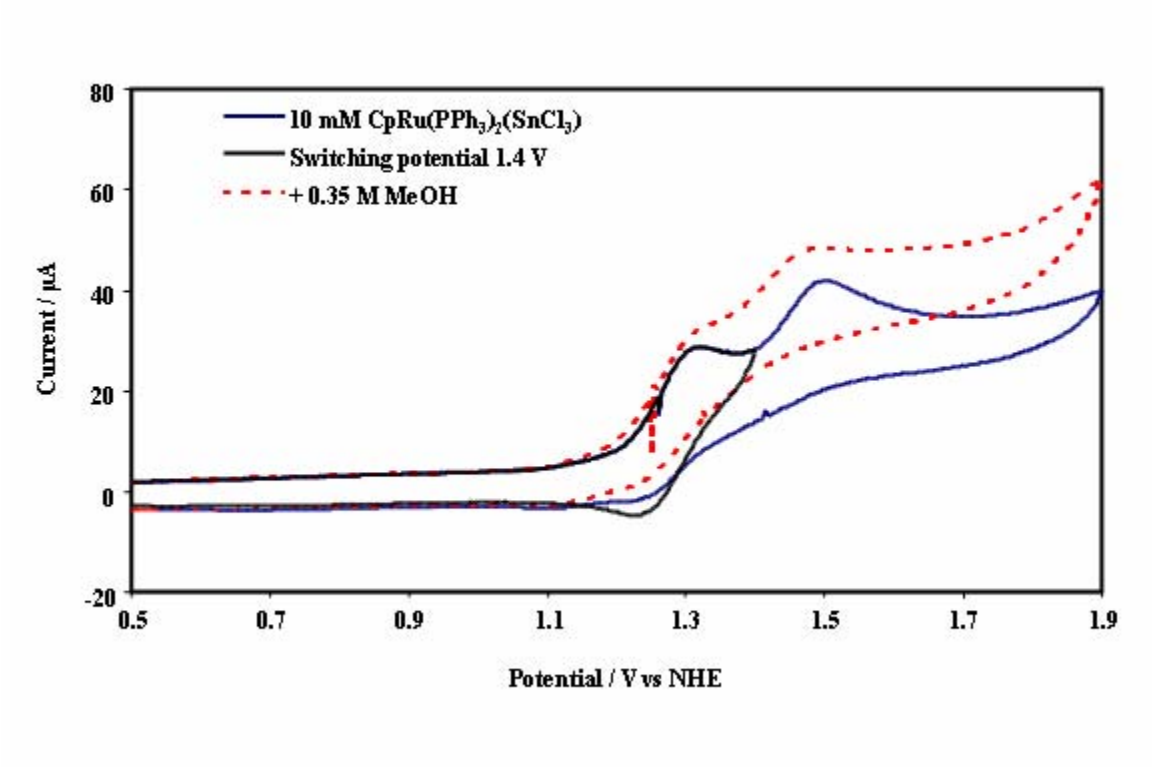

Figure 4-5. Cyclic voltammograms of **20** under nitrogen in 3.5 mL of CH_3CN / 0.1 M TBAT; glassy carbon working electrode; Ag/Ag^+ reference electrode; 50 mV/s scan rate, solutions as specified in figure.

The CV of $CpRu(PPh_3)_2(SnCl_3)$ (**20**) in acetonitrile (Table 4-2) is very similar to $CpRu(Ph_2PCH_2CH_2NMe_2)_2Cl$ (**28**), displaying two irreversible oxidation waves, at 1.32 and 1.50 V. At a switching potential of 1.40 V, the first oxidation wave is chemically reversible (Figure 4-5). This first oxidation wave has been assigned to the Ru(II/III) couple of **20**. This assignment was made by comparing the CVs of **20** in CH_3CN (Figure 4-2) to that in DCE (Figure 3-3). The second wave is irreversible, regardless of

the switching potential. This oxidation process is similar to the second oxidation wave observed for **28** in CH_3CN, and has been assigned to the oxidation of an acetonitrile complex. The formation of a solvent coordinated complex has been previously reported,[205] during CV studies of an analogous ruthenium hydride complex, $CpRu(PPh_3)_2H$ in acetonitrile (Eq. 4.7).

$$CpRu(PPh_3)_2H \xrightarrow[CH_3CN]{-\ 1e^-} 0.5\ [CpRu(PPh_3)_2(CH_3CN)]^+ + 0.5\ [CpRu(PPh_3)_2(H)_2]^+ \quad (4.7)$$

The CVs of the $Ru/SnCl_3$ complexes $CpRu(Ph_2PCH_2CH_2NMe_2)_2(SnCl_3)$ (**29**) and $CpRu(amphos)_2(SnCl_3)$ (**32**) were studied in several solvents. A single irreversible oxidation wave was observed for **29** and **32** in $MeNO_2$, CH_2Cl_2 and CH_3CN. In methanol a significant increase in current was observed when **29** and **32** were added, but no oxidation waves were observed. The catalytic current of the methanol oxidation reaction obscures the Ru(II/III) redox couple.

The chloride ligands in complexes $CpRu(Ph_2PCH_2CH_2NMe_2)_2(SnCl_3)$ (**29**) and $CpRu(PPh_3)_2(SnCl_3)$ (**20**) were substituted with the less electron withdrawing phenyl groups to yield complexes **30** and **27**. A single oxidation wave, assigned to the Ru(II/III) couple was observed in the CV of complexes $CpRu(Ph_2PCH_2CH_2NMe_2)_2(SnPh_3)$ (**30**) and $CpRu(PPh_3)_2(SnPh_3)$ (**27**). The Ru(II/III) oxidation waves of the $SnPh_3$ complexes **30** and **27** are shifted to lower potentials than those of the corresponding $SnCl_3$ complexes. As predicted by Holt,[126] and supported by the NMR and CV data, $(SnPh_3)^-$ is a weaker Lewis acid than $(SnCl_3)^-$.

Electrochemical Oxidation of Methanol

The cyclic voltammograms of the Ru/Sn complexes $CpRu(PPh_3)_2(SnPh_3)$ (**27**), $CpRu(Ph_2PCH_2CH_2NMe_2)_2(SnCl_3)$ (**29**), $CpRu(Ph_2PCH_2CH_2NMe_2)_2(SnPh_3)$ (**30**) and $CpRu(amphos)_2(SnCl_3)$ (**32**) all exhibit a catalytic current in the presence of methanol. The onset of this catalytic current for the heterobimetallic complexes coincides with the oxidation of the metal center from Ru(II) to Ru(III), regardless of what solvent is being used. A similar current increase was observed in the cyclic voltammograms of $CpRu(PPh_3)_2(SnCl_3)$ (**20**) and $CpRu(TPPMS)_2(SnCl_3)$ (**23**). For the monometallic complexes $CpRu(Ph_2PCH_2CH_2NMe_2)_2Cl$ (**28**) and $CpRu(amphos)_2Cl$ (**31**) no catalytic current was observed within the potential window (0 – 2.0 V) when methanol was introduced.

The electrochemical oxidation of methanol in 0.1 M TBAT/MeOH was performed at 1.4 V with **28 - 32**. The anodic potential was chosen during previous studies,[169] and used for these experiments so as to have a direct correlation to the previous results. At 1.4 V the Ru metal center of **28**, **30** and **31** will be oxidized from Ru(II) to Ru(III). Although no oxidation wave was observed for **29** and **32** in methanol, by extrapolating from **28** and **31** the Ru(II/III) couple for **29** and **32** can be estimated as 1.56 and 1.62 V respectively. $CpRu(Ph_2PCH_2CH_2NMe_2)_2(SnCl_3)$ (**29**) and $CpRu(amphos)_2(SnCl_3)$ (**32**) are oxidized at an anodic potential of 1.4 V; this process can be observed in the CVs that display a current increase.

The oxidation products formed during the electrolysis are dimethoxymethane and methyl formate (Table 4-3). DMM and MF are the same products observed during earlier studies of Ru-TPPMS electrocatalysts[169] in neat methanol. The evolution of

Table 4-3. Bulk electrolysis data for the oxidation of methanol by **27 - 32**

Complex[a]	TON[b]	Current Efficiency[c] (%)	DMM (10^{-5} moles)	MF (10^{-5} moles)	Product Ratio (DMM/MF)
$CpRu(TPPMS)_2(SnCl_3)$[d] (**23**)	40.0 ± 2.6	90.1 ± 6.9	127 ± 6	13.0 ± 0.6	9.8 ± 1.0
$CpRu(amphos)_2Cl$ (**31**)	8.85 ± 0.60	37.8 ± 1.5	28.7 ± 1.4	2.3 ± 0.1	12.6 ± 1.0
$CpRu(amphos)_2(SnCl_3)$ (**32**)	10.3 ± 0.6	52.1 ± 2.1	27.9 ± 1.4	8.2 ± 0.4	3.4 ± 1.0
$CpRu(Ph_2PCH_2CH_2NMe_2)_2Cl$ (**28**)	9.66 ± 0.59	37.7 ± 1.9	27.2 ± 1.4	6.6 ± 0.3	2.5 ± 0.6
$CpRu(Ph_2PCH_2CH_2NMe_2)_2(SnCl_3)$ (**29**)	10.0 ± 0.6	47.6 ± 2.1	24.6 ± 1.2	10.6 ± 0.5	2.3 ± 1.0
$CpRu(Ph_2PCH_2CH_2NMe_2)_2(SnPh_3)$ (**30**)	2.14 ± 0.14	8.2 ± 0.4	7.5 ± 0.4	N.O.	∞
$CpRu(PPh_3)_2(SnPh_3)$ (**27**)[e]	0.80 ± 0.06	4.2 ± 0.1	2.8 ± 0.1	N.O.	∞
$CpRu(PPh_3)_2(SnCl_3)$ (**20**)[d,e]	3.37 ± 0.20	13.1 ± 0.7	8.65 ± 0.43	3.15 ± 0.16	2.7 ± 1.0
$CpRu(PPh_3)_2Cl$ (**19**)[d,e]	2.60 ± 0.15	7.3 ± 0.5	6.84 ± 0.34	2.26 ± 0.11	3.0 ± 1.0

[a] All electrolyses performed at 1.4 V in 0.1 M TBAT/MeOH with 10 mM catalyst for 5 hours. [b] Moles of product formed per mole of catalyst. [c] Calculated using Eq. 1.21. [d] Reference 169. [e] Performed at 1.7 V in 0.7 M TBAT/CH_2Cl_2 with 10 mM catalyst, 0.35 M methanol for 5 hours.

DMM and MF was monitored as a function of time and plotted in Figures 4-6 and 4-7 respectively. For complexes **28**, **29**, **31** and **32**, DMM is formed at a faster rate than MF,

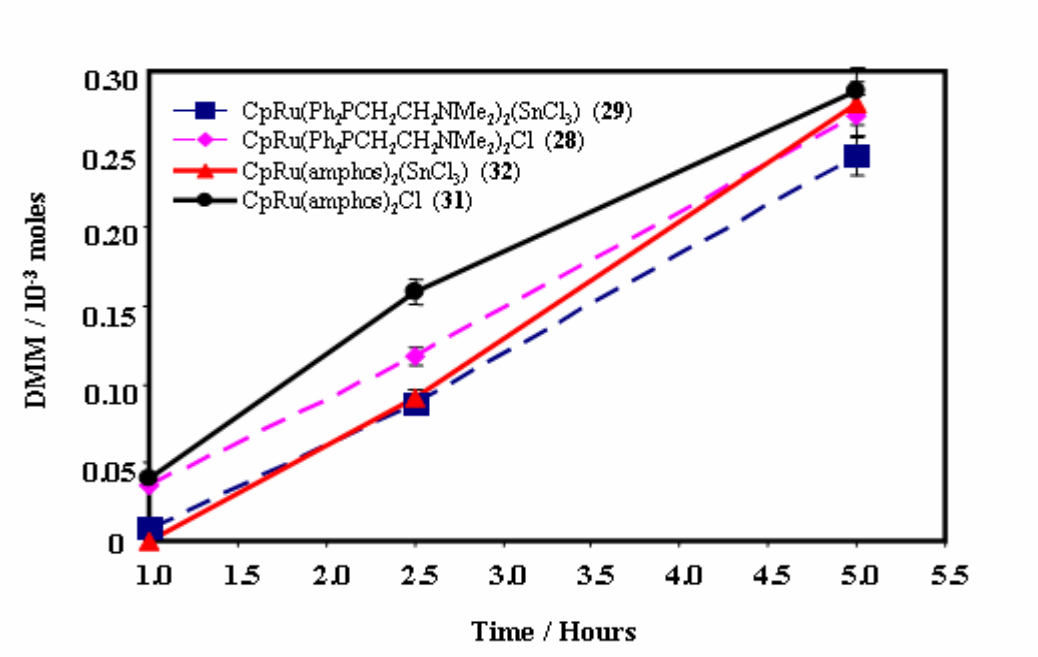

Figure 4-6. Formation of DMM during the electrooxidation of methanol at 1.4 V with Ru catalysts as specified.

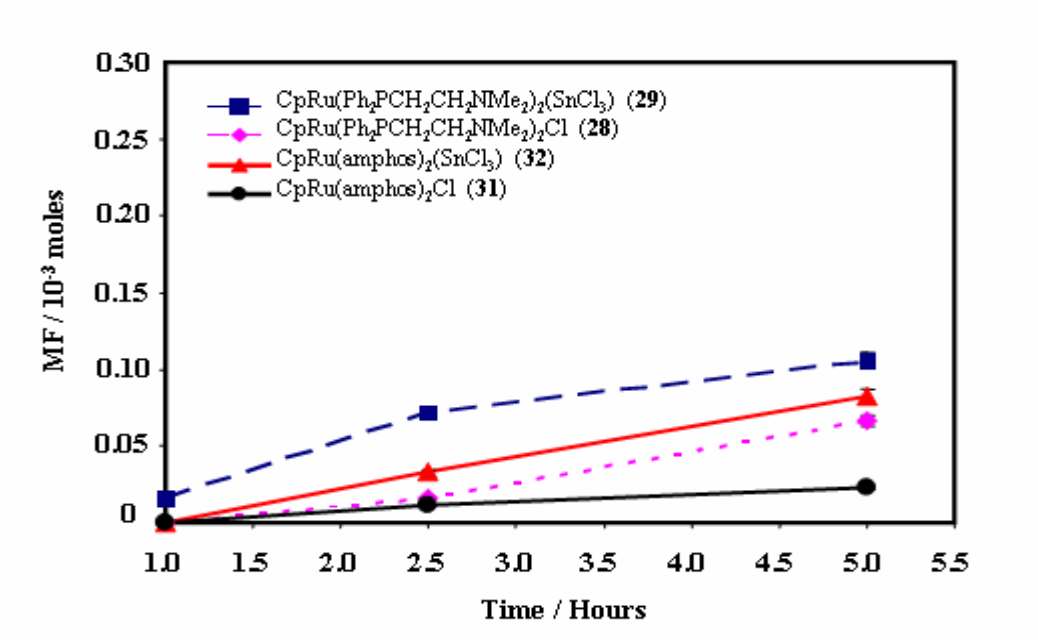

Figure 4-7. Formation of MF during the electrooxidation of methanol at 1.4 V with Ru catalysts as specified.

and its formation is favored all throughout the reaction. The Ru-aminophosphine complexes are not as active, efficient or selective as the Ru-TPPMS complexes (Table 3-5),[169] forming smaller quantities of products with a lower current efficiency.

After 5 hours of electrolysis with **28**, **29**, **31** and **32**, oxidative currents gradually decrease to approximately 60 % of the initial value. During this time the yellow solutions developed a dark brown color. Analysis of the resulting solutions by $^{31}P\{^{1}H\}$ NMR was employed to determine what happened to the catalysts during the electrolysis. At the end of the electrolysis, two singlets corresponding to the major phosphorus species were observed. Based on the chemical shift, one species was identified as the oxide of the phosphine ligand. The other singlet had a chemical shift close to the starting material, and was presumed to be a structurally similar species. Similar reaction products were identified when the electrolysis was performed with the TPPMS complexes.

The role of tin during the catalysis is unclear. Two possibilities exist:

1. Activating the Ru metal center: Increasing the electrophilicity of Ru was suggested by Gusevskaya (Eq. 3.5) during the thermal dehydrogenation of methanol.
2. Binding site for methanol: A similar role was invoked by Shinoda (Scheme 3-3) during the thermal dehydrogenation of methanol.

Both possibilities are affected by the Lewis acidity of the tin(II) ligand. To determine the role of tin, the phenyl substituted complexes $CpRu(Ph_2PCH_2CH_2NMe_2)_2(SnPh_3)$ (**30**) and $CpRu(PPh_3)_2(SnPh_3)$ (**27**) were used as catalysts during the electrooxidation of methanol. Both complexes catalyzed the electrooxidation of methanol, forming DMM (Table 4-3) as the only oxidation product. In neat methanol, $CpRu(Ph_2PCH_2CH_2NMe_2)_2(SnPh_3)$ (**30**) is a poor electrocatalyst, forming smaller quantities of products with a lower current efficiency than $CpRu(Ph_2PCH_2CH_2NMe_2)_2(SnCl_3)$ (**29**) and

$CpRu(Ph_2PCH_2CH_2NMe_2)_2Cl$ (**28**). A similar trend was observed when the catalytic activity of $CpRu(PPh_3)_2(SnPh_3)$ (**27**) was compared to $CpRu(PPh_3)_2(SnCl_3)$ (**20**) and $CpRu(PPh_3)_2Cl$ (**19**) (Table 4-3). The fact that the $SnPh_3$ complexes are less active than the $SnCl_3$ complexes implies that the Lewis acidity of the tin(II) ligand is an important factor in the activity of the catalysts. The mechanistic role of tin is still unclear since decreasing its Lewis acidity influences not only the electrophilicity of the neighboring Ru, but also the ability of tin to bind methanol.

The electrochemical oxidation of methanol was also investigated in nitromethane ($MeNO_2$), propylene carbonate (PC) and acetonitrile (CH_3CN) with $CpRu(amphos)_2(SnCl_3)$ (**32**) and $CpRu(PPh_3)_2(SnCl_3)$ (**20**). The CVs of **20** (Figure 4-5) and **32** (Figure 4-8) exhibited the anticipated catalytic current when methanol was introduced. The potential applied during the electrolysis is after the Ru(II/III) oxidation wave (Table 4-4), but within the solvent window of CH_3CN, $MeNO_2$ and PC. Although a catalytic current was observed in the CV when methanol was introduced, no oxidation products were detected during the electrolysis (Table 4-4).

Table 4-4. Bulk electrolysis data for the oxidation of methanol by **28** and **29**

Complex[a]	Electrolyte	Ru(II/III) E_{pa} (V)	Anodic Potential (V)	TON[b]
$CpRu(PPh_3)_2(SnCl_3)$ (**20**)	0.1 M TBAT / CH_3CN	1.32	1.70	0
$CpRu(PPh_3)_2(SnCl_3)$ (**20**)	0.1 M TBAT / $MeNO_2$	1.42	1.70	0
$CpRu(amphos)_2(SnCl_3)$ (**32**)	0.1 M TBAT / CH_3CN	1.59	1.80	0
$CpRu(amphos)_2(SnCl_3)$ (**32**)	0.1 M TBAT / $MeNO_2$	1.64	1.80	0
$CpRu(amphos)_2(SnCl_3)$ (**32**)	0.1 M TBAT / PC	1.73	1.80	0

[a] All electrolyses performed with 10 mM catalyst and 0.35 M methanol for 5 hours. All potentials reported vs NHE. [b] Moles of product formed per mole of Ru complex.

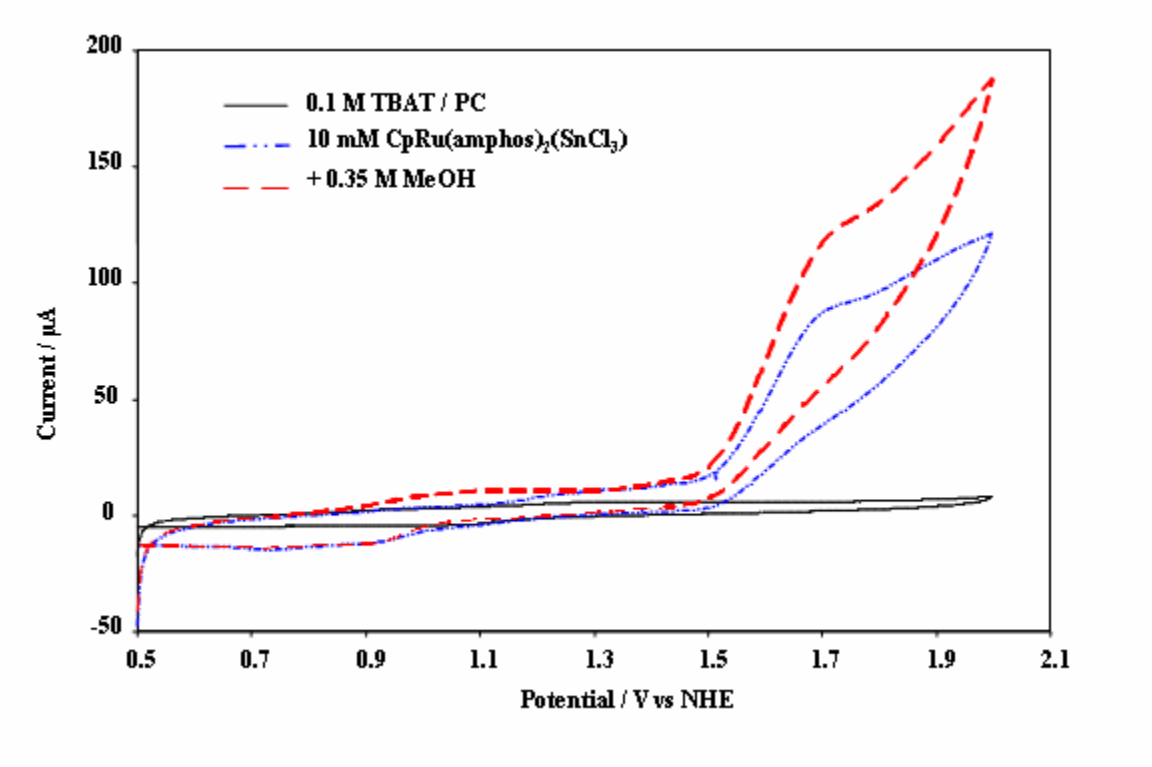

Figure 4-8. Cyclic voltammograms of **32** under nitrogen in 3.5 mL of PC / 0.1 M TBAT; glassy carbon working electrode; Ag/Ag^{+} reference electrode; 50 mV/s scan rate, solutions as specified in figure.

Since $CpRu(amphos)_2(SnCl_3)$ (**32**) and $CpRu(PPh_3)_2(SnCl_3)$ (**20**) are catalytically active in methanol and DCE, their inactivity in CH_3CN, $MeNO_2$ and PC must be as a result of the solvents. Previous results with chelating phosphine ligands (dppm, dppe and dppp) have established the necessity of a vacant coordination site on Ru for the reaction to proceed. The methanol oxidation reaction is probably retarded by the formation of solvent coordinated adducts. The formation of solvent adducts was invoked during the CV studies of **20** and **28** in CH_3CN. The ability of a solvent to coordinate to a metal center is affected by the Lewis basicity / donor number of the solvent. Donor number is a qualitative measurement of Lewis basicity, developed by Gutmann in 1976.[206,207] Strong Lewis bases have high donor numbers, and readily form adducts with Lewis acids. Acetonitrile and propylene carbonate are moderate Lewis bases (Table 4-5). Because of

Table 4-5. Donor number of selected Lewis bases

Lewis Base[a]	Donor Number kcal. mol^{-1}
CH_2Cl_2	0
DCE	0
CH_3NO_2	2.1
CH_3CN	14.1
PC	15.1
H_2O	18.0 (33.0[b])
CH_3OH	19.0
pyridine	33.1

[a] Reference 206. [b] Bulk donor number (donor number of the Lewis base in the associated liquid)

this they should readily form adducts with the Lewis acidic metal centers of $CpRu(amphos)_2(SnCl_3)$ (**32**) and $CpRu(PPh_3)_2(SnCl_3)$ (**20**). By comparing the donor numbers of methanol and nitromethane it is evident that methanol is a better Lewis base than nitromethane. It should however be noted that these measurements were performed in dichloroethane as the solvent. A better value would be the donor number of nitromethane in nitromethane as solvent (bulk donor number). The bulk donor number of nitromethane is expected to be greater than the corresponding donor number in dichlorethane, compare water in Table 4-5. It is thought that the large excess of nitromethane, acetonitrile and propylene carbonate favors the formation of solvent adducts, overcoming the thermodynamic preference if any for methanol.

Heterogeneous Studies

Preparation of Modified Toray Carbon Paper (MTCP) Electrodes

Two methods were utilized for preparing the modified electrodes:

- Method A) The metal complex and Nafion® suspension were combined. After reaching equilibrium the resulting mixture is used to coat the TCP electrode.
- Method B) The TCP electrode is coated with the Nafion® membrane before immersing in a solution of the metal complex.

These electrodes are extremely stable in solvents commonly used in electrochemistry, such as water, propylene carbonate, nitromethane and acetonitrile. They are however unstable in chlorinated solvents, rapidly degrading in methylene chloride.

MTCP-1. 200 μL of a stock solution containing Nafion® (0.25 wt %) and $CpRu(amphos)_2Cl$ (0.0167 wt %) dissolved in methanol was deposited on the surface of a TCP electrode. After drying, the modified electrode was washed with methanol and water before storing in aqueous KCl under an atmosphere of nitrogen.

MTCP-2. 200 μL of a stock solution containing Nafion® (0.833 wt %) and $CpRu(amphos)_2(SnCl_3)$ (0.0167 wt %) dissolved in methanol was deposited on the surface of a TCP electrode. After drying, the modified electrode was washed with acetonitrile before storing in acetonitrile under an atmosphere of nitrogen.

MTCP-3. 200 μL of a 2.5 wt % Nafion® suspension was deposited on the surface of a TCP electrode. After drying, the modified electrode was immersed overnight in an acetonitrile or nitromethane solution of $CpRu(amphos)_2Cl$ (0.1 wt %). Electrodes modified by this method were stored in this solution under an atmosphere of nitrogen when not in use.

MTCP-4. These electrodes were prepared in an analogous manner to MTCP-3 with $CpRu(amphos)_2(SnCl_3)$ as the metal complex.

MTCP-5. These electrodes were prepared in an analogous manner to MTCP-3 with $CpRu(Ph_2PCH_2CH_2NMe_2)_2(SnPh_3)$ as the metal complex.

Table 4-6. Formal potentials for the modified electrodes MTCP-1 to MTCP-5

Complex	Electrode	Electrolyte	E_{pa} (V vs NHE)	$E_{1/2}$ (V vs NHE)	ΔE_p (mV)	i_{pa} / i_{pc}
$CpRu(amphos)_2Cl$ (**31**)	MTCP-1	0.1 M KCl / H_2O	0.90	0.81	185	1.15
$CpRu(amphos)_2Cl$ (**31**)	MTCP-1	0.1 M TBAT / MeOH	0.97	0.90	142	1.08
$CpRu(amphos)_2(SnCl_3)$ (**32**)	MTCP-2	0.1 M TBAT / CH_3CN	1.38	1.36	42	1.03
$CpRu(amphos)_2Cl$ (**31**)	MTCP-3	0.1 M TBAT / MeOH	0.92	0.85	146	1.06
$CpRu(amphos)_2Cl$ (**31**)	MTCP-3	0.1 M TBAT / $MeNO_2$	1.06	0.93	264	1.15
$CpRu(amphos)_2Cl$ (**31**)	MTCP-3	0.1 M TBAT / CH_3CN	0.82	0.77	110	1.13
$CpRu(amphos)_2(SnCl_3)$ (**32**)	MTCP-4	0.1 M TBAT / CH_3CN	1.51			
$CpRu(amphos)_2(SnCl_3)$ (**32**)	MTCP-4	0.1 M TBAT / $MeNO_2$	1.73			
$CpRu(Ph_2PCH_2CH_2NMe_2)_2(SnPh_3)$ (**30**)	MTCP-5	0.1 M TBAT / CH_3CN	1.36			

Cyclic Voltammetry

Cyclic voltammetry was used to probe the stability of $CpRu(Ph_2PCH_2CH_2NMe_2)_2(SnPh_3)$ (**30**), $CpRu(amphos)_2Cl$ (**31**) and $CpRu(amphos)_2(SnCl_3)$ (**32**) in the modified electrodes. Electrodes modified with $CpRu(amphos)_2Cl$ (**31**) were stable in solutions of methanol, acetonitrile, nitromethane and water, with no evidence of leaching. These CVs were also very reproducible even upon repeated cycling and prolonged storage. When placed in 0.1 M TBAT/PC the complex rapidly leached from the electrode surface into solution. No leaching was observed when the electrodes were placed in propylene carbonate without supporting electrolyte. This indicated that the cation of the electrolyte was displacing the Ru complex from the Nafion® matrix. Attempts at stabilizing the electrodes by varying the supporting electrolyte ($NaBPh_4$, NH_4PF_6) were unsuccessful. Because of the rapid leaching observed in PC, this solvent was not used during further studies of the modified electrodes.

When attached to the electrode surface, a single chemically reversible oxidation wave was observed for MTCP-1 and MTCP-3 (Table 4-6). This redox process was assigned to the Ru(II/III) couple of $CpRu(amphos)_2Cl$ (**31**). The reversibility of this electron transfer process is a good indication that the complex and its oxidized form are both stable within the Nafion® matrix. When immobilized, the Ru(II/III) couple of **31** is typically shifted by 30 to 80 mV with respect to the Ru(II/III) couple of the complex in solution (Table 4-2).

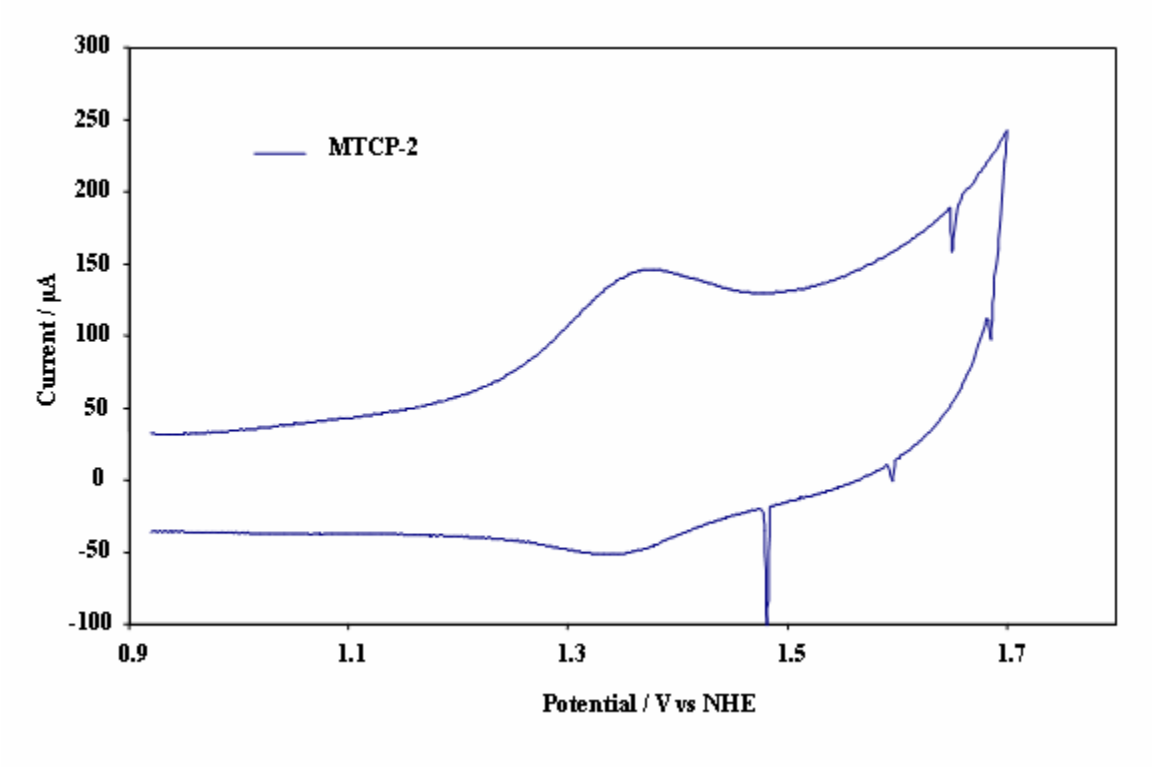

Figure 4-9. Cyclic voltammograms of MTCP-2, electrode modified with $CpRu(amphos)_2(SnCl_3)$ (**32**) under nitrogen in 3.5 mL of CH_3CN / 0.1 M TBAT; Ag/Ag^+ reference electrode; 50 mV/s scan rate.

The CVs of MTCP-2 and MTCP-4 are very stable and reproducible when analyzed in the aprotic solvents nitromethane and acetonitrile. For MTCP-2 in acetonitrile the oxidation of $CpRu(amphos)_2(SnCl_3)$ (**32**) is reversible (Table 4-6, Figure 4-9). The Nafion® matrix stabilizes $[CpRu(amphos)_2(SnCl_3)]^+$, allowing it to be reduced reversibly. This was unexpected since in solution and in MTCP-4, the oxidation of **32** is irreversible (Table 4-3 and 4-6). No redox waves were initially observed in the CVs of MTCP-2 and MTCP-4 when analyzed in water or methanol. The absence of the Ru(II/III) oxidation wave was thought to be as a result of the catalytic current obscuring its presence. Upon repeated scans a redox couple similar to the Ru(II/III) couple of **32** is observed. This was the first indication that in the presence of methanol and water MTCP-2 and MTCP-4 may be unstable. $^{31}P\{^1H\}$ NMR was used to monitor the stability of $CpRu(amphos)_2(SnCl_3)$

(**32**) in the Nafion® suspensions prior to coating the TCP electrode. Based on the NMR studies complex **32** is stable for at least two days in the Nafion® suspension, prior to preparing MTCP-2. The actual decomposition pathway for the immobilized complex is uncertain, but it seems to require the passage of current in a protic solvent. The decomposition was also observed when the CV is performed in acetonitrile and nitromethane solutions containing methanol.

One attempt at stabilizing the complex during the CV studies in methanol was the use of $CpRu(Ph_2PCH_2CH_2NMe_2)_2(SnPh_3)$ (**30**) in the modified electrodes (MTCP-5). This attempt however was unsuccessful and MTCP-5 also degraded when analyzed in water and methanol.

Summary

A series of Ru/Sn complexes containing the amphiphilic ligands $Ph_2PCH_2CH_2NMe_2$ and $Ph_2PCH_2CH_2NMe_3BF_4$ was synthesized and studied. Complexes **28**, **29**, **31** and **32** are soluble and stable in both protic and aprotic solvents. Cyclic voltammetry of these complexes was performed in methylene chloride, acetonitrile, nitromethane, propylene chloride, methanol and water. The electrochemical oxidation of methanol was performed with **28**, **29**, **31** and **32** in neat methanol. The products formed during the electrolysis are DMM and MF. The aminophosphine complexes (**28**, **29**, **31** and **32**) are not as efficient or selective as the TPPMS complexes (**22** and **23**) studied in chapter 3. The decreased activity is attributed to the stronger Ru-P bond and the decreased cone angle of the aminophosphine complexes. These two factors will inhibit phosphine dissociation, and retard the methanol oxidation reaction.

Complexes containing the $SnPh_3$ ligand $CpRu(PPh_3)_2(SnPh_3)$ (**27**) and $CpRu(Ph_2PCH_2CH_2NMe_2)_2(SnPh_3)$ (**30**), form smaller quantities of oxidation products

than the corresponding $SnCl_3$ complexes $CpRu(PPh_3)_2(SnPh_3)$ (**20**) and $CpRu(Ph_2PCH_2CH_2NMe_2)_2(SnPh_3)$ (**29**) respectively. This result indicates that the Lewis acidity of the tin(II) metal center is important to the activity of the catalyst.

Chemically modified electrodes were prepared with Nafion® exchanged membranes containing $CpRu(amphos)_2Cl$ (**31**), $CpRu(amphos)_2(SnCl_3)$ (**32**) and $CpRu(Ph_2PCH_2CH_2NMe_2)_2(SnPh_3)$ (**30**). Electrodes modified with **31** were studied in solutions of water, methanol, nitromethane and acetonitrile. These electrodes were stable and no evidence of leaching was observed. Electrodes containing the heterobimetallic complexes could only be studied in nitromethane and acetonitrile. In solutions of water and methanol, the heterobimetallic complexes quickly decompose. Because of the instability of the electrodes in methanol and the retardation of the oxidation reaction by nitromethane and acetonitrile, no catalytic studies were performed with these electrodes.

CHAPTER 5
EXPERIMENTAL PROTOCOLS

General Considerations

Standard Schlenk / vacuum techniques were used throughout. All NMR solvents were degassed via three freeze-pump-thaw cycles and stored over 4 Å molecular sieves. ^{1}H and $^{31}P\{^{1}H\}$NMR spectra are referenced to the residual proton in the deuterated solvent and to 85 % H_3PO_4, respectively. High-resolution mass spectrometry was performed by the University of Florida analytical service. Elemental analysis was performed by the Robertson Microlit Laboratories, Madison, NJ. $ClCH_2CH_2N(CH_3)_2$,[208] *cyclo*-$C_5H_5CH_2CH_2N(CH_3)_2$,[209] $CpRu(PPh_3)_2Cl$,[210] $Cp(PPh_3)Ru(\eta^1\text{-dppm})Cl$,[211] $CpRu(\eta^2\text{-dppm})Cl$,[212] $CpRu(\eta^2\text{-dppe})Cl$,[212] $CpRu(\eta^2\text{-dppp})Cl$,[213] $RuCl_2(PPh_3)_3$,[214] $Ru(\eta^2\text{-}Ph_2PCH_2CH_2NMe_2)_2Cl_2$,[215] $(Ind)Ru(PPh_3)_2(SnCl_3)$,[216] $CpRu(PPh_3)_2(SnCl_3)$,[125] $(\eta^5\text{-}C_5H_4(CH_2)_2N(CH_3)_2H^+)Ru(\eta^2\text{-dppm})Cl$,[217] and $IrCl(CO)_2(H_2N(C_6H_4)CH_3)$[218] were prepared as previously described. TPPMS was prepared using a slight modification of the published procedure.[219] Tetra-n-butylammonium triflate (TBAT), and $RuCl_3{\cdot}xH_2O$ were purchased from Sigma-Aldrich. $(Ind)Ru(PPh_3)_2Cl$ was purchased from Strem Chemicals. Toray carbon paper (0.37 mm thickness) was purchased from fuelcellstore.com. Copper wire (0.5 mm diameter, 99.9999 %) was purchased from Alfa Aesar. All other starting materials were purchased in reagent grade purity and used without further purification.

Electrochemistry

Electrochemical experiments were performed at ambient temperature in a glove box under a nitrogen atmosphere using an EG&G PAR model 263A potentiostat/galvanostat. Cyclic voltammetry (CV) was performed with a normal three-electrode configuration consisting of a working electrode (glassy carbon 3 mm diameter or TCP electrode area 2 cm^{-2}), a Pt flag counter electrode and a reference electrode. For experiments performed in 1,2-dichloroethane (DCE) or methanol, the reference electrode consisted of an acetonitrile solution of freshly prepared 0.01 M $AgNO_3$ and 0.1 M TBAT along with a silver wire. The Ag^+ solution and silver wire were contained in a 75 mm glass tube fitted at the bottom with a Vycor tip. For aqueous solutions a Ag/AgCl reference electrode (Bioanalytical Systems) was used. Constant potential electrolysis was carried out with similar equipment except for the working electrode being replaced with a vitreous carbon electrode. All potentials are reported vs. NHE and are not corrected for the junction potential of the reference electrode. The E^0 values for the ferrocene/ferrocenium couple in the electrolytes used is shown in Table 5-1.

Table 5-1. Formal potentials of the ferrocene/ferrocenium couple

Electrolyte	$Fc^{+/0}$ (V vs NHE)[a]
0.7 M TBAT / DCE	0.50
0.7 M TBAT/CH_2Cl_2	0.50
0.1 M TBAT/MeOH	0.50
0.1 M TBAT/PC	0.58
0.1 M TBAT/CH_3CN	0.41
0.1 M TBAT/$MeNO_2$	0.48

[a] Recorded at ambient temperature, scan rates = 50 mV/s.

Electrode Fabrication

Toray carbon paper (TCP) electrodes were fabricated as follows: TCP was cut into 1.5 cm x 1.0 cm blocks, treated with acetone, 0.1 M HCl and water to remove any impurities. The TCP blocks were then dried overnight at 60 °C. Electrical contact to the TCP was made through a copper wire attached with a conductive silver paste. After curing overnight at 60 °C, the electrode was cleaned as before with acetone, 0.1 M HCl and water, before drying at 60 °C for 5 hours. The silver electrical contact was then encapsulated with an insulating epoxy to give a TCP electrode with an area of approximately 2 cm^{-2}. After curing overnight at 60 °C the electrode was cleaned again as described above and stored in an inert atmosphere.

Product Analysis

Electrolysis products were analyzed by gas chromatography on a Shimadzu GC-17A chromatograph containing a 15 m x 0.32 mm column of AT™-WAX (Alltech®, 0.5 μm film) on fused silica. The column was attached to the injection port with a neutral 5 m x 0.32 mm AT™-WAX deactivated guard column. The electrolysis products were quantitatively determined with the use of *n*-heptane as an internal standard. Products were identified by comparison to authentic samples.

Preparation of Modified Electrodes

Method A. Stock solutions of Nafion (0.5 - 2.5 wt %) and Ru complex (0.1 – 0.5 wt %) were prepared by slowly adding methanol solutions of the Ru complex to a rapidly stirred suspension of 5 wt % Nafion. The resulting mixture was left stirring under N_2 overnight to allow the ion exchange process to reach completion. The TCP electrodes were then coated with the Nafion/Ru mixture (50 μL increments), and evaporation of the

solvent assisted with a gentle flow of nitrogen. The electrodes were then dried at 60 °C for 30 minutes before rinsing with methanol, water and allowed to air dry at ambient temperature overnight. Electrodes modified by this method (MTCP-A) were stored under an atmosphere of nitrogen when not in use.

Method B. TCP electrodes were coated with 200 μL of a Nafion suspension (1 – 5 wt %) rinsed with water and dried overnight at 60 °C. The Nafion modified electrodes are then taken into the glove box before immersing overnight in a solution (0.1 – 0.5 wt %) of the Ru complex. Electrodes modified by this method (MTCP-B) were stored in this solution under an atmosphere of nitrogen when not in use.

Synthesis

$CpRu(PPh_3)(\mu\text{-}Cl)(\mu\text{-}dppm)HgCl_2$ (16)

A 50 mL Schlenk flask was charged with mercury acetate (0.21 g, 0.65 mmol) and 20 mL of DCE. To this suspension, $CpRu(PPh_3)(Cl)(\eta^1\text{-}dppm)$ (**6**) (0.56 g, 0.65 mmol) dissolved in 20 mL of DCE was slowly added while stirring. After two hours acetyl chloride (12 drops) dissolved in 20 mL of DCE was slowly added. All volatiles were removed in vacuo after an additional hour of stirring. The resulting yellow solid was then redissolved and filtered through Hyflo Super Cel with 50 mL of DCE. This orange solution was then concentrated to approximately 5 mL before hexanes (20 mL) was added. The resulting yellow solid was collected on a sintered glass frit and dried overnight at 80 °C under vacuum. Yield: 0.59 g, 81 %. ^1H NMR (CD_2Cl_2): δ 7.81 – 6.50 (m, 35H, $Ph_2PCH_2PPh_2$ + PPh_3), 4.85 (s, 5H, Cp), 3.25 – 2.95 (m, 2H, $Ph_2PCH_2PPh_2$). $^{31}P\{^1H\}$ NMR ($CDCl_3$): δ 39.9 (d, Ru-PPh_3, J_{PP} = 40 Hz), 35.0 (dd, Ru-$PPh_2CH_2PPh_2$, J_{PP} = 40 Hz, 10 Hz), 30.1 (d, Hg-$PPh_2CH_2PPh_2$, J_{PP} = 10 Hz).

$CpRu(PPh_3)(\mu\text{-}Cl)(\mu\text{-}dppm)Hg(OAc)_2$ (18)

Mercury (II) acetate (0.03 g, 0.10 mmol) and 5 mL of CH_2Cl_2 was placed in a 25 mL Schlenk flask. The Schlenk flask was then fitted with an addition funnel containing $CpRu(PPh_3)(\eta^1\text{-}dppm)Cl$ (0.08 g, 0.10 mmol) in 5 mL of CH_2Cl_2. Approximately 10 minutes after the addition was complete, the mercury acetate was completely dissolved and stirring continued for an additional hour. The solution was then filtered through Hyflo Super Cel before evaporating to dryness at low pressure. The resulting solid was then recrystallized from CH_2Cl_2/hexanes. Yield: 95 %. ^1H NMR ($CDCl_3$): δ $^{31}P\{^1H\}$ NMR ($CDCl_3$): δ 41.9 (d, Ru-*P*Ph_3, J_{PP} = 43 Hz), 36.9 (dd, Ru-*P*$Ph_2CH_2PPh_2$, J_{PP} = 43 Hz, 28 Hz), 24.1 (d, Hg-PPh_2CH_2*P*Ph_2, J_{PP} = 28 Hz).

$CpRu(TPPMS)_2Cl$ (22)

In a 250 mL flask, $CpRu(PPh_3)_2Cl$ (1.0 g, 1.4 mmol) and TPPMS (0.89 g, 2.3 mmol) in 100 mL of toluene were refluxed under N_2 for two days. The resulting orange solid was then collected on a medium frit, washed with approximately 200 mL of diethyl ether and dried under vacuum at 80 °C. Yield: 0.97 g, 90 %. ^1H NMR (DMSO-d_6): δ 7.72 – 7.52 (m, 4H), 7.25 – 7.08 (m, 24H), 4.07 (s, 5H, Cp). $^{31}P\{^1H\}$ NMR (DMSO-d_6): δ 40.1 (s). HRMS (FAB): calc. for $C_{41}H_{33}O_6Na_2P_2RuS_2$ *m/z* 895.0033 $[M - Cl^- - 2\ H_2O]^+$, found 894.9935. Anal. Calc. for $C_{41}H_{37}O_8Na_2ClP_2RuS_2$: C, 50.96; H, 3.86. Found: C, 50.71; H, 3.68.

$CpRu(TPPMS)_2(SnCl_3)$ (23)

$CpRu(TPPMS)_2Cl$ (0.71 g, 0.76 mmol) and $SnCl_2$ (0.17 g, 0.89 mmol) in 25 mL ethanol were stirred under N_2 at room temperature overnight. The solution was then evaporated to dryness and the resulting yellow solid recrystallized from ethanol/diethyl

ether. Yield: 0.73 g, 85 %. ^{1}H NMR (CD_3OD): δ 7.86 – 7.70 (m, 4H), 7.35 – 7.08 (m, 24H), 4.65 (s, 5H, Cp). $^{31}P\{^{1}H\}$ NMR (CD_3OD): δ 46.0 (s, TPPMS, $^{2}J_{P,Sn}$ = 422 Hz). Anal. Calc. for $C_{41}H_{37}O_8Na_2Cl_3P_2RuS_2Sn$: C, 42.60; H, 3.23. Found: C, 42.87; H, 3.07.

CpRu(η^2-dppm)($SnCl_3$) (24)

A 50 mL Schlenk was charged with CpRu(η^2-dppm)Cl (0.59 g, 1.0 mmol), anhydrous $SnCl_2$ (0.21 g, 1.1 mmol) and 40 mL of ethanol. This orange mixture was then refluxed for 5 hours. The resulting bright yellow solid was then filtered and recrystallized from CH_2Cl_2/hexane before drying under vacuum at 60 °C. Yield: 0.66 g, 85 %. ^{1}H NMR ($CDCl_3$): δ 7.62 – 7.28 (m, 20H, $Ph_2PCH_2PPh_2$), 5.16 (m, 1H, $Ph_2PCHPPh_2$), 5.08 (s, 5H, Cp), 4.76 (m, 1H $Ph_2PCHPPh_2$). $^{31}P\{^{1}H\}$ NMR ($CDCl_3$): δ 8.3 (s, $PPh_2CH_2PPh_2$).

CpRu(η^2-dppp)($SnCl_3$) (26)

A 50 mL round bottom flask was charged with CpRu(η^2-dppp)Cl (0.24 g, 0.39 mmol), anhydrous $SnCl_2$ (0.09 g, 0.47 mmol) and 25 mL of ethanol before fitting with a reflux condenser. This orange mixture was then refluxed overnight under an atmosphere of nitrogen. The resulting bright yellow solid was then collected on a sintered glass frit and washed with ethanol before drying in vacuo at 60 °C. Yield: 0.29 g, 91 %. ^{1}H NMR ($CDCl_3$): δ 7.48 – 7.22 (m, 20H, $Ph_2PCH_2CH_2CH_2PPh_2$), 4.84 (s, 5H, *Cp*), 2.8 – 2.7 (m, 4H, $Ph_2PCH_2CH_2CH_2PPh_2$), 1.54 (s, 2H, $Ph_2PCH_2CH_2CH_2PPh_2$). $^{31}P\{^{1}H\}$ NMR ($CDCl_3$): δ 33.9 (s, $PPh_2CH_2CH_2CH_2PPh_2$). HRMS (FAB): calc. for $C_{32}H_{31}P_2Ru$ *m/z* 579.0944 $[M - SnCl_3^-]^+$, found 579.2200.

$CpRu(PPh_3)_2(SnPh_3)$ (27)

A 100 mL Schlenk flask was charged with $CpRu(PPh_3)_2(SnCl_3)$ (1.0 g, 1.1 mmol) and 50 mL of benzene, before fitting with an addition funnel containing 2.4 mL of phenyllithium (1.8M in di-n-butylether). Phenyllithium was then added dropwise to the yellow suspension, resulting in a purple solution. Stirring was continued for 4 hours at room temperature before quenching with 1 mL of ethanol. After removing the solvent, the resulting yellow solid was dried in vacuo for 2 hours. The yellow solid was then dissolved in approximately 100 mL of diethyl ether and filtered through a pad of Hyflo Super Cel before drying in vacuo at 60 °C overnight. Yield: 1.02 g, 90 %. ^{1}H NMR ($CDCl_3$): δ 7.19 – 6.98 (m, 45H), 4.27 (s, 5H, Cp). $^{31}P\{^1H\}$ NMR ($CDCl_3$): δ 53.0 (s, *P*Ph_3, $^2J_{PSn}$ = 270 Hz). HRMS (FAB): calc. for $C_{53}H_{44}P_2RuSn$ *m/z* 964.0977 $[MH^+ - C_6H_6]^+$, found 964.0941.

$CpRu(Ph_2PCH_2CH_2N(CH_3)_2)_2Cl$ (28)

A two necked 100 mL round bottom flask fitted with a reflux condenser and a rubber septum was charged with $Ru(\eta^2\text{-}Ph_2PCH_2CH_2NMe_2)_2Cl_2$ (0.65 g, 0.95 mmol), cyclopentadiene (0.19 g, 2.8 mmol) and 50 mL of ethanol. This red mixture was then refluxed for three days under an atmosphere of nitrogen. After refluxing, the solvent was removed under vacuum and the resulting orange solid washed with 90 mL of n-hexanes before recrystallizing with CH_2Cl_2/n-hexanes. Yield: 0.50 g, 74 %. ^{1}H NMR ($CDCl_3$): δ 7.47 – 7.15 (m, 20H), 4.29 (s, 5H, Cp), 3.12 (m, 2H), 2.94 (m, 2H), 2.63 (s, 12H, $N(CH_3)_2$), 2.42 (m, 2H), 2.20 (m, 2H). $^{31}P\{^1H\}$ NMR ($CDCl_3$): δ 36.6 (s, $Ph_2PCH_2CH_2NMe_2$). HRMS (FAB): calc. for $C_{37}H_{46}ClN_2P_2Ru$ *m/z* 717.1872 $[MH]^+$, found 717.1889.

$CpRu(Ph_2PCH_2CH_2N(CH_3)_2)_2(SnCl_3)$ (29)

A 25 mL Schlenk flask was charged with $CpRu(Ph_2PCH_2CH_2N(CH_3)_2)_2Cl$ (0.84 g, 1.11 mmol), $SnCl_2$ (0.33 g, 1.75 mmol) and 20 mL of 1,2-dichloroethane. The resulting mixture was stirred at room temperature for two days before refluxing for 6 hours. After removing the solvent under vacuum, the orange solid was dissolved in CH_2Cl_2 and filtered through a pad of Hyflo Super Cel. A yellow solid was then precipitated with n-hexanes before recrystallizing with CH_2Cl_2/n-hexanes. Yield: 0.97 g, 96 %. ^{1}H NMR ($CDCl_3$): δ 7.44 – 7.19 (m, 20H), 4.71 (s, 5H, Cp), 3.09 (m, 4H), 2.86 – 2.74 (m, 14H), 2.56 (m, 2H). $^{31}P\{^1H\}$ NMR ($CDCl_3$): δ 39.4 (s, $Ph_2PCH_2CH_2NMe_2$, $^2J_{PSn}$ = 412 Hz). HRMS (FAB): calc. for $C_{37}H_{45}Cl_2N_2P_2RuSn$ *m/z* 871.0500 $[M\text{-}Cl^-]^+$, found 871.0543.

$CpRu(Ph_2PCH_2CH_2N(CH_3)_2)_2(SnPh_3)$ (30)

A 50 mL Schlenk flask was charged with $CpRu(Ph_2PCH_2CH_2N(CH_3)_2)_2(SnCl_3)$ (0.25 g, 0.28 mmol) and 50 mL of toluene before cooling to -78 °C. The Schlenk flask was then fitted with an addition funnel containing 0.70 mL of phenyllithium (1.7M in di-n-butylether) and 2 mL of toluene. Phenyllithium was then added dropwise, resulting in the formation of a purple solution. Stirring was continued for 4 hours at room temperature before quenching with 1 mL of ethanol. After drying in vacuo, the resulting yellow solid was dissolved in n-hexanes and filtered through a pad of Hyflo Super Cel. Complex **30** was then isolated by chromatography on SiO_2 with 99:1 (chloroform/triethylamine) as eluent. Yield: 0.19 g, 64 %. ^{1}H NMR ($CDCl_3$): δ 7.52 – 7.09 (m, 35H), 4.21 (s, 5H), 2.3 – 2.1 (m, 4H), 1.81 (s, 12H), 1.6 – 1.7 (m, 4H). $^{31}P\{^1H\}$ NMR ($CDCl_3$): δ 43.8 (s, $Ph_2PCH_2CH_2N(CH_3)_2$, $^2J_{PSn}$ = 262 Hz).

$CpRu(Ph_2PCH_2CH_2N(CH_3)_3BF_4)_2Cl$ (31)

A 500 mL two-necked round bottom flask containing $CpRu(PPh_3)_2Cl$ (1.00 g, 1.37 mmol) and 150 mL of toluene was fitted with a reflux condenser and a pressure equalizing addition funnel before heating to reflux. To the refluxing orange mixture, a solution of amphos (0.99 g, 2.8 mmol) in 50 mL of methylene chloride was added dropwise. After four days of reflux, the solvent was removed under vacuum and the resulting yellow solid was washed with 200 mL of petroleum ether and 100 mL of toluene before recrystallizing from CH_2Cl_2 / diethyl ether. Yield: 0.96 g, 76 %. ^{1}H NMR (DMSO-d_6): δ 7.49 – 7.21 (m, 20H), 4.48 (s, 5H, Cp), 3.21 – 2.85 (m, 24H), 2.57 (m, 2H). $^{31}P\{^1H\}$ NMR (DMSO-d_6): δ 35.9 (s, amphos). HRMS (FAB): calc. for $C_{39}H_{51}BClF_4N_2P_2Ru$ *m/z* 833.2294 $[M\text{-}BF_4^-]^+$, found 833.2287.

$CpRu(Ph_2PCH_2CH_2N(CH_3)_3BF_4)_2(SnCl_3)$ (32)

$CpRu(amphos)_2Cl$ (0.20 g, 0.22mmol) and $SnCl_2$ (0.50 g, 0.33mmol) in 50 mL of ethanol were refluxed under N_2 overnight. The solution was then evaporated to dryness and the resulting yellow solid was recrystallized from ethanol/diethyl ether. Yield: 0.21 g, 88 %. ^{1}H NMR (acetone-d_6): δ 7.65 – 7.43 (m, 20H), 5.00 (s, 5H, Cp), 3.49 (m, 2H), 3.11 (s, 18H, $N(CH_3)_2$), 2.94 (m, 4H), 2.44 (m, 2H). $^{31}P\{^1H\}$ NMR (acetone-d_6): δ 39.5 (s, $Ph_2PCH_2CH_2NMe_3BF_4$, $^2J_{P,Sn}$ = 405 Hz).

$Ph_2PCH_2CH_2N(CH_3)_2$

1.25 g of Li chips and 100 mL of THF were placed in a 250 mL Schlenk flask fitted with a pressure equalizing addition funnel. To the vigorously stirred Li suspension, Ph_2PCl (10 g, 0.045 moles) in 50 mL of THF was slowly added. After stirring at R.T. for 12 hours, the resulting Ph_2PLi solution was transferred to a two necked round bottom

flask fitted with a rubber septum and an addition funnel. While stirring the deep red Ph_2PLi solution, $ClCH_2CH_2N(CH_3)_2$ (5.0 g, 0.036 moles) in 50 mL of THF was slowly added before heating for 12 hours at 60 °C. The resulting mixture was then hydrolyzed with 50 mL of degassed water, before adding 200 mL of diethyl ether. The organic layer was extracted with 250 mL of water and dried over $MgSO_4$ before the solvent was removed under vacuum to yield an oil. Purification of the oil was achieved using flash chromatography through a column of neutral alumina with diethyl ether as the eluent. Yield: 7.86 g, 84 %. The compound was identified by comparison to literature data.[220]

$Ph_2PCH_2CH_2N(CH_3)_3BF_4$

Me_3OBF_4 (1.65 g, 0.011 mol) and 80 mL of CH_2Cl_2 were added to a 250 mL Schlenk flask, fitted with a pressure equalizing addition funnel. The flask was then cooled to -98 °C before a solution of $Ph_2PCH_2CH_2N(CH_3)_2$ (3.01 g, 0.012 mol) in 30 mL of CH_2Cl_2 was added dropwise. When the addition was complete the mixture was stirred at -98 °C for 5 hours then at rt overnight. The resulting white solid was collected on a sintered frit and washed exhaustively with diethyl ether, before recrystallizing from CH_2Cl_2 / diethyl ether. Yield: 3.36 g, 84 %. ^{1}H NMR (acetone-d_6): δ 7.42 – 7.55 (m, 10H, *Ph*$_2$P), 3.68 (m, 2H, $Ph_2PC\mathit{H}_2CH_2NMe_3$), 3.38 (s, 9H, $Ph_2PCH_2CH_2N\mathit{Me}_3$), 2.85 (m, 2H, $Ph_2PCH_2C\mathit{H}_2NMe_3$). $^{31}P\{^1H\}$ NMR (acetone-d_6): δ -19.5 (s, $Ph_2\mathit{P}CH_2CH_2NMe_3$).

$[(\eta^5\text{-}C_5H_4(CH_2)_2N(CH_3)_2H)Ru(\mu\text{-dppm})(\mu\text{-}CO)_2IrCl_2]Cl$

A 100 mL round bottom flask was charged with $(\eta^5\text{-}C_5H_4(CH_2)_2N(CH_3)_2H^+)Ru(\eta^2\text{-dppm})Cl$ (1.3 g, 2.0 mmol), $IrCl(CO)_2(H_2N(C_6H_4)CH_3)$ (0.81 g, 2.0 mmol) and 50 mL of toluene. This mixture was then refluxed for 24 hrs and the resulting yellow precipitate collected on a sintered glass

frit. The crude product was then placed into a Soxhlet extractor and impurities extracted overnight with benzene, before drying overnight in vacuo at 60 °C. Yield: 1.25 g, 65 %. ^{1}H NMR (DMSO-d_6): δ 7.52-7.18 (m, 20H, *Ph*$_2$PCH$_2$P*Ph*$_2$), 5.30 (s, 2H, *Cp*), 5.07 (s, 2H, *Cp*), 3.17 (m, 2H, Ph$_2$PC*H*$_2$PPh$_2$), 2.70 (m, 10H, C$_5$H$_4$(C*H*$_2$)$_2$N(C*H*$_3$)$_2$H$^+$). ^{31}P{^{1}H} NMR (d_6-DMSO): δ 59.8 (d, Ru-Ph$_2$*P*CH$_2$PPh$_2$, J_{PP} = 59 Hz), 12.4 (d, Ir-*P*Ph$_2$CH$_2$PPh$_2$, J_{PP} = 59 Hz). IR (KBr) 1800, 1780 cm^{-1}. HRMS (FAB) calcd for $C_{36}H_{37}Cl_2IrNO_2P_2Ru$ *m/z* 942.0349 [M-Cl$^-$]$^+$, found 942.0377.

Crystallographic Structure Determination of CpRu(PPh$_3$)(μ-Cl)(μ-dppm)HgCl$_2$ (16)

Data were collected at 173 K on a Siemens SMART PLATFORM equipped with a CCD area detector and a graphite monochromator utilizing MoKα radiation (λ = 0.71073 Å). Cell parameters were refined using up to 8192 reflections. A full sphere of data (1850 frames) was collected using the ω-scan method (0.3° frame width). The first 50 frames were remeasured at the end of data collection to monitor instrument and crystal stability (maximum correction on I was < 1 %). Absorption corrections by integration were applied based on measured indexed crystal faces.

The structure was solved by the Direct Methods in *SHELXTL5,* and refined using full-matrix least squares. The non-H atoms were treated anisotropically, whereas the hydrogen atoms were calculated in ideal positions and were riding on their respective carbon atoms. The asymmetric unit consists of the complex and two dichloroethane molecules of crystallization. One of those molecules had one of its chlorine atoms disordered and was refined in two parts (Cl6 & Cl6'). Their site occupation factors were dependently refined to 0.67(2) for Cl, and consequently 0.33(2) for Cl6'. A total of 581 parameters were refined in the final cycle of refinement using 10968 reflections with I >

$2\sigma(I)$ to yield R_1 and wR_2 of 2.07 % and 5.23 %, respectively. Refinement was done using F^2.

LIST OF REFERENCES

(1) Moureu, C.; Dufraisse, C. *Chem. Rev.* **1926**, *3*, 113-162.

(2) Sheldon, R. A.; Kochi, J. K. *Metal-Catalyzed Oxidations of Organic Compounds*; Academic Press: New York, 1981.

(3) *Ruthenium Catalysts and Fine Chemistry*; Bruneau, C.; Dixneuf, P. H.; Eds.;. Topics in Organometallic Chemistry; Springer: New York, 2004.

(4) Sheldon, R. A.; Arends, I. W. C. E. In *Advances in Catalytic Activation of Dioxygen by Metal Complexes*; Simandi, L. I., Ed.; Kluwer: Dordrecht, 2003; pp 123-155.

(5) Egami, H.; Onitsuka, S.; Katsuki, T. *Tetrahedron Lett.* **2005**, *46*, 6049-6052.

(6) Shapley, P. A.; Zhang, N. J.; Allen, J. L.; Pool, D. H.; Liang, H. C. *J. Am. Chem. Soc.* **2000**, *122*, 1079-1091.

(7) Murahashi, S. I.; Komiya, N. *Catal. Today* **1998**, *41*, 339-350.

(8) Chatterjee, D.; Mitra, A.; Shepherd, R. E. *Inorg. Chim. Acta* **2004**, *357*, 980-990.

(9) Marko, I. E.; Giles, P. R.; Tsukazaki, M.; Chelle-Regnaut, I.; Urch, C. J.; Brown, S. M. *J. Am. Chem. Soc.* **1997**, *119*, 12661-12662.

(10) Neumann, R.; Khenkin, A. M.; Juwiler, D.; Miller, H.; Gara, M. *J. Mol. Catal. A - Chem.* **1997**, *117*, 169-183.

(11) Pearson, A. J.; Kwak, Y. *Tetrahedron Lett.* **2005**, *46*, 3407-3410.

(12) Brown, D. S.; Kerr, W. J.; Lindsay, D. M.; Pike, K. G.; Ratcliffe, P. D. *Synlett* **2001**, 1257-1259.

(13) Jiang, L.; Sun, G.; Sun, S.; Liu, J.; Tang, S.; Li, H.; Zhou, B.; Xin, Q. *Electrochim. Acta* **2005**, *50*, 5384-5389.

(14) Camara, G. A.; De Lima, R. B.; Iwasita, T. *J. Electroanal. Chem.* **2005**, *585*, 128-131.

(15) Yoshida, P. G. *Fuel cell vehicles race to a new automotive future*; Office of Technology Policy, U.S. Dept. of Commerce, 2003.

(16) Stone, C.; Morrison, A. E. *Solid State Ionics* **2002**, *152-153*, 1-13.

(17) Kim, D.; Cho, E. A.; Hong, S.-A.; Oh, I.-H.; Ha, H. Y. *J. Power Sources* **2004**, *130*, 172-177.

(18) Parsons, R.; VanderNoot, T. *J. Electroanal. Chem.* **1988**, *257*, 9-45.

(19) Hartnig, C.; Spohr, E. *Chem. Phys.* **2005**, *319*, 185-191.

(20) Li, X. *Fuel cells*; Taylor & Francis Group: New York, 2006.

(21) Arico, A. S.; Srinivasan, S.; Antonucci, V. *Fuel Cells* **2001**, *1*, 133-161.

(22) Wasmus, S.; Kuver, A. *J. Electroanal. Chem.* **1999**, *461*, 14-31.

(23) Goodenough, J. B.; Hamnett, A.; Kennedy, B. J.; Manoharan, R.; Weeks, S. A. *J. Electroanal. Chem.* **1988**, *240*, 133-145.

(24) Beden, B.; Kadirgan, F.; Lamy, C.; Leger, J. M. *J. Electroanal. Chem.* **1981**, *127*, 75-85.

(25) Chandrasekaran, K.; Wass, J. C.; Bockris, J. O. *J. Electrochem. Soc.* **1990**, *137*, 518-524.

(26) Ianniello, R.; Schmidt, V. M.; Stimming, U.; Stumper, J.; Wallau, A. *Electrochim. Acta* **1994**, *39*, 1863-1869.

(27) Dinh, H. N.; Ren, X.; Garzon, F. H.; Zelenay, P.; Gottesfeld, S. *J. Electroanal. Chem.* **2000**, *491*, 222-233.

(28) Yajima, T.; Uchida, H.; Watanabe, M. *J. Phys. Chem. B* **2004**, *108*, 2654-2659.

(29) Wasmus, S.; Vielstich, W. *J. Appl. Electrochem.* **1993**, *23*, 120-124.

(30) Iwasita, T. *Electrochim. Acta* **2002**, *47*, 3663-3674.

(31) Enyo, M.; Machida, K.-i.; Fukuoka, A.; Ichikawa, M. In *Electrochemistry in Transition*; Murphy, O. J., Ed.; Plenum Press: New York, 1992, pp 359-369.

(32) Ross, P. N. *Electrochim. Acta* **1991**, *36*, 2053-2062.

(33) Leger, J. M.; Lamy, C. *Ber. Bunsen-Ges.* **1990**, *94*, 1021-1025.

(34) Guo, Y. G.; Hu, J. S.; Zhang, H. M.; Liang, H. P.; Wan, L. J.; Bai, C. L. *Adv. Mater.* **2005**, *17*, 746-+.

(35) Wang, K.; Gasteiger, H. A.; Markovic, N. M.; Ross, P. N. *Electrochim. Acta* **1996**, *41*, 2587-2593.

(36) Tsaprailis, H.; Birss, V. I. *Electrochem. Solid-State Lett.* **2004**, *7*, A348-A352.

(37) Lee, S. A.; Park, K. W.; Choi, J. H.; Kwon, B. K.; Sung, Y. E. *J. Electrochem. Soc.* **2002**, *149*, A1299-A1304.

(38) McLeod, E. J.; Birss, V. I. *Electrochim. Acta* **2005**, *51*, 684-693.

(39) Liu, N.; Kourtakis, K.; Figueroa, J. C.; Chen, J. G. G. *J. Catal.* **2003**, *215*, 254-263.

(40) Zellner, M. B.; Chen, J. G. G. *J. Electrochem. Soc.* **2005**, *152*, A1483-A1494.

(41) Lei, H. W.; Suh, S.; Gurau, B.; Workie, B.; Liu, R. X.; Smotkin, E. S. *Electrochim. Acta* **2002**, *47*, 2913-2919.

(42) Chu, D.; Gilman, S. *J. Electrochem. Soc.* **1996**, *143*, 1685-1690.

(43) Rolison, D. R.; Hagans, P. L.; Swider, K. E.; Long, J. W. *Langmuir* **1999**, *15*, 774-779.

(44) Kua, J.; Goddard, W. A. *J. Am. Chem. Soc.* **1999**, *121*, 10928-10941.

(45) Watanabe, M.; Motoo, S. *J. Electroanal. Chem.* **1975**, *60*, 276-283.

(46) Arico, A. S.; Antonucci, P. L.; Modica, E.; Baglio, V.; Kim, H.; Antonucci, V. *Electrochim. Acta* **2002**, *47*, 3723-3732.

(47) Sugimoto, W.; Aoyama, K.; Kawaguchi, T.; Murakami, Y.; Takasu, Y. *J. Electroanal. Chem.* **2005**, *576*, 215-221.

(48) Cathro, K. J. *J. Electrochem. Soc.* **1969**, *116*, 1608-1611.

(49) Lima, A.; Coutanceau, C.; Léger, J. M.; Lamy, C. *J. Appl. Electrochem.* **2001**, *31*, 379-386.

(50) Goetz, M.; Wendt, H. *J. Appl. Electrochem.* **2001**, *31*, 811-817.

(51) Gurau, B.; Viswanathan, R.; Liu, R. X.; Lafrenz, T. J.; Ley, K. L.; Smotkin, E. S.; Reddington, E.; Sapienza, A.; Chan, B. C.; Mallouk, T. E.; Sarangapani, S. *J. Phys. Chem. B* **1998**, *102*, 9997-10003.

(52) Reddington, E.; Sapienza, A.; Gurau, B.; Viswanathan, R.; Sarangapani, S.; Smotkin, E. S.; Mallouk, T. E. *Science* **1998**, *280*, 1735-1737.

(53) Choi, W. C.; Kim, J. D.; Woo, S. I. *Catal. Today* **2002**, *74*, 235-240.

(54) Arico, A. S.; Poltarzewski, Z.; Kim, H.; Morana, A.; Giordano, N.; Antonucci, V. *J. Power Sources* **1995**, *55*, 159-166.

(55) Sullivan, M. G.; Utomo, H.; Fagan, P. J.; Ward, M. D. *Anal. Chem.* **1999**, *71*, 4369-4375.

(56) Jusys, Z.; Massong, H.; Baltruschat, H. *J. Electrochem. Soc.* **1999**, *146*, 1093-1098.

(57) Takasu, Y.; Kawaguchi, T.; Sugimoto, W.; Murakami, Y. *Electrochim. Acta* **2003**, *48*, 3861-3868.

(58) Jusys, Z.; Kaiser, J.; Behm, R. J. *Langmuir* **2003**, *19*, 6759-6769.

(59) Lund, H.; Hammerich, O.; Editors *Organic Electrochemistry, Fourth Edition*, Dekker: New York, 2001.

(60) Geneste, F.; Moinet, C.; Ababou-Girard, S.; Solal, F. *Inorg. Chem.* **2005**, *44*, 4366-4371.

(61) Meyer, T. J.; Huynh, M. H. V. *Inorg. Chem.* **2003**, *42*, 8140-8160.

(62) Navarro, M.; De Giovani, W. F.; Romero, J. R. *J. Mol. Catal. A-Chem.* **1998**, *135*, 249-256.

(63) Moyer, B. A.; Meyer, T. J. *J. Am. Chem. Soc.* **1978**, *100*, 3601-3603.

(64) Samuels, G. J.; Meyer, T. J. *J. Am. Chem. Soc.* **1981**, *103*, 307-312.

(65) Moyer, B. A.; Thompson, M. S.; Meyer, T. J. *J. Am. Chem. Soc.* **1980**, *102*, 2310-2312.

(66) Gagne, R. R.; Marks, D. N. *Inorg. Chem.* **1984**, *23*, 65-74.

(67) Rossi, A.; De Giovani, W. F. *J. Mol. Catal. A: Chem.* **2006**, *243*, 40-43.

(68) Thompson, M. S.; Meyer, T. J. *J. Am. Chem. Soc.* **1982**, *104*, 4106-4115.

(69) De Giovani, W. F.; Romero, J. R.; Madurro, J. M. *Quim. Nova* **1988**, *11*, 367-369.

(70) Madurro, J. M.; Chiericato, G., Jr.; De Giovani, W. F.; Romero, J. R. *Tetrahedron Lett.* **1988**, *29*, 765-768.

(71) Navarro, M.; De Giovani, W. F.; Romero, J. R. *Synth. Commun.* **1990**, *20*, 399-406.

(72) Farrer, B. T.; Thorp, H. H. *Inorg. Chem.* **2000**, *39*, 44-49.

(73) Neyhart, G. A.; Cheng, C.-C.; Thorp, H. H. *J. Am. Chem. Soc.* **1995**, *117*, 1463-1471.

(74) Cheng, C.-C.; Goll, J. G.; Neyhart, G. A.; Welch, T. W.; Singh, P.; Thorp, H. H. *J. Am. Chem. Soc.* **1995**, *117*, 2970-2980.

(75) Carter, P. J.; Cheng, C.-C.; Thorp, H. H. *J. Am. Chem. Soc.* **1998**, *120*, 632-642.

(76) Deronzier, A.; Moutet, J. C. In *Electrochemical reactions catalyzed by transition metal complexes*; McCleverty, J.A., Meyer, T.J., Eds.; Comprehensive Coordination Chemistry II Vol. 9; Elsevier: Oxford, 2004; pp 471 - 507.

(77) Lima, E. C.; Fenga, P. G.; Romero, J. R.; De Giovani, W. F. *Polyhedron* **1998**, *17*, 313-318.

(78) Gerli, A.; Reedijk, J.; Lakin, M. T.; Spek, A. L. *Inorg. Chem.* **1995**, *34*, 1836-1843.

(79) Roecker, L.; Meyer, T. J. *J. Am. Chem. Soc.* **1987**, *109*, 746-754.

(80) Roecker, L.; Meyer, T. J. *J. Am. Chem. Soc.* **1986**, *108*, 4066-4073.

(81) Lebeau, E. L.; Meyer, T. J. *Inorg. Chem.* **1999**, *38*, 2174-2181.

(82) Muller, J. G.; Acquaye, J. H.; Takeuchi, K. J. *Inorg. Chem.* **1992**, *31*, 4552-4557.

(83) Kieboom, A.P.G.; Moulijn, J.A.; Sheldon, R.A. In *Catalysis: an Integrated Approach*; Van Santen, R. A.; Van Leeuwen, P. W. N. M.; Moulijn, J. A.; Averill, B. A.; Eds.; Elsevier: New York, 1999; Chapter 2.

(84) Oyama, S. T.; Hightower, J. W. In *Catalytic Selective Oxidation*; Oyama, S. T.; Desikan, A. N.; Hightower, J. W., Eds.; ACS Symposium Series 523; American Chemical Society: Washington, DC, 1993; pp 1 - 15.

(85) Molenveld, P.; Engbersen, J. F. J.; Reinhoudt, D. N. *Chem. Soc. Rev.* **2000**, *29*, 75-86.

(86) Rowlands, G. J. *Tetrahedron* **2001**, *57*, 1865-1882.

(87) Ishii, Y.; Hidai, M. *Catal. Today* **2001**, *66*, 53-61.

(88) Laneman, S.A.; Stanley, G.G., In *Homogeneous Transition Metal Catalyzed Reactions*; Moser, W.R.; Slocum, D.W.; Eds.; Advances in Chemistry Series 230; American Chemical Society: Washington, DC, 1992; p 349.

(89) Quebatte, L.; Solari, E.; Scopelliti, R.; Severin, K. *Organometallics* **2005**, *24*, 1404-1406.

(90) Gauthier, S.; Scopelliti, R.; Severin, K. *Organometallics* **2004**, *23*, 3769-3771.

(91) Shapley, P.A., In *Activation and Functionalization of C-H Bonds*; Goldberg, K.I.; Goldman, A.S.; Eds.; ACS Symposium Series 885; American Chemical Society: Washington, DC, 2004; p 349.

(92) Matare, G.; Tess, M. E.; Abboud, K. A.; Yang, Y.; McElwee-White, L. *Organometallics* **2002**, *21*, 711-716.

(93) Tess, M. E.; Hill, P. L.; Torraca, K. E.; Kerr, M. E.; Abboud, K. A.; McElwee-White, L. *Inorg. Chem.* **2000**, *39*, 3942-3944.

(94) Shibasaki, M.; Yoshikawa, N. *Chem. Rev.* **2002**, *102*, 2187-2209.

(95) Severin, K. *Chem. Eur. J.* **2002**, *8*, 1514-1518.

(96) Rida, M. A.; Smith, A. K. *Mod. Coord. Chem.* **2002**, 154-162.

(97) Wheatley, N.; Kalck, P. *Chem. Rev* **1999**, *99*, 3379-3419.

(98) Baranger, A. M.; Bergman, R. G. *J. Am. Chem. Soc* **1994**, *116*, 3822-3835.

(99) Adams, R. D.; Barnard, T. S. *Organometallics* **1998**, *17*, 2885-2890.

(100) Xiao, J.; Puddephatt, R. J. *Coord. Chem. Rev.* **1995**, *143*, 457-500.

(101) Yang, Y.; Abboud, K. A.; McElwee-White, L. *Dalton Trans.* **2003**, 4288-4296.

(102) Anderson, R.; Griffin, K.; Johnston, P.; Alsters, P. L. *Adv. Synth. Catal.* **2003**, *345*, 517-523.

(103) Hayashi, M.; Yamada, K.; Nakayama, S.; Hayashi, H.; Yamazaki, S. *Green Chem.* **2000**, *2*, 257-260.

(104) Paavola, S.; Zetterberg, K.; Privalov, T.; Csoregh, I.; Moberg, C. *Adv. Synth. Catal.* **2004**, *346*, 237-244.

(105) Steinhoff, B. A.; King, A. E.; Stahl, S. S. *J. Org. Chem.* **2006**, *71*, 1861-1868.

(106) Buffin, B. P.; Clarkson, J. P.; Belitz, N. L.; Kundu, A. *J. Mol. Catal. A: Chem.* **2005**, *225*, 111-116.

(107) Guan, B. T.; Xing, D.; Cai, G. X.; Wan, X. B.; Yu, N.; Fang, Z.; Yang, L. P.; Shi, Z. J. *J. Am. Chem. Soc.* **2005**, *127*, 18004-18005.

(108) Paquette, L., Ed. *Encyclopedia of reagents for organic synthesis*; John Wiley & Sons: New York, 1995.

(109) Ding, R.; Katebzadeh, K.; Roman, L.; Bergquist, K.-E.; Lindstroem, U. M. *J. Org. Chem.* **2006**, *71*, 352-355.

(110) Kelly, T. R.; Whiting, A.; Chandrakumar, N. S. *J. Am. Chem. Soc.* **1986**, *108*, 3510-3512.

(111) Olah, G. A.; Kobayashi, S.; Tashiro, M. *J. Am. Chem. Soc.* **1972**, *94*, 7448-7461.

(112) Kobayashi, S.; Busujima, T.; Nagayama, S. *Chem. Eur. J.* **2000**, *6*, 3491-3494.

(113) Tschinkl, M.; Schier, A.; Riede, J.; Gabbaie, F. P. *Organometallics* **1999**, *18*, 1747-1753.

(114) King, J. B.; Gabbaie, F. P. *Organometallics* **2003**, *22*, 1275-1280.

(115) Haneline, M. R.; Tsunoda, M.; Gabbaie, F. P. *J. Am. Chem. Soc.* **2002**, *124*, 3737-3742.

(116) Gardinier, J. R.; Gabbai, F. P. *Dalton Trans.* **2000**, 2861-2865.

(117) Peng, A.; Ding, Y. *Synthesis* **2003**, 205-208.

(118) Periana, R. A.; Taube, D. J.; Evitt, E. R.; Loffler, D. G.; Wentrcek, P. R.; Voss, G.; Masuda, T. *Science* **1993**, *259*, 340-343.

(119) Song, H.-B.; Zhang, Z.-Z.; Mak, T. C. W. *New J. Chem.* **2002**, *26*, 113-119.

(120) Deming, R. L.; Allred, A. L.; Dahl, A. R.; Herlinger, A. W.; Kestner, M. O. *J. Am. Chem. Soc.* **1976**, *98*, 4132-4137.

(121) Yang, Y.; McElwee-White, L. *Dalton Trans.* **2004**, 2352-2356.

(122) Smith, P. J.; Ed. *Chemistry of Tin, Second Edition*, 1997.

(123) Cotton, J. D.; Knox, S. A. R.; Stone, F. G. A.J. Chem. Soc. A **1968**, 2758-2762.

(124) Kummer, R.; Graham, W. A. G. *Inorg. Chem.* **1968**, *7*, 1208-1214.

(125) Robles-Dutenhefner, P. A.; Moura, E. M.; Gama, G. J.; Siebald, H. G. L.; Gusevskaya, E. V. *J. Mol. Catal. A-Chem.* **2000**, *164*, 39-47.

(126) Holt, M. S.; Wilson, W. L.; Nelson, J. H. *Chem. Rev.* **1989**, *89*, 11-49.

(127) Kretschmer, M.; Pregosin, P. S. *Inorg. Chim. Acta* **1982**, *61*, 247-254.

(128) Consiglio, G.; Morandini, F.; Ciani, G.; Sironi, A.; Kretschmer, M. *J. Am. Chem. Soc.* **1983**, *105*, 1391-1392.

(129) Vetere, V.; Faraoni, M. B.; Santori, G. F.; Podesta, J. C.; Casella, M. L.; Ferretti, O. A. *Catal. Today* **2005**, *107-108*, 266-272.

(130) Einaga, H.; Yamakawa, T.; Shinoda, S. *J. Mol. Catal. A-Chem.* **1995**, *97*, 35-40.

(131) Ohnishi, T.; Yamakawa, T.; Shinoda, S. *J. Chem. Soc., Dalton Trans.* **1997**, 789-794.

(132) Yamakawa, T.; Hiroi, M.; Shinoda, S. *J. Chem. Soc., Dalton Trans.* **1994**, 2265-2269.

(133) Choudhury, J.; Podder, S.; Roy, S. *J. Am. Chem. Soc.* **2005**, *127*, 6162-6163.

(134) Szymanska-Buzar, T. **2003**, *122*, 121-129.

(135) Czelusniak, I.; Szymanska-Buzar, T. *J. Mol. Catal. A: Chem.* **2002**, *190*, 131-143.

(136) Kegl, T.; Kollar, L. *J. Mol. Catal. A: Chem.* **1997**, *122*, 95-101.

(137) Kollar, L.; Consiglio, G.; Pino, P. *J. Organomet. Chem.* **1987**, *330*, 305-314.

(138) Casey, C. P.; Martins, S. C.; Fagan, M. A. *J. Am. Chem. Soc.* **2004**, *126*, 5585-5592.

(139) Shinoda, S.; Ohnishi, T.; Yamakawa, T. **1997**, *1*, 25-34.

(140) Shinoda, S.; Itagaki, H.; Saito, Y. *J. Chem. Soc., Chem. Commun.* **1985**, 860-861.

(141) Roper, W. R.; Wright, L. J. **1982**, *234*, C5-C8.

(142) Kung, H. H.; Smith, K. J. In *Methanol Production and Use*; Cheng, W; Kung, H.H., Chemical Industries; Dekker: New York, 1994; Vol. 57 Chapter 5.

(143) Haynes, A.; Maitlis, P. M.; Morris, G. E.; Sunley, G. J.; Adams, H.; Badger, P. W.; Bowers, C. M.; Cook, D. B.; Elliott, P. I. P.; Ghaffar, T.; Green, H.; Griffin, T. R.; Payne, M.; Pearson, J. M.; Taylor, M. J.; Vickers, P. W.; Watt, R. J. *J. Am. Chem. Soc.* **2004**, *126*, 2847-2861.

(144) Chang, C. D. In *Methanol Production and Use*; Cheng, W; Kung, H.H., Chemical Industries; Dekker: New York, 1994; Vol. 57 Chapter 4.

(145) Wachs, I. E.; Briand, L. E. WO Patent 2002022539, 2002

(146) Yoneoka, M.; Ikarashi, T.; Watabe, K.; Nakumura, K. EP Patent 625502, 1994

(147) Yuan, Y.; Liu, H.; Imoto, H.; Shido, T.; Iwasawa, Y. *J. Catal.* **2000**, *195*, 51-61.

(148) Yuan, Y.; Tsai, K.; Liu, H.; Iwasawa, Y. *Top. Catal.* **2003**, *22*, 9-15.

(149) Liu, H.; Bayat, N.; Iglesia, E. *Angew. Chem.-Int. Edit.* **2003**, *42*, 5072-5075.

(150) Liu, H. C.; Iglesia, E. *J. Phys. Chem. B* **2003**, *107*, 10840-10847.

(151) U.S. Environmental Protection Agency, http://www.epa.gov/OMS/diesel.htm (accessed February 1, 2006), part of U.S. Environmental Protection Agency, http://www.epa.gov/ (accessed February 1, 2006).

(152) Anthony, C. R.; McElwee-White, L., Eds. *Materials, Chemicals and Energy from Forest Biomass*; 921 ed.; American Chemical Society: Washington, D.C., 2006.

(153) Otsuka, K.; Ina, T.; Yamanaka, I. *Appl. Catal. A-Gen.* **2003**, *247*, 219-229.

(154) Fedkiw, P. S., Jr.; Liu, R.; Trainham, J. A., III US Patent 5,223,102, 1993

(155) Yamanaka, I.; Otsuka, K. *Chem. Lett.* **1988**, 753-756.

(156) Otsuka, K.; Yamanaka, I. *Appl. Catal.* **1986**, *26*, 401-404.

(157) Lin, W. F.; Wang, J. T.; Savinell, R. F. *J. Electrochem. Soc.* **1997**, *144*, 1917-1922.

(158) Wasmus, S.; Wang, J. T.; Savinell, R. F. *J. Electrochem. Soc.* **1995**, *142*, 3825-3833.

(159) Liu, R.; Fedkiw, P. S. *J. Electrochem. Soc.* **1992**, *139*, 3514-3523.

(160) Childers, C. L.; Huang, H. L.; Korzeniewski, C. *Langmuir* **1999**, *15*, 786-789.

(161) Rieger, P. H. *Electrochemistry*; Chapman & Hall: New York, 1987.

(162) Kissinger, P. H., Ed.; *Laboratory techniques in electroanalytical chemistry*; Dekker: New York, 1996.

(163) Schnatbaum, K.; Schafer, H. J. *Synthesis* **1999**, 864-872.

(164) Denooy, A. E. J.; Besemer, A. C.; Vanbekkum, H. *Tetrahedron* **1995**, *51*, 8023-8032.

(165) Einaga, H.; Yamakawa, T.; Shinoda, S. *J. Coord. Chem.* **1994**, *32*, 117-119.

(166) Suárez, T.; Fontal, B.; Reyes, M.; Bellandi, F.; Contreras, R.; León, G.; Cancines, P. *React. Kinet. Catal. Lett.* **2002**, *76*, 161-169.

(167) Mandal, S. K.; Chakravarty, A. R. *Indian J Chem A* **1990**, *29A*, 18-21.

(168) Gamasa, M. P.; Gimeno, J.; Gonzalez-Bernardo, C.; Martin-Vaca, B. M.; Monti, D.; Bassetti, M. *Organometallics* **1996**, *15*, 302-308.

(169) Anthony, C. R.; McElwee-White, L. *J. Mol. Catal. A - Chem.* **2005**, *227*, 113-117.

(170) Shaw, B.R. In *Electrochemistry, Past and Present*; Stock, J.S., Orna, M.V., Eds.; ACS Symposium Series 390; American Chemical Society: Washington, DC, 1989; pp 318 - 338.

(171) Navratilova, Z.; Kula, P. *Electroanalysis* **2003**, *15*, 837-846.

(172) Walcarius, A. *Anal. Chim. Acta* **1999**, *384*, 1-16.

(173) Seen, A. J. *J. Mol. Catal. A: Chem.* **2001**, *177*, 105-112.

(174) Chen, T. Y.; Leddy, J. *Langmuir* **2000**, *16*, 2866-2871.

(175) Gierke, T. D.; Hsu, W. Y.In *Perfluorinated Ionomer Membranes*; Eisenberg, A.; Yeager, H.L., Eds.; ACS Symposium Series 180; American Chemical Society: Washington, DC, 1982; pp 283 - 307.

(176) Mauritz, K. A.; Moore, R. B. *Chem. Rev.* **2004**, *104*, 4535-4585.

(177) Olah, G. A.; Meidar, D. *Synthesis* **1978**, 671-672.

(178) Seen, A. J.; Townsend, A. T.; Bellis, J. C.; Cavell, K. J. *J. Mol. Catal. A: Chem.* **1999**, *149*, 233-242.

(179) Kuwana, T.; French, W. G. *Anal. Chem.* **1964**, *36*, 241.

(180) Zen, J. M.; Kumar, A. S.; Tsai, D. M. *Electroanalysis* **2003**, *15*, 1073-1087.

(181) Bard, A. J. *Integrated Chemical Systems: A Chemical Approach to Nanotechnology*; Wiley: New York, 1994.

(182) Malinauskas, A. *Synth. Met.* **1999**, *107*, 75-83.

(183) Podlovchenko, B. I.; Andreev, V. N. *Russ. Chem. Rev.* **2002**, *71*, 837-851.

(184) Rolison, D. R.; Bessel, C. A. *Acc. Chem. Res.* **2000**, *33*, 737-744.

(185) Santiago, M. B.; Velez, M. M.; Borrero, S.; Diaz, A.; Casillas, C. A.; Hofmann, C.; Guadalupe, A. R.; Colon, J. L. *Electroanalysis* **2006**, *18*, 559-572.

(186) Vickers, S. J.; Ward, M. D. *Electrochem. Commun.* **2005**, *7*, 389-393.

(187) Deronzier, A. In *Conducting Polymers and Polymer Electrolytes: from Biology to Photovoltaics*; Rubinson, J.F.; Mark, H.B., Eds.; ACS Symposium Series 832; American Chemical Society: Washington, DC, 2003; pp 141-153.

(188) Yao, K.; Shimazu, K.; Nakata, M.; Yamagishi, A. *J. Electroanal. Chem.* **1998**, *443*, 253-261.

(189) Paula, M. M. S.; Franco, C. V. *J. Coord. Chem.* **1996**, *40*, 71-82.

(190) Guo, Z.; Dong, S. *Anal. Chem.* **2004**, *76*, 2683-2688.

(191) Shaidarova, L. G.; Gedmina, A. V.; Chelnokova, I. A.; Budnikov, G. K. *J. Anal. Chem.* **2005**, *60*, 533-539.

(192) Vining, W. J.; Meyer, T. J. *J. Electroanal. Chem.* **1985**, *195*, 183-187.

(193) Dobson, J. C.; Meyer, T. J. *Inorg. Chem.* **1988**, *27*, 3283-3291.

(194) Moss, J. A.; Leasure, R. M.; Meyer, T. J. *Inorg. Chem.* **2000**, *39*, 1052-1058.

(195) Hogan, C. F.; Forster, R. J. *Anal. Chim. Acta* **1999**, *396*, 13-21.

(196) Deronzier, A.; Eloy, D.; Jardon, P.; Martre, A.; Moutet, J.-C. *J. Electroanal. Chem.* **1998**, *453*, 179-185.

(197) Murray, R. W.; Ewing, A. G.; Durst, R. A. *Anal. Chem.* **1987**, *59*, 379A - 390A.

(198) Murray, R. W. *Molecular Design of Electrode Surfaces*; Wiley: New York, 1992.

(199) Aubert, P.-H.; Audebert, P.; Capdevielle, P.; Maumy, M.; Roche, M. *New J. Chem.* **1999**, *23*, 297-301.

(200) Vining, W. J.; Meyer, T. J. *Inorg. Chem.* **1986**, *25*, 2023-2033.

(201) Navarro, M.; Collomb, M.-N.; Deronzier, A. *J. Electroanal. Chem.* **2002**, *520*, 150-156.

(202) Ebadi, M.; Alexiou, C.; Lever, A. B. P. *Can. J. Chem.* **2001**, *79*, 992-1001.

(203) Oyaizu, K.; Haryono, A.; Natori, J.; Tsuchida, E. *J. Chem. Soc., Faraday Trans.* **1998**, *94*, 3737-3742.

(204) Swavey, S.; Narra, M.; Srour, H. *J. Coord. Chem.* **2005**, *58*, 1463-1476.

(205) Smith, K. T.; Roemming, C.; Tilset, M. *J. Am. Chem. Soc.* **1993**, *115*, 8681-8689.

(206) Gutmann, V. *Coord. Chem. Rev.* **1976**, *18*, 225-255.

(207) McNaught, A. D.; Wilkinson, A. *Compendium of Chemical Terminology, 2nd Edition*; Blackwell Science: Boston, 1997.

(208) Picquet, M.; Stutzmann, S.; Tkatchenko, I.; Tommasi, I.; Zimmermann, J.; Wasserscheid, P. *Green Chem.* **2003**, *5*, 153-162.

(209) Rees, W. S., Jr.; Dippel, K. A. *Org. Prep. Proced. Int.* **1992**, *24*, 527-532.

(210) Bruce, M. I.; Wallis, R. C. *Aust. J. Chem.* **1979**, *32*, 1471-1485.

(211) Bruce, M. I.; Humphrey, M. G.; Patrick, J. M.; White, A. H. *Aust. J. Chem.* **1983**, *36*, 2065-2072.

(212) Ashby, G. S.; Bruce, M. I.; Tomkins, I. B.; Wallis, R. C. *Aust. J. Chem.* **1979**, *32*, 1003-1016.

(213) Suzuki, T.; Tokunaga, M.; Wakatsuki, Y. *Org. Lett.* **2001**, *3*, 735-737.

(214) Ortiz-Frade, L. A.; Ruiz-Ramirez, L.; Gonzalez, I.; Marin-Becerra, A.; Alcarazo, M.; Alvarado-Rodriguez, J. G.; Moreno-Esparza, R. *Inorg. Chem.* **2003**, *42*, 1825-1834.

(215) Shen, J.-Y.; Slugovc, C.; Wiede, P.; Mereiter, K.; Schmid, R.; Kirchner, K. *Inorg. Chim. Acta* **1998**, *268*, 69-76.

(216) Oro, L. A.; Ciriano, M. A.; Campo, M.; Foces-Foces, C.; Cano, F. H. *J. Organomet. Chem.* **1985**, *289*, 117-131.

(217) Chu, H. S.; Lau, C. P.; Wong, K. Y.; Wong, W. T. *Organometallics* **1998**, *17*, 2768-2777.

(218) Klabunde, U. *Inorg. Syn.* **1974**, *15*, 82-84.

(219) Roman, P. J., Jr.; Paterniti, D. P.; See, R. F.; Churchill, M. R.; Atwood, J. D. *Organometallics* **1997**, *16*, 1484-1490.

(220) Smith, R. T.; Baird, M. C. *Inorg. Chim. Acta* **1982**, *62*, 135-139.

BIOGRAPHICAL SKETCH

Corey Ricardo Carlo Anthony was born in Kingston, Jamaica on December 31st, 1976. His interest in the sciences was sparked at an early age by his sisters and their toy chemistry kit. Corey spent his formative years at St. Theresa Preparatory School before attending St. George's College High School where his love for chemistry took root. After completing high school Corey went on to pursue a tertiary level education at the University of the West Indies at Mona. He thoroughly enjoyed his college years and graduated in 1998 with a Bachelor of Science degree in pure and applied chemistry. Corey then got his first full time job at the Jamaica Forensic Science Laboratory as a forensic science examiner. He worked at the forensic lab for two years before enrolling at the University of Florida. In spring of 2001 he joined the McElwee-White research group and began his Ph.D. studies in organometallic chemistry. After six years of research, he graduated from the University of Florida with a Doctorate of Philosophy in chemistry.